ÉCOLE DE TECHNOLOGIE SUPÉRIEURE
UNIVERSITÉ DU QUÉBEC

THESIS PRESENTED TO
ÉCOLE DE TECHNOLOGIE SUPÉRIEURE

IN PARTIAL FULFILLMENT OF THE REQUIREMENTS FOR
THE DEGREE OF MASTER OF ENGINEERING
M. Ing.

BY
WANG, Jun

PACKING DESIGN OF MEMS PRESSURE, TEMPERATURE AND OTHER SENSORS

MONTREAL, OCTOBER 3 2008

PRÉSENTATION DU JURY (ANGLAIS) –THESIS M. ENG.

THIS THESIS HAS BEEN EVALUATED

BY THE FOLLOWING BOARD OF EXAMINERS

M. Vahé Nerguizian, directeur de mémoire
Département de génie électrique à l'École de technologie supérieure

M. René Jr. Landry, codirecteur de mémoire
Département de génie électrique à l'École de technologie supérieure

M. Jean-François Boland, président du jury
Département de génie électrique à l'École de technologie supérieure

M. Gino Rinaldi, examinateur externe
Conseil National de Recherches du Canada, Ottawa

THIS THESIS HAS BEEN PRESENTED AND DEFENDED

BEFORE A BOARD OF EXAMINERS AND PUBLIC

AUGUST 28 2008

AT ÉCOLE DE TECHNOLOGIE SUPÉRIEURE

CONCEPTION D'EMPAQUETAGE DES MICROS CAPTEURS DE PRESSION, DE TEMPERATURE ET AUTRES EN MEMS.

WANG, Jun

RÉSUMÉ

Dans certaines recherches précédentes, la fabrication des capteurs de pression se basait sur les puces MEMS à base de SiC (Silicon Carbide). Cependant, des chercheurs de l'Université Concordia ont démontré récemment que SiCN (Silicon Carbide Nitride) avait un avantage plus important par rapport au Si (Silicon) ou SiC à haute température. Il serait donc un matériel potentiel dans un environnement hostile. Dans ce mémoire, un bref historique sur les capteurs MEMS à haute température sera introduit. Certaines questions dont le choix du matériel, la fabrication, l'empaquetage, et l'application des capteurs de température MEMS seront discutées. Une approche pour le conditionnement des capteurs de pression à haute température sera présentée et quelques prototypes seront créés avec succès. En outre, certaines simulations pour ces prototypes seront étudiées et les résultats des simulations seront examinés.

PACKING DESIGN OF MEMS PRESSURE, TEMPERATURE AND OTHER SENSORS

WANG, Jun

ABSTRACT

High temperature MEMS pressure sensor packaging demands much more requirements for packaging process than common pressure sensors. The choice of material for high temperature MEMS pressure sensor is an important issue. Some previous researches concentrated on a SiC MEMS pressure sensor chip. However, the researchers from Concordia University recently found that SiCN had important advantages over Si or SiC at high temperature and would be a potential material in harsh environment. In this thesis, a brief background about high temperature MEMS sensor is introduced. Some issues in the material choice, fabrication, packaging, and application of high temperature MEMS sensor are discussed. Two kinds of methods for packaging high temperature pressure sensors are designed to create prototypes and the designed prototypes are evaluated under the sensor working condition. In addition, some simulations for those designed prototypes are studied and the results of simulations are discussed.

ACKNOWLEDGEMENT

This thesis would not have been possible without the love and guidance of those who have supported my efforts. I would like to express my deep appreciation to my major advisor, Prof. Vahé Nerguizian for all his support, encouragement, and dedication throughout my research. I am grateful to my co-advisor, Prof. René Jr. Landry, for his helpful advices and insightful support in this research. I would like to thank the committee members for their positive comments and personal encouragements. I also want to acknowledge other CRIAQ members, especially Prof. Ion Stiharu, Dr. Gino Rinaldi, Mr. Patrice Dionne, Mr. Daniel Summers, and Dr. Sergey Andronenko. Thank you all!

SYNTHÈSE

Cette recherche vise en particulier à développer des empaquetages des capteurs de pression MEMS pour les applications aérospatiales dans les turbines des moteurs d'avions à des températures élevées et environnement corrosif. L'ensemble du mémoire est divisé en 5 chapitres et chaque chapitre est résumé, comme montré ci-après.

La commande des turbines à gaz du moteur pourrait rendre un moteur plus efficace et plus fiable. Le moteur a besoin des capteurs de pression à haute température qui fournissent des données dynamiques de pression et de température. Des capteurs de pression à haute température traditionnels sont grands, lourdes et coûteux. Le projet CRIAQ 6.2 prévoit l'utilisation des MEMS à base de micro-capteurs qui améliorent les performances et la sécurité des turbines à gaz des moteurs.

La particularité d'empaquetage des capteurs MEMS à haute température est discutée. Haute conductivité thermique, thermomécanique compatibilité, haute résistance aux chocs thermiques, haute résistance et haute compatibilité chimique sont nécessaires pour les applications à haute température. Certains des matériels appropriés seront mis en place. Les capteurs à haute température sont généralement fabriqués avec du SiC, du SiCN ou du SiN. Dans cette étude, AlN, alumine et SiCN sont choisis pour faire agir comme substrat de l'empaquetage. La colle époxyde n'est pas un matériel convenable pour connecter la puce et le substrat pour des applications à haute température. Cotronics Corporation a certains colles céramiques à base l'alumine qui peuvent bien fonctionner à haute température. La liaison des fils électrique et de saisie est également discutée. Le fil d'aluminium ne peut pas passer les essais de traction destructifs après des cycles thermiques entre -55 °C et 400 °C. Le fil en or est beaucoup mieux que le fil en aluminium car pour les essais de traction du fil en or il n'y a pas de différence significative avant et après les cycles thermiques entre -55 °C et 500 °C. Le fil en platine a une meilleure stabilité à haute température que le fil en or. Par contre le fil de liaison en

platine qui peut supporter un environnement du moteur à 600 °C est rarement utilisé dans l'industrie. L'alliage Kovar a une dilatation thermique similaire aux matériaux d'empaquetage. Ainsi, il devient de plus en plus un matériel de boîtier convenable mieux que l'acier inoxydable.

Deux prototypes détaillés d'empaquetage de capteur MEMS de pression à haute température sont présentés dans ce mémoire. Les puces de capteur pourraient être des puces en SiCN (l'université de Concordia travaille sur ce procédé) ou des puces en SiC (le matériel le plus populaire pour les applications à haute température). La technologie de métallisation de Ti/Pt/Au est parvenue à une maturité et elle pourrait se développer sur des substrats par un dépôt chimique en phase vapeur. Trois candidats de matériaux pour le substrat seront simulés dans le chapitre 5 (AlN, composé d'alumine et SiCN céramique). Les substrats d'alumine composés peuvent être préparés par moulage ou l'empotage. Les substrats de céramique SiCN peuvent également être préparés par une coulée en moule. Les substrats AlN peuvent être faits par pressage à chaud ou par frittage de pression. Tous les substrats doivent être intégrés aux broches en platine. Le fil en or est utilisé pour le prototype 1 et la soudure à point en or (flip chip) est utilisée pour le prototype. Pour le collage et l'étanchéité, un adhésif à base d'alumine Resbond 940HT de Cotronics Corporation est choisi. Cet adhésif est également utilisé pour relier le substrat à un boîtier en alliage Kovar qui vise à protéger les capteurs.

Une analyse de FEM et de brèves étapes de la FEA sont introduites, le contenu et l'analyse sont discutés. La conception de 4 prototypes est modélisée. Deux éléments (SOLID5 et SOLID90) sont appliqués dans les modèles des paramètres de matériaux et les modèles de dimensions sont saisis, puis le programme ANSYS est utilisé pour les calculs, et les résultats sont présentés par ANSYS post-processeur.

Différents types de simulation sont effectués, et les résultats de simulation sont présentés.

- Les simulations de distribution de contrainte thermo mécanique montrent que la partie qui subit le plus de contraintes est le bord de la membrane du capteur avec application de pression ou bien sans l'application de pression.
- L'empaquetage conventionnel a le moins de contraintes thermique que celui de la méthode de la puce retournée (flip chip).
- Si les dimensions géométriques des capteurs sont proportionnellement changées, la taille des capteurs n'a pas d'incidence sur la contrainte thermique.
- Si seulement l'épaisseur de la membrane du capteur change (autres parties conservent la même dimension), l'augmentation de l'épaisseur de la membrane de la puce du capteur peut diminuer avec les contraintes thermiques.
- Avec l'augmentation de la température, la déformation augmentera également. Pour la déformation de la membrane, il y a eu une augmentation de 12% du déplacement au centre de la membrane lors de changements de température de 0 degré Celsius à 600 degrés Celsius.
- Pour chaque matériel, on a différentes contraintes thermiques La liaison du platine est meilleur que celle de l'or. Al_2O_3 n'est pas un bon matériel de base par rapport au AlN et au SiCN. Une puce de SiC avec une liaison de matériaux de base de SiCN et platine semblent être la meilleure combinaison matérielle. Une puce SiCN avec des matériaux de base d'AlN est également bon pour la liaison en platine et la liaison en or. La plupart des combinaisons aux SiCN sont mieux que le carbure de silicium.
- La simulation transitoire de transfert de chaleur montre que le SiCN ne convient pas pour des applications avec une température à évolution rapide en raison de sa faible conductivité thermique.
- Un calcul de transfert de chaleur par simulation dans MATLAB est validé par une vérification transitoire de transfert de chaleur.
- Si la température des contraintes libres est proche du point médian de la température étendue de charge, il est conseillé de réduire les contraintes thermiques.

- Une simulation en FEMLAB est complétée en utilisant le même modèle que le logiciel ANSYS, leurs résultats similaires confirment la validité des modèles.
- La comparaison entre la connexion d'or imparfaite (80% densité, 63% du module) et la connexion parfaite (100% densité, module 100%) est générée avec une pression de charge de 1M Pa et la température de la pièce. Les contraintes thermiques sont presque les mêmes.

En conclusion, si le fil de liaison en platine est disponible, l'empaquetage conventionnel doit être adopté parce que le boîtier a le moins de stress thermique et le fil en platine a une meilleure stabilité à haute température que l'or. Sinon, l'empaquetage en puce retournée (flip-chip) pourrait protéger l'intérieur de la pièce et cette solution est plus raisonnable.

TABLE OF CONTENTS

Page

LIST OF TABLES

LIST OF FIGURES

Page

LIST OF ABREVIATIONS

AES	Auger Electron Spectrometry
Al_2O_3	Alumina
AlN	Aluminum Nitride
ANSYS	Product of ANSYS company. Software for FE analysis and static simulation
Au	Gold
BeO	Beryllium Oxide
C4	Controlled Collapse Chip Connection
CAE	Computer-Aided Engineering
CFRP	Carbon-Fiber-Reinforced Plastic
CNS/ATM	Communications, Navigation, Surveillance, and Air Traffic Management
CRIAQ	Consortium for Research and Innovation in Aerospace in Quebec
CTE	Coefficient of Thermal Expansion
CVD	Chemical Vapor Deposition
DRIE	Deep Reactive Ion Etching
DSP	Difference Scalar Potential
ESEM	Environmental Scanning Electron Microscope
FADEC	Full Authority Digital Engine Control
FE	Finite Element
FEM/FEA	Finite Element Method/Finite Element Analysis
FQRNT	Le Fonds Québécois de la Recherche sur la Nature et les Technologies

GaAs	Gallium Arsenide
GSP	General Scalar Potential
GUI	Graphic User Interface
HAR	High Aspect Ratio
HF	Hydrogen Fluoride
IC	Integrated Circuit
ISO	International Organization for Standardization
KOH	Potassium Hydroxide
LIGA	German acronym for (X-ray) lithography (Lithographie), Electroplating (Galvanoformung), and Molding (Abformung)
MEMS	Micro ElectroMechanical Systems
MESFET	Metal Epitaxial Semiconductor Field Effect Transistor
MTF	Mean Time to Failure
NaOH	Sodium Hydroxide
NEMS	Nano ElectroMechanical Systems
NOx	Nitrogen Oxides
PDC	Polymer Derived Ceramic
PDE	Partial Differential Equation
PECVD	Plasma-Enhanced Chemical Vapor Deposition
PRT	Platinum Resistance Thermometer
Pt	Platinum
PVD	Physical Vapor Deposition

redox	Oxidation-Reduction.
RF	Radio Frequency
RIE	Reactive Ion Etching
RSP	Reduced Scalar Potential
RTD	Resistance Temperature Detector
SiN	Silicon Nitride (Si_3N_4)
SiC	Silicon Carbide
SiCN	Silicon Carbide Nitride
SIMS	Secondary Ions Mass Spectrometry
SOI	Silicon-On-Insulator
TAO	Thermo Acoustic Oscillation
Tg	Transition temperatures
Ti	Titanium
TMAH	TetraMethylAmmonium Hydroxide
UV	Ultraviolet
VRQ	Valorisation-Recherche Québec

INTRODUCTION

Background

Microsystems technologies are believed to be an important part of the technological foundation upon which the world can continue to improve the standard of living in the twenty-first century [1]. Micro electromechanical systems (MEMS) have been studied intensely for over two decades. MEMS generally range in size from a micrometer (a millionth of a meter) to a millimeter (thousandth of a meter). MEMS are also referred to as micro machines, or Micro Systems Technology (MST). MEMS are separate and distinct from the hypothetical vision of Molecular Nanotechnology or Molecular Electronics. Si-based MEMS, fabricated by surface and bulk micromachining techniques derived from IC processing technology, dominate the current MEMS market [2].

MEMS devices are designed and fabricated to realize functional purposes in some fields. Among these MEMS devices, MEMS sensors are widely used in many fields. MEMS sensor is fabricated by using MEMS technology and its function purposes, e.g. pressure and temperature measurements are realized by detecting the signal change of some parameter in the MEMS device. This signal is caused by converting one type of energy to another through the MEMS device [3].

A pressure sensor is designed to convert input pressures to electrical outputs. Pressure is an expression of the force required to stop a gas or fluid from expanding, and is usually stated in terms of force per unit area [4].

A temperature sensor (thermometer) is designed to detect a change in a physical parameter such as resistance or output voltage that corresponds to a temperature change. There are two basic types of temperature sensing: contact temperature sensing and non-

contact measurement [5]. The word thermometer is derived from two smaller word fragments: thermo from the Greek for heat and meter from Greek, meaning to measure.

To form these functional MEMS sensors, proper assembly and packaging techniques are required. Packaging is the science, art, and technology of enclosing or protecting products for distribution, storage, sale, and use. It also refers to the process of design, evaluation, and production of packages. For a typical MEMS sensor packaging fabrication, it could include pre-package test, wafer mounting, wafer sawing, wafer cleaning, die inspection, die attaching, wire bonding, sealing, ink marking, and final test. Most of MEMS packaging processes and techniques are from IC industry, but MEMS sensor packaging still has its own characteristic. MEMS sensor usually has moving parts and needs contact environment. Some MEMS sensors have hermitic parts. In fact, MEMS sensor packaging design should be considered at the beginning of MEMS sensor chip design using concurrent engineering. Different type sensors usually have different packaging requirement, so a number of packaging approaches have been developed for MEMS sensor [6].

MEMS sensors for low-temperature pressure measurements have been studied for a few decades, and many devices have been made in many applications. However, high-temperature pressure sensors for hazard environment are still in the laboratory. Some interesting works were presented in different ways to assure high-temperature MEMS functional sensor [7]. High-Temperature MEMS packaging represents a challenging and costly task in the manufacturing of MEMS. On average, almost 70 % of the cost of a high temperature MEMS sensor is in the package [8].

High temperature MEMS pressure sensor packaging is an important part of the project, MEMS for control and monitoring of gas turbine engines, funded by Consortium for Research and Innovation in Aerospace in Quebec (CRIAQ). It demands much more requirements for packaging process than common pressure sensors. Therefore, high

temperature MEMS sensor packaging is a difficulty, but it is the pivot for the whole system. This thesis will concentrate on the packaging of the sensors which will be used in the Pratt & Whitney Canada (P&WC) engines. Those sensors could be high-temperature MEMS pressure sensors, acoustic MEMS sensors, and temperature sensors because each part of a jet engine has different environment for those sensors. In this thesis, two kinds of methods for packaging high temperature pressure sensors are designed to create prototypes, and the designed prototypes are evaluated under the sensor operating condition [9].

At the micron scale, the theories of conventional size constructs are not always suitable to explain some phenomenon's observed in the small size MEMS devices. Therefore, proper finite element analysis (FEA) is necessary for the study of MEMS design and fabrication. The FEA simulations for the designed prototypes are also a part of work in this thesis.

The entire thesis is divided into 5 chapters and each chapter has an overview, as shown in the following.

Overview of chapters

Chapter 1 presents the objective of this research (and it is also one of the objectives of CRIAQ 6.2). Some problems in the industry, jet engine environment, and MEMS sensor are briefly introduced.

Chapter 2 discusses some high temperature MEMS sensor packaging key issues, including the choice of packaging materials and packaging processes.

Chapter 3 describes a solution for high temperature MEMS pressure sensor packaging, and evaluates packaging materials and designed prototypes.

Chapter 4 introduces the way to simulate designed prototypes by using finite element analysis.

Chapter 5 shows the results and discussions of the simulations.

CHAPTER 1

PROBLEMS IN THE INDUSTRY

Gas turbine jet engine closed-loop active control could create thermo acoustic instabilities, and increase fuel mileage for aircraft engines. High temperature MEMS sensors are necessary because the hot section of a jet engine works at up to 600 degrees Celsius. The objectives of CRIAQ project 6.2 are to provide the industrial partners with MEMS sensors that will enhance the performance and safety of gas turbine jet engines.

Objective of this research

This research aims specifically to develop a MEMS sensor package for the aerospace applications in the turbines of the airplane engines to high temperatures and corrosive environment.

The measurement of the useful parameters like the pressure, the temperature and other in the engines of airplane is very important to ensure the control and the monitoring of the health of the plane. The usage of several MEMS sensors at various places in an engine would allow the detection of the anomalies and the fast correction of these.

The environment of the engines is very severe. It presents extreme temperatures close to 600 degrees Celsius and very corrosive gases, such as sulfides, NO_X, CO and CO_2 [10]. The packaging of MEMS sensors in this environment requires a detailed attention and presents a major design challenge. Not only is the packaging a challenge, but also the connection of sensors signals to the external world.

The methodology to achieve our object includes the following statements:

1. To make a review of literature on the technology of packaging of MEMS
2. To analyze existing MEMS sensor packaging.

3. To find a solution to package these MEMS sensors to meet the specifications identified by the involved industrial company.
4. To simulate the prototypes by using finite element analysis.

The main purpose of this research is to find out a solution for packaging a MEMS pressure sensor which can work on jet engine combustion environment and is summarized as high temperature 600 degrees Celsius, high dynamic pressure and chemically corrosive.

1.1 Gas Turbine Jet Engine Control

Future jet engine must provide high efficiency and reliability at low cost. Pressure sensors and temperature sensors in an engine can supply dynamic pressure and temperature data which could make a feedback control system work. Fuel mixture has a key role for the engine performance and it is a key object for jet engine control system [11]. Lean fuel mixture combustion means that more than the stoichiometric amount of air needed to burn a certain amount fuel is taken to the engine, the fuel will combust completely and some oxygen will be left over in the exhaust gases. Currently, the fuel mixture aircraft operators use is 40 to 45 percent of the fuel of a typical 14:1 air-to-fuel mixture [12]. Jet engines running lean fuel mixtures could cause Thermo Acoustic Oscillations (TAO's) which occur in systems where a long tube open at the cold end is extended to the closed end at the warm boundary, which usually happens in the fill line or the vent line where the tube is capped off at the hot end, or the flow rate in the tube is small [13]. TAO's can be very damaging for an engine as the oscillations are accompanied by considerable heat conduction down the tube. This can increase the heat leak of the system by several orders of magnitude. Lean mixtures also increase nitrogen oxides (NOx) emissions, especially where hot spots form within the engine.

Proper fuel mixture will prevent combustor thermo acoustic instabilities, reduce emissions and increase fuel mileage for aircraft engines. Traditionally this kind of

problem is resolved with pre-programmed open-loop Full Authority Digital Engine Control (FADEC) adjustments; however, there is no guarantee that such techniques can deal with all of the instabilities [14]. The solution is active fuel control [11] that relies on feedback signals from pressure sensors and temperature sensors that are integrated onto engine's fuel injectors. According to Glennan Microsystems Inc., this technology could improve turbine stability under lean operating conditions while reducing nitrogen oxides by 75 percent and carbon dioxide by 15 percent below current emissions standards [12]. In Okojie's work [14], active control as a solution was proposed. Both temperature sensors and pressure sensors are considered necessary. The presence of these sensors will help the control and the monitoring of the health of the engines of the airplanes. The problem consists in finding suitable sensors that is not always easy for a harsh environment like in a jet engine.

1.2 Jet Engine Environment

The major components of a jet engine are similar across the major different types of jet engines, although not all engine types have all components. The major parts include: Air intake (Inlet), Compressor or Fan, Shaft, Combustor or Flame holders or Combustion Chamber, Turbine, Afterburner or reheat (chiefly UK), and Nozzle. According to their working temperature, Air intake and Compressor belong to cold section of a jet engine; the others after combustor belong to hot section [10].

For a cold section part (like an air intake), the environment temperature is from -60 degrees Celsius to 70 degrees Celsius, therefore some commercial MEMS sensors in the market are suitable for this section. However, for a hot section part (like a combustor), the sensors should be able to work in a harsh environment of:

- High temperature up to 600 degrees Celsius
- Ambient gas composed of chemically reactive species such as oxygen in air, hydrocarbon/hydrogen in fuel, and catalytically poisoning species such as NOx and SOx in combustion products [10].

- Vibration
- Noise

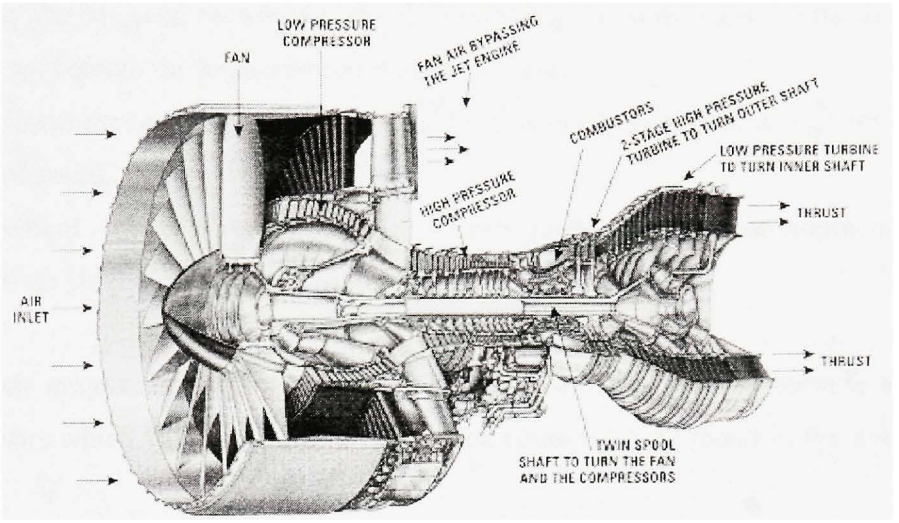

Figure 1.1 Pratt & Whitney PW4084 turbofan.

Cited from www.allstar.fiu.edu/aero/turbine2.html (2008)

Aerospatial industry is one of the most dynamic components of the Quebec economy. CRIAQ (Consortium for Research and Innovation in Aerospace in Quebec) is a non-profit consortium, established with the financial support of Valorisation-Recherche Québec (VRQ), le Fonds Québécois de la Recherche sur la Nature et les Technologies (FQRNT), industries and universities, to promote and perform collaborative pre-competitive industry research projects primarily at universities. CRIAQ's objectives are to increase the competitiveness of the aerospace industry, and enhance the collective knowledge base in aerospace through improved education and training of students [15].

1.3 CRIAQ project 6.2

This research is a part of CRIAQ project 6.2 which is titled MEMS Based Gas Turbines Control. The objectives of CRIAQ project 6.2 are to provide the industrial partners with

MEMS (Micro Electro Mechanical Systems)-based micro sensors that will enhance the performance and safety of gas turbine jet engines. In particular:

- prove the concept of MEMS based control and monitoring systems for gas jet engines through the integration of existent systems;
- develop a pressure sensor to measure the dynamic pressure in a high temperature environment;
- implement temperature sensors for health monitoring or development testing purposes [15].

This thesis emphasizes high temperature pressure sensor packaging because the other type sensors which will be applied in jet engine control can be found in the commercial market.

1.4 High temperature MEMS pressure sensor

The piezoresistive effect describes a change in the electrical resistance of a material due to applied pressure to this material. When a certain pressure applies on a piezoresistive material which is usually thin in order to be able to show big resistance difference, deformation is created and its resistance changes. This is the principle of piezoresistive pressure sensor which is the most popular MEMS pressure sensor.

Because the piezoresistive pressure sensor is highly temperature sensitive, the temperature must be known before the output voltage of the sensor can be converted to a moderately accurate pressure reading. For a typical piezoresistive pressure sensor, the piezoresistive elements (i.e., the diffused resistors) are located on an n-type epitaxial layer of typical thickness 2-10μm. The epitaxial layer is held by a p-type substrate. The pressure sensitive diaphragm is formed by silicon back-end bulk micromachining (see Figure 1.1). For this process, anisotropic etchants like TetraMethylAmmonium Hydroxide (TMAH) and Potassium hydroxide (KOH) are used [16].

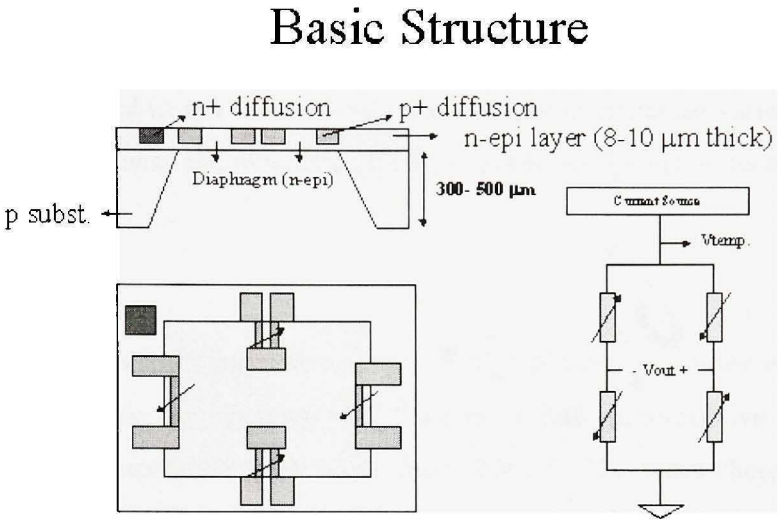

Figure 1.2 Piezoresistive pressure sensors.

Cited from Piezoresistive Pressure and Temperature Sensor Cluster (2007, P. 1)

1.5 RTCA/DO-160

RTCA, Inc. is a private, not-for-profit corporation that develops consensus-based recommendations regarding communications, navigation, surveillance, and air traffic management (CNS/ATM) system issues. DO-160's title is Environmental Conditions and Test Procedures for Airborne Equipment. It includes standard procedures and environmental test criteria for testing airborne equipment for the entire spectrum of aircraft from light general aviation aircraft and helicopters through the "Jumbo Jets" and SST categories of aircraft. The document includes 26 Sections and three Appendices. Examples of tests covered include vibration, power input, radio frequency susceptibility, lightning, and electrostatic discharge. DO-160E is the newest one which superseded DO-160, DO-160A, DO-160B, DO-160C, and DO-160D. DO-160 is recognized by the International Organization for Standardization (ISO) as de facto international standard ISO-7137 since DO-160D [17].

The application of RTCA/DO-160 is strict and expensive to be respected for MEMS sensor systems; it also takes a long time. This is the reason why this standard will not be applied and concerned in this thesis. Some test, such as temperature variation, humidity, vibration, waterproofness and magnetic effects, could be used when units are packaged.

1.6 Summary

A high temperature MEMS pressure sensor is a MEMS pressure sensor which can work in a high temperature environment. SiCN material has piezoresistive property even though operation temperature goes more than 1000 °C (the researchers of Concordia University did some tests). In this research, the sensor should work inside the hot section of a jet engine. Working in such a hostile environment is a big challenge for a MEMS pressure sensor. Both material and packaging could cause problems to conventional semiconductor pressure sensors. In the next chapters, high temperature MEMS pressure sensor packaging will be discussed in depth.

CHAPTER 2

HIGH TEMPERATURE MEMS PACKAGING

2.1 Introduction

In this chapter, different points will be considered. It is desired to know what the problem in the high temperature packaging is and how to choose suitable materials for packaging. Some candidate materials' characteristics for sensor chip and sensor chip dimensions are to be found. The choice of some candidate materials for constraint base and the comparison of some adhesives that could be used for die bonding and sealing at high temperature need also to be determined. The electrical attachment materials and the effect of high temperature on bonded wires are very important for the reliability of the component. Finally, a suitable housing material that could be compatible with the thermal expansion characteristic of the other parts is needed.

2.2 High temperature packaging consideration

The most decisive issues in designing MEMS packages for high temperature and harsh environment are

- thermal stresses caused by the thermal expansion mismatches between various package elements including substrates, dies, adhesives, etc.,
- thermal shock resistance induced by environment temperature changing during MEMS operation,
- heat dissipation to keep the temperature similar inside the package and reduce thermal expansion mismatches.

Material properties can significantly affect how well the package can meet the requirements, in fact they can determine whether the MEMS components fail or work properly. Materials for high temperature and harsh environment MEMS packaging should be selected according to the following criteria.

Thermomechanical compatibility: Thermal expansion differences between the die and the substrate as well as between the different packaging components bring thermal stresses to the MEMS package. Those stresses can break the package or the MEMS. In order to solve this problem, the thermal expansion mismatch between the die, the substrate, and other packaging components should be small enough at all temperatures from requirement. Thermal expansion mismatch may rise with temperature and can make the thermal stress problem worse. For this reason, all the packaging component materials in a package should have similar coefficient of thermal expansion in all temperatures.

Thermal conductivity: Package thermal resistance must be very low in order to dissipate heat and keep the temperature similar inside package. Packaging components such as substrate, metallization, and die attach thermal conductivities must be high enough in all operating temperatures. In this research, MEMS die does not create heat and environment temperature does not change very fast in an engine, therefore not very high thermal conductivity material like SiCN is also considered as packaging material.

Thermal shock resistance: Package components should have high thermal shock resistance (parameter R) to avoid thermal MEMS physical or functional failures caused by thermal stresses during environment temperature changing. The thermal shock parameter (R) is defined by

$$R = \frac{\sigma(1-\nu)}{\alpha E} \qquad (1)$$

where ν is Poisson's ratio, α is coefficient of thermal expansion, σ is strength, and E is elastic modulus (or Young's modulus) [18].

Chemical compatibility: Any packaging component should not react with the die and both packaging components during packaging process. Packaging components should also confront jet engine corrosive gas.

Hermeticity: The package should have atmospheric integrity to keep cavity to measure pressure.

Simplicity, size, and weight: The whole package should be simple enough to be able to be fabricated, small in size, and lightweight for aircraft applications. The die may have the dimensions in the order of micrometers, but whole package dimensions may be up to several centimeters.

Metallization: Metallization should not react with the die and the substrate at assembly and service temperatures. Electro migration of conductors must be prevented or minimized to prevent failures by shorting. The temperature coefficient of resistance should be as small as possible within the intended temperature range [18].

2.3 High temperature sensor chip

Conventional silicon semiconductor MEMS sensors are easily fabricated because silicon techniques are mature in the IC and MEMS industry. Pressure sensors increasingly suffer from instability and failure when the operation is extended to high end of their temperature range. The reasons include degradation of metal/semiconductor electrical contacts and weakening of bond wires due to temperature-driven intermetallic diffusion (for the silicon technique, generally is under 300 degree Celsius). Thus, high temperature MEMS systems need to be constructed from some different materials, including ceramics. Several ceramics' properties such as mechanical robustness, chemical inertness, and electrical stability make them highly suitable for high temperature harsh environment MEMS applications [19]. Silicon carbide (SiC) is the most popular material, but silicon carbide nitride (SiCN) is chosen to be developed at Concordia University for CRIAQ project 6.2.

2.3.1 SiCN

Silicon CarboNitride (SiCN) is a mechanically, chemically and thermally robust polymer derived ceramic material, which has not only, but also possesses functional properties. This property yields SiCN as an excellent choice for sensor applications in high temperatures with harsh chemical conditions.

SiCN is a recent development in the ceramic materials, which boasts outstanding mechanical robustness, excellent oxidation-resistance and semi-conductivity after annealing heat treatment. SiCN ceramics can be fabricated from photo-sensitive liquid precursor mixture using light energy such as laser and UV light to cure into a solid polymer, and then heat treated to transform into SiCN ceramics. This Polymer Derived Ceramic (PDC) fabrication approach with UV light or laser enables fabrication of SiCN that is much like the fabrication of microsystems, using techniques such as UV lithography, micro-molding and stereo-lithography [20]. Figure 2.1, Figure 2.2 and Figure 2.3 show characteristics of three different commercial SiCN materials (NCP200, T2-1 and VT50) [21].

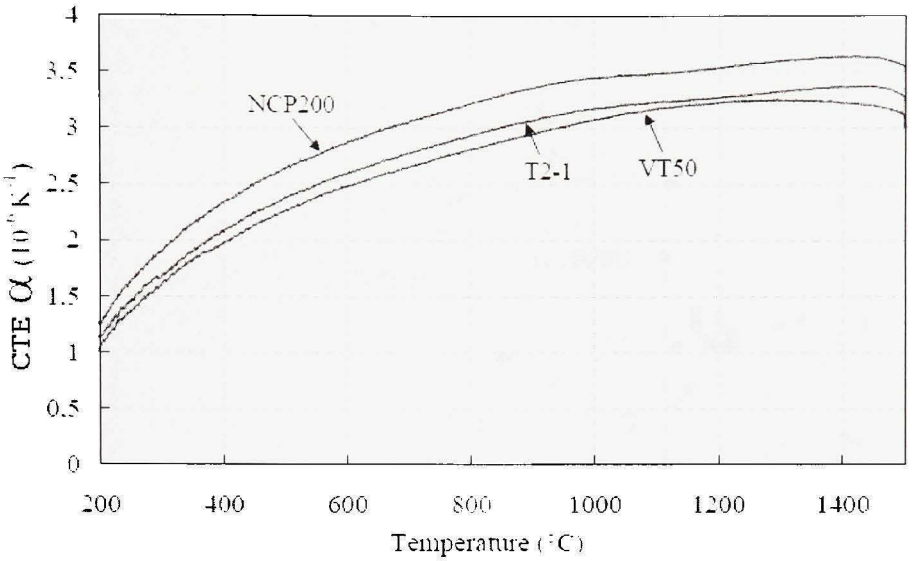

Figure 2.1 Coefficients of thermal expansion (CTE) of 3 commercial SiCN.
Cited from Thermochemistry and Constitution of Precursor-Derived Si-(B-)C-N Ceramics (2002, P.107)

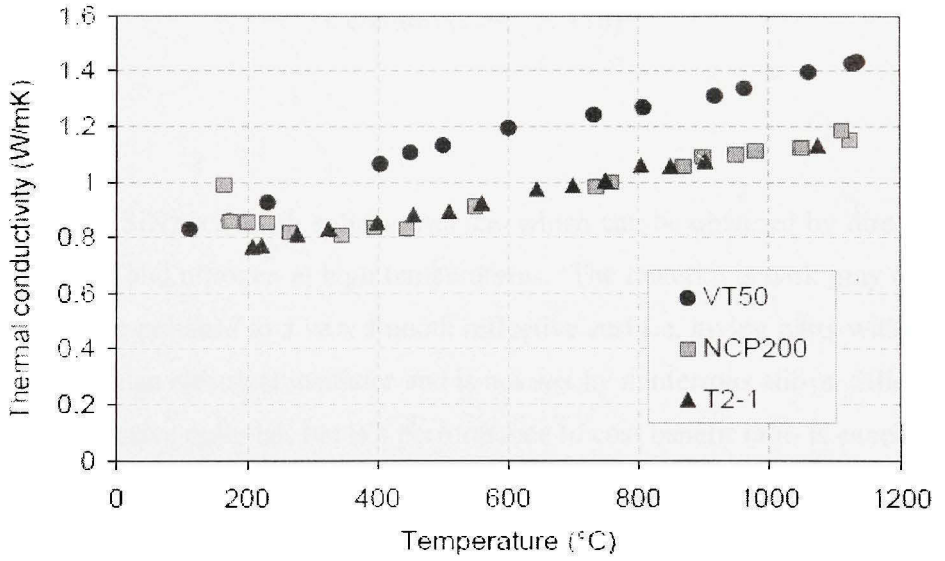

Figure 2.2 Thermal conductivity of 3 commercial SiCN.
Cited from Thermochemistry and Constitution of Precursor-Derived Si-(B-)C-N Ceramics (2002, P. 114)

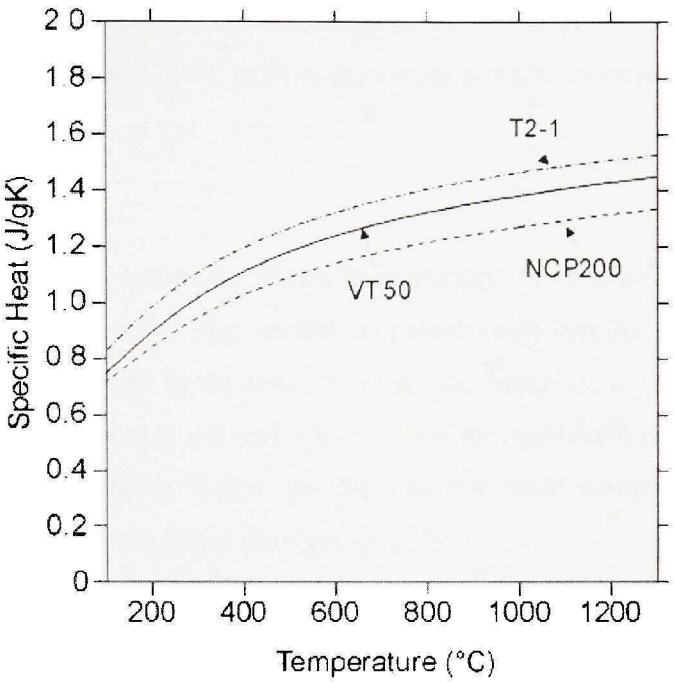

Figure 2.3 Specific heat of 3 commercial SiCN.

Cited from Thermochemistry and Constitution of Precursor-Derived Si-(B-)C-N Ceramics (2002, P. 110)

2.3.2 SiN

Silicon nitride (SiN) is a hard, solid substance, which can be obtained by direct reaction between silicon and nitrogen at high temperatures. 'The material is dark gray to black in color and can be polished to a very smooth reflective surface, giving parts with a striking appearance. It is an electrical insulator and is not wet by nonferrous alloys. Silicon nitride is a rather expensive material, but it's performance to cost benefit ratio is excellent in the applications where it can outperform the normally utilized materials with long life and very reliable low maintenance operation' [22].

In microelectronic technology, silicon nitride is usually formed using chemical vapor deposition (CVD) method, or one of its variants, such as plasma-enhanced chemical

vapor deposition (PECVD). It is usually used either as an insulator layer to electrically isolate different structures or as an etch mask in bulk micromachining.

2.3.3 SiC

'Silicon Carbide is the only chemical compound of carbon and silicon. The material has been developed into a high quality technical grade ceramic with very good mechanical properties. It is used in abrasives, refractories, ceramics, and numerous high-performance applications. The material can also be made an electrical conductor and has applications in resistance heating, flame igniters and electronic components. Structural and wear applications are constantly developing' [23].

'Silicon carbide is composed of tetrahedral of carbon and silicon atoms with strong bonds in the crystal lattice. This produces a very hard and strong material. Silicon carbide is not attacked by any acids or alkalis or molten salts up to 800°C. In air, SiC forms a protective silicon oxide coating at 1200°C and is able to be used up to 1600°C. The high thermal conductivity coupled with low thermal expansion and high strength gives this material exceptional thermal shock resistant qualities. Silicon carbide ceramics with little or no grain boundary impurities maintain their strength to very high temperatures, approaching 1600°C with no strength loss. Chemical purity, resistance to chemical attack at temperature, and strength retention at high temperatures has made this material very popular as wafer tray supports and paddles in semiconductor furnaces' [23].

Silicon carbide (SiC) is an attractive material for high-temperature applications because of its mechanical robustness, chemical inertness, and electrical stability at elevated temperatures. It has better high temperature characteristics than silicon and GaAs material (see Table 2.1)[24]. Table 2.1 is presented in 1993, some data have been changed such as silicon material maximum work temperature is more than 300°C and SiC material can work up to 600°C. Figure 2.4 shows some SiC properties.

Table 2.1

Comparison of semiconductor materials

(Cited from Advances in silicon carbide device processing and substrate fabrication for high power microwave and high temperature electronics, 1993)

Property	Silicon	GaAs	SiC	Units
Band gap	1.1	1.4	2.9	eV
Max. Temp.	150	200	500	°C
Thermal Conductivity (α)	1.5	0.5	5	W/cm°C
Breakdown Field (E_b)	0.3	0.3	3	10^6v/ctn
Elect. Mob. @ 10^{17}cm-3(μ)	800	4800	260	cm^2/V sec
Saturated Elec. Vel. (V_{Sat})	1.0	0.6	2.5	10^7cm/sec
Dielectric Constant	11.8	12 8	9.7	
Figure of Merit	1	7.8	152	

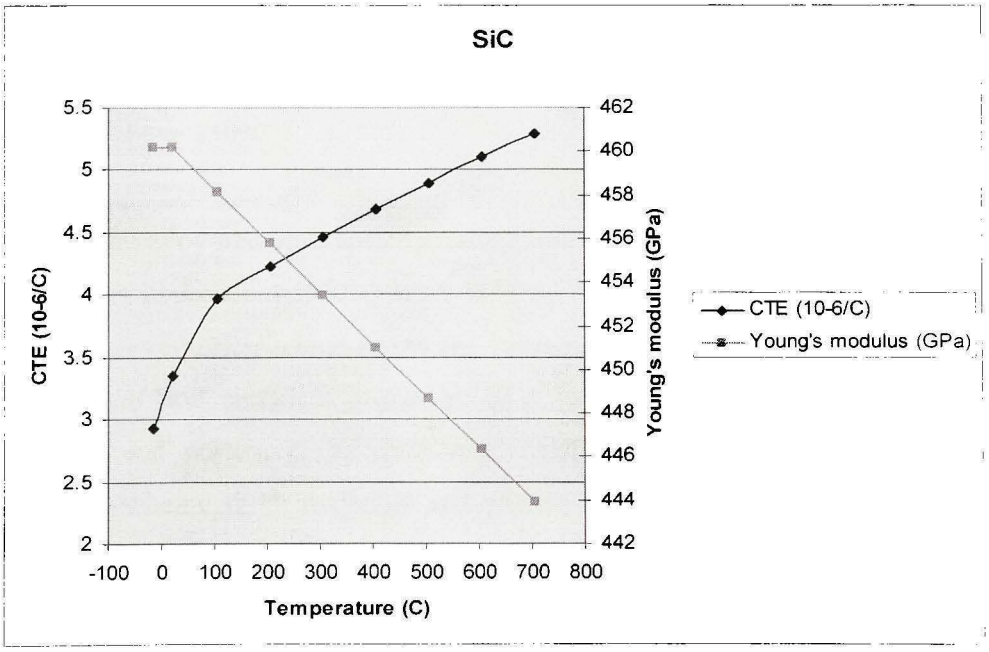

Figure 2.4 SiC material properties with temperature.

Recent pressure sensor researches concentrate on silicon carbide material. Some SiC high-temperature pressure sensors have been proposed, designed and implemented to work in the 600°C environment, such as piezoresistive pressure sensors [25] and capacitive pressure sensors [26].

2.3.4 Shape and size of sensor chips

Commercial piezoresistive pressure sensor chips are usually cuboid, but cylinder is possible and the size of a sensor chip usually varies from 2mm and more in length to 0.1mm in the diameter. The strain gauge determinates the minimum size of a chip.

2.4 Constraint base (packaging substrate)

The basic function of the packaging substrate is to provide a framework for attaching the device die, metallization for electrical interconnection (such as wirebond), mounting the leads connecting the chip to the external environment, building nonelectrical signal paths, mechanical and possibly also electromagnetic shielding. Plastic/polymer-type materials are not suitable for 500°C operation because of melting and depolymerization at temperatures above 350°C.

Most metal and alloy materials suffer severely from corrosion, especially, from oxidation at temperatures approaching 500°C in air [27]. So the remaining material system suitable for substrate is ceramics, which meets the basic requirements for a substrate: excellent stable chemical and electrical properties in a harsh environment, especially at high temperatures and corrosive gas ambience. After selecting the substrate material, a metallization scheme (both materials and processing) and associated sealing materials matching the substrate material must be identified or developed simultaneously. In order to reduce the thermal stress of the die-attach, the CTE of the substrate material must match that of the device material (such as SiC). The properties of substrate surface and the interfaces formed at high temperature with other packaging materials, such as the die-

attach material, also become very important. At high temperatures, the surfaces of some ceramics (nitrides and carbides) gradually react with gas ambience, such as oxygen and water vapor, and therefore would lead to changes in properties such as surface resistivity and surface adhesiveness. Concerns such as these regarding the surface properties of "well-known" ceramic materials in high-temperature corrosive gas ambience may lead to valuable results from research into packaging materials for high-temperature MEMS [27].

SiC and SiCN materials also could be constraint base material, but they are described in the section earlier, so they are not mentioned in this section.

2.4.1 AlN

'Aluminum nitride (AlN) is stable at very high temperatures in inert atmospheres. In air, AlN surface oxidation occurs above 700°C, and even at room temperature, surface oxide layers of 5-10 nm have been detected. Above this temperature bulk oxidation occurs. Aluminum nitride is stable in hydrogen and carbon dioxide atmospheres up to 980°C. The material dissolves slowly in mineral acids through grain boundary attack, and in strong alkalis through attack on the aluminum nitride grains. The material hydrolyzes slowly in water. Aluminum nitride is resistant to attack from most molten salts including chlorides and cryolite' [28].

Metallization methods are available to allow AlN to be used in electronics applications similar to those of alumina and BeO.

A survey of current packaging materials, suggest that aluminum nitride (AlN) is an ideal candidate for packaging [29]. Figure 2.5 shows AlN CTE property.

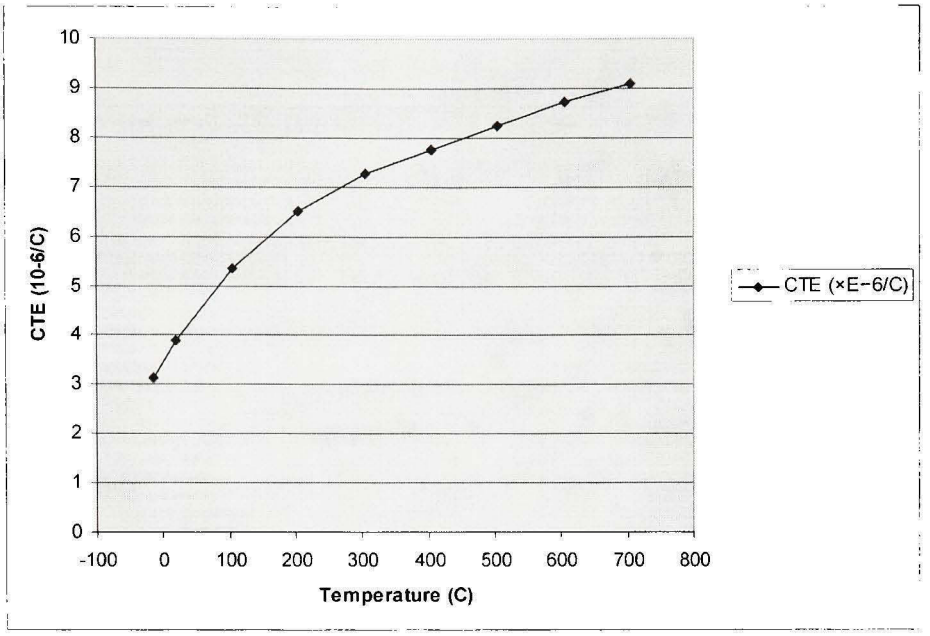

Figure 2.5 AIN material CTE properties.

2.4.2 Alumina

Aluminum oxide is an amphoteric oxide of aluminum with the chemical formula Al_2O_3. It is also commonly referred to as alumina in the mining, ceramic and materials science communities.

Aluminum oxide is an electrical insulator but has a relatively high thermal conductivity. In its most commonly occurring in crystalline form, called corundum or α-aluminum oxide, its hardness makes it suitable for use as an abrasive and as a component in cutting tools.

'Alpha phase alumina is the strongest and stiffest of the oxide ceramics. Its high hardness, excellent dielectric properties, refractoriness and good thermal properties make it the material of choice for a wide range of applications.

High purity alumina is usable in both oxidizing and reducing atmospheres to 1925°C. It resists attack by all gases except wet fluorine and is resistant to all common reagents except hydrofluoric acid and phosphoric acid. Elevated temperature attack occurs in the presence of alkali metal vapors particularly at lower purity levels.

The composition of the ceramic body can be changed to enhance particular desirable material characteristics. An example would be additions of chrome oxide or manganese oxide to improve hardness and change color. Other additions can be made to improve the ease and consistency of metal films fired to the ceramic for subsequent brazed and soldered assembly' [30].

Figure 2.6 shows 96% alumina properties.

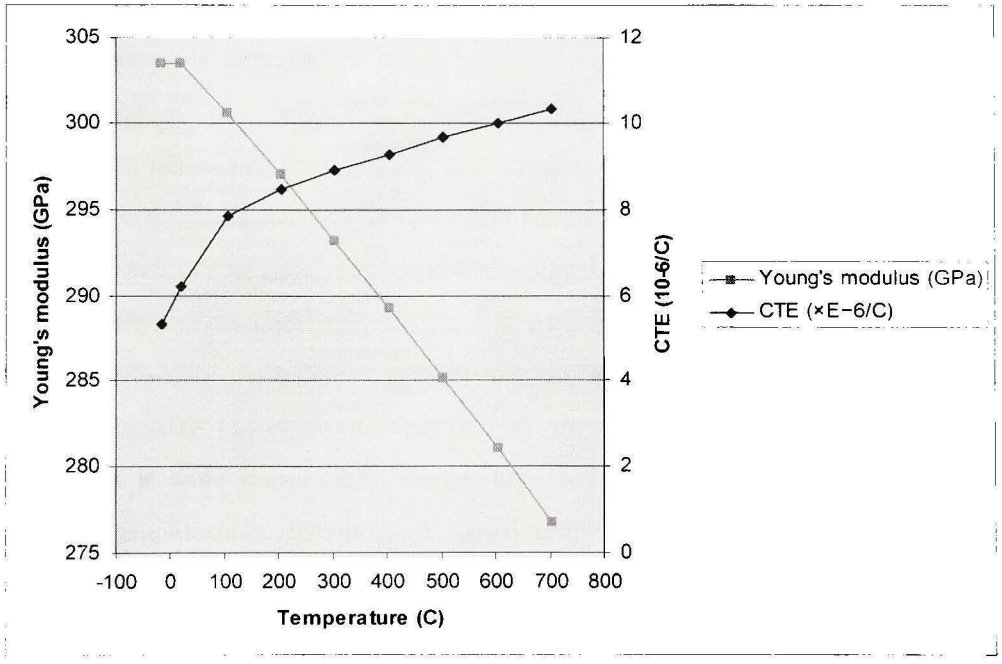

Figure 2.6 96% alumina properties.

2.5 Die bonding and sealing

'An ideal die-attaching material suitable for use in a wide temperature range is a need for innovative materials to package harsh-environment MEMS devices. In addition to the superior chemical and electrical stabilities at high temperatures and in a corrosive environment, the die-attaching materials must possess good thermal and electrical conductivity, unique features of metallic material; meanwhile, the CTE of such a material should match those of the die and the ceramic substrate. Ideally, if the CTE of the substrate slightly mismatches that of the die, the die-attach material should be able to compensate the CTE mismatch between the die and the substrate. A material with low Young's modulus and narrow elastic region certainly would help to absorb thermal strain, thus reducing the stresses in the die and the substrate. However, this would reduce the lifetime of the die-attach material part in a dynamic thermal environment because of the accumulated permanent strain.

The basic purpose of hermetic sealing is to create and maintain a stable and sometimes inert ambience for the packaged device. This simple function at low (room) temperature is difficult to achieve at temperatures approaching 600 degrees Celsius because, first, at such high temperatures most soft or flexible sealing materials such as plastic/polymer-based materials can no longer operate; second, sealing very often applies between different materials. The CTE mismatches of these materials make hermetic sealing difficult over a wide temperature range, especially under thermal cycling condition. Third, high temperatures activate and significantly promote thermal processes such as diffusion and degassing at material surfaces, thus it becomes difficult to maintain an ambience in a small enclosure by sealing. Therefore, it is expected that creative sealing concepts are necessary to meet the requirements for packaging many high temperature MEMS devices' [7].

Adhesive is key material for the die bonding and sealing. High temperature Epoxy has a 315°C (600°F) limit and its strength reduces while environment temperature increases.

Pyrex (Borosilicate glass) has a thermal expansion coefficient about one-third that of ordinary glass. This reduces material stresses caused by temperature gradients, thus making it more resistant to breaking. Pyrex begins to soften at 821 °C (1510 °F); at this temperature, the viscosity of Pyrex® Brand 7740 Pyrex is 10.76 Pa·s (107.6 poise). Pyrex is less dense than ordinary glass.

Adhesive materials used in an aircraft need to withstand low (−55°C), as well as high (600°C) temperatures. However, there are few adhesives suitable for the whole temperature range. 'A solution would be a material with a combination of a low-temperature adhesive and a high-temperature adhesive, called a mixed-adhesive joint. In a bonded joint, the thermal stresses are generated essentially by the different thermal expansion properties of the adhesive and the adherents and, to a lesser extent, by the shrinkage of the adhesive produced by curing. The case of a mixed-adhesive joint is more complicated because there are two adhesives with different glass transition temperatures (Tg). To determine the stress-free temperature in a mixed adhesive joint, sandwich specimen of aluminum-adhesive-CFRP (Carbon-Fibre-Reinforced Plastic) were fabricated and the thermal strains were measured with strain gauges. In a mixed adhesive joint, two stress-free temperatures were found: the stress-free temperature of the high temperature adhesive, which is its cure temperature, and the stress-free temperature of the low temperature adhesive, which is its transition temperature' [31]. The only problem is that glass material cure temperature is too high, which may destroy the sensor chip or package during die bonding and sealing process.

Aluminum compound material adhesive also shows high temperature ability. An example of aluminum compound is Durabond 950 from Cotronics Corporation [32]. Durabond 950 Adhesive is specially formulated to bond metals, ceramics and dissimilar materials for use to 731°C (1200°F). Epoxy adhesives are limited to 315°C (600°F), lose strength at elevated temperatures and will start to thermally decompose. Silicone based materials are designed for sealing applications and not suited for structural bonds at high

temperatures. Durabond is a metallic ceramic composite and can not soften or decompose at temperatures up to 731°C (1200°F). Durabond adhesive contains no Epoxies or Silicones which would limit their use to 315°C (600°F).

This adhesive was developed for high strength, high temperature bonding. It is easy to apply and cures at low temperature. This metallic composite adhesive offers some of the ductility and impact resistance associated with soldering and welding. Durabond adhesive can be drilled, tapped, machined, etc. It is easily machinable and can be ground, sanded or polished, so it might be used to wafer-to-wafer bonding.

2.6 Wire bonding

Harsh-environment MEMS packaging offers new challenges to the device packaging field. Discussions on the basic requirements of properties of the materials necessary for packaging harsh-environment MEMS are followed to an electrical interconnection system that is based on a ceramic substrate and thick-film metallization, with a compatible conductive die-attach scheme for chip-level packaging of low-power, harsh-environment MEMS devices [7].

2.6.1 Electrical attachment materials

2.6.1.1 Nickel (Ni)

Nickel is a silvery white metal that takes on a high polish. It belongs to the transition metals, and is hard and ductile. It occurs most usually in combination with sulfur and iron in pentlandite, with sulfur in millerite, with arsenic in the mineral nickeline, and with arsenic and sulfur in nickel glance. Melting point of nickel is 1455 degrees Celsius [33].

2.6.1.2 Gold (Au)

Gold is a good conductor of heat and electricity, and is not affected by air and most reagents. Heat, moisture, oxygen, and most corrosive agents have very little chemical effect on gold, making it well-suited for use in coins and jewelry; conversely, halogens will chemically alter gold, and aqua regia dissolves it via formation of the chlorаurate ion [33]. Some properties of gold [7] are given in Figure 2.7.

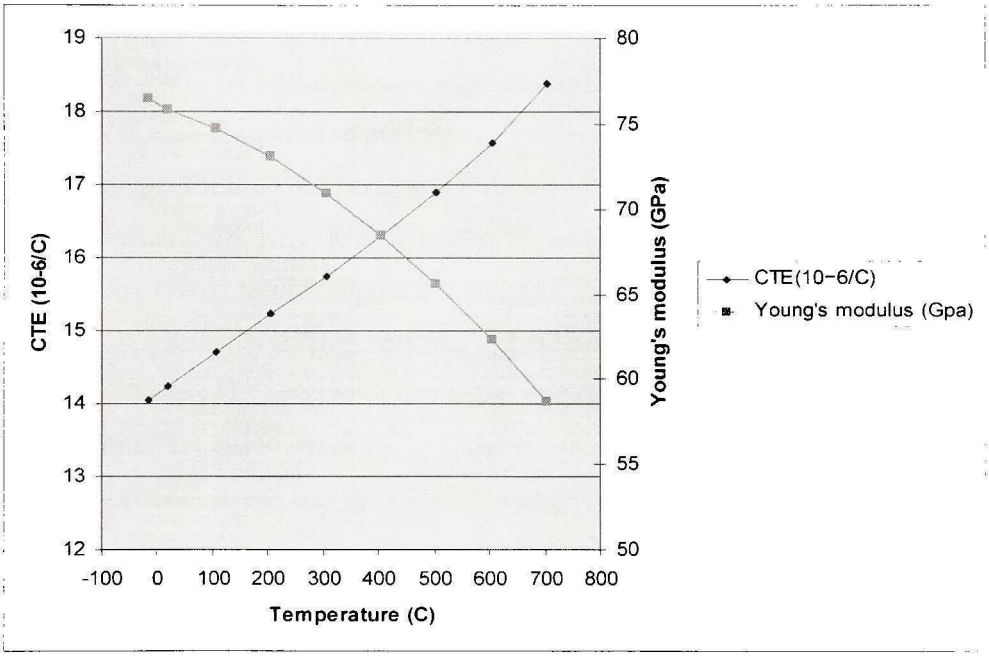

Figure 2.7 Au material properties.

2.6.1.3 Platinum (Pt)

Platinum is a chemical element in the periodic table that has the atomic symbol Pt and an atomic number of 78. A heavy, malleable, ductile, precious, grey-white transition metal, platinum is resistant to corrosion and occurs in some nickel and copper ores along with some native deposits. Platinum is used in jewellery, laboratory equipment; electrical contacts, dentistry, and automobile emissions control devices.

Platinum possesses high resistance to chemical attack, excellent high-temperature characteristics, and stable electrical properties. All these properties have been exploited for industrial applications. Platinum does not oxidize in air at any temperature, but can be corroded by cyanides, halogens, sulfur, and caustic alkalis. This metal is insoluble in hydrochloric and nitric acid, but does dissolve in the mixture known as aqua regia (forming chloroplatinic acid). Common oxidation states of platinum include +2, and +4. The +1 and +3 oxidation states are less common, and are often stabilized by metal bonding in bimetallic (or polymetallic) species [34].

Although over 80% of packages are wire bonded, wire bonding technique has some problem for the high temperature packaging. An investigation of aluminum and gold wire bonding processes for high temperature electronics indicates ultrasonic wire bonding of 8 and 15 mil aluminum wire and 3 mil gold wire on various metallized substrates. Aluminum wire bonds to nickel-plated aluminum nitride (AlN) and silicon nitride (SiN) substrates were thermally cycled between -55 °C and 400 °C, and gold wires bonded to gold-coated AlN and SiN substrates were thermally cycled between -55 °C and 500 °C. In Mustain's work [35], the thermal cycling was accomplished according to MIL-STD-883E criteria. An environmental scanning electron microscope (ESEM) was used to examine the wire/pad and pad/substrate interface areas before and after the thermal cycling. After thermal cycling [35], the samples were subjected to destructive pull testing at room temperature. The results of the testing revealed no significant degradation of the bonds after thermal cycling. The results of Al wire bonding and Au wire bonding for high temperature packaging are introduced as followings.

2.6.2 Aluminum wire bonding -55 to 400 °C

Figure 2.8 shows nickel metallization on standard DBC (AlN) and SiN substrates with aluminum wire bonds at elevated temperatures. 8 and 15 mil Al wires were bonded to Ni-coated bonding pads using conventional ultrasonic wire bonding.

'SEM and EDX analyses show some surface contamination at the wire/pad areas after thermal cycling. Following thermal cycling between –55°C and 400 °C, the nickel-plated layer containing nickel phosphide breaks down into nickel and phosphorous. The phosphorous then appears on the surface as contamination. Destructive pull test results show that the pull strength of the aluminum wire bonds exceeded MIL standard pull strengths. SEM and EDX analyses of the substrate region beneath the bond revealed no cratering problems with the nickel-plated AlN substrates. However, for the nickel-plated SiN substrates, cratering was observed' [35].

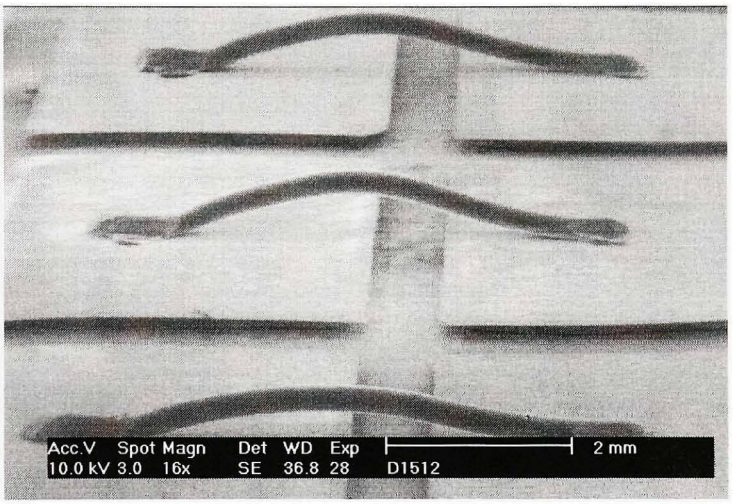

Figure 2.8 15 mil Al wires ultrasonically bonded to a Ni plated bond pad.
Cited from IEEE Electronic Components and Technology Conference (2005, P. 1625)

2.6.3 Gold wire bonding -55 to 500 °C

Three mil gold wires were bonded to Au pads on gold plated AlN and SiN substrates using conventional thermosonic wire bonding. SEM and EDX analyses were performed before and after thermal cycling test. There was no significant difference between the EDX spectra before and after thermal test [35].

SEM and EDX of the substrate region beneath the bonds did not reveal any cratering problems with gold-plated AlN and SiN substrates. Figure 2.9 shows a 3mil gold wire bonging on an Au plated AlN substrate.

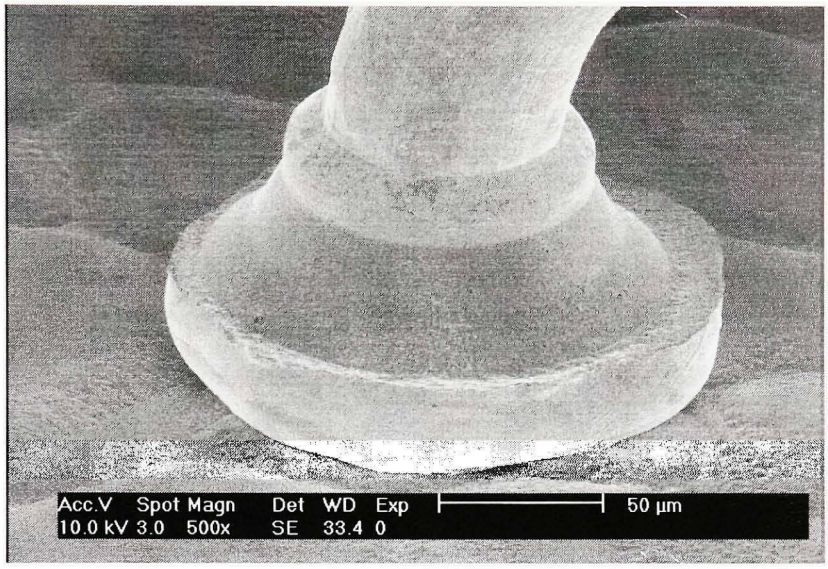

Figure 2.9 3mil gold wire bonding on Au plated AlN substrate.
Cited from IEEE Electronic Components and Technology Conference (2005, P. 1627)

2.6.4 Platinum wire bonding

Obviously, platinum wire has better high temperature stability than gold, but only few platinum wires bonding has done in the laboratory. As an example, an application of parallel-gap welding for bonding 5-mil annealed Pt wire to a 5000 A-Pt pad (with an underlying base of Ti, MO, and W) sputter deposited on a sapphire substrate has been systematically examined by Fendrock. 'Optimum bonding parameters- force, voltage, duration, gap, and electrode width-have been developed for Cu-Cr and MO-Carbide electrodes which attain bond pull strengths approaching the tensile strength of the Pt wire without sapphire substrate microcracking. The MO-Carbide electrodes produced stronger

bonds with less oxidation and pitting, and exhibited less electrode-wire adhesion than the Cu-Cr electrodes' [36].

2.7 Housing

Materials useful for packaging electronic components usually exhibit certain properties. For example, the packaging material should provide dissipation of static electricity and shielding from static discharges and electric fields that may be generated, e.g., when the electronic component moves inside the package or when the packaging material is rubbed against other materials. The packaging material should protect itself from outer environment physical damage and make itself be installed easily. The packaging material should also function as a barrier against moisture vapor and oxygen to protect the electronic component from degradation while it is being stored. Housing is a way of packaging electronic components.

In high temperature packaging application, housing cover materials are usually metals, alloys and ceramics. As an example, Kovar is a nickel-cobalt ferrous alloy. It is designed to be compatible with the thermal expansion characteristic of sealing to borosilicate glass. Its composition is typically 29% nickel, 17% cobalt, 0.2% silicon, 0.3% manganese, and 53.5% iron (by weight) [37]. Melting point of Kovar is 1450 degrees Celsius.

2.8 Signal cable

Dacon Systems Inc. produces some high temperature signal cables which could be used as connection between sensor packages and an aircraft control system. The wires of these cables use nickel or nickel alloys as conductor, and insulated by mica type or fiberglass. These cables can work up to 1200 degrees Celsius [38].

2.9 Summary

In this chapter, the particularity of high temperature MEMS sensor packaging is discussed. High thermal conductivity, thermomechanical compatibility, high thermal shock resistance, high strength and high chemical compatibility are requested for high temperature applications. Some suitable materials are introduced. Sensor chip for high temperature application are usually fabricated by SiC, SiCN and SiN. In this study, AlN, Alumina and SiCN are chosen to make packaging substrate. Epoxy is not a suitable die attach material for high temperature applications. Cotronics has some ceramic-based adhesives which can bond metals and ceramics. Wire bonding and electrical attachment are also discussed. Aluminum wire can not pass destructive pull test after thermal cycling between –55°C and 400°C. Gold wire is much better than aluminum wire and there is no significant difference between before and after thermal cycling between –55°C and 500°C. Platinum wire has better high temperature stability than gold. But Platinum wire bonding which can satisfy 600°C engine environment applications is rarely used in the industry. Kovar alloy has similar thermal expansion characteristic than other high temperature packaging materials. So it becomes more suitable housing material than stainless steel.

CHAPTER 3

HIGH TEMPERATURE PRESSURE SENSOR PACKAGING SOLUTIONS

3.1 Introduction

In this chapter, different points will be considered, such as: packaging strategy (to know exactly what type of design and simulation will be performed), metallization (to choose a technique to prepare metal pad), substrate (to prepare the substrate before attaching the chip), die bonding and sealing (to choose an adhesive to bond die and substrate, seal the cavity inside), wire bonding (to decide what kind of wire will be used) and flip chip (to choose a material to connect die and substrate).

All the packaging solutions in this chapter will be presented by two designed prototypes. Sensor chip should be completed before packaging. SiC material sensor chip fabrication is like Si material, and SiCN material chip has different process [39].

3.2 Designed prototype 1 (conventional package prototype)

This method derivates from most MEMS pressure sensor package (that is why it is called conventional package method). The idea for this method is to select proper materials to package. The designed prototype consisted of a pressure sensor die mounted on a substrate (i.e. constraint base). The die could be SiC or SiCN and it attaches to a ceramic substrate (it could be AlN, Al_2O_3 or SiCN) by using adhesives (Al_2O_3). A schematic model of this prototype is shown in Figure 3.1.

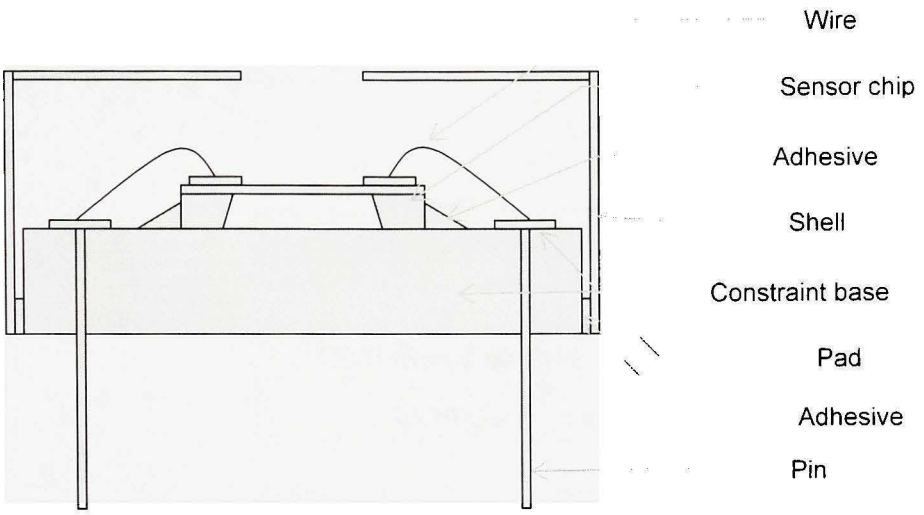

Figure 3.1 Side view of prototype 1 (conventional package prototype).

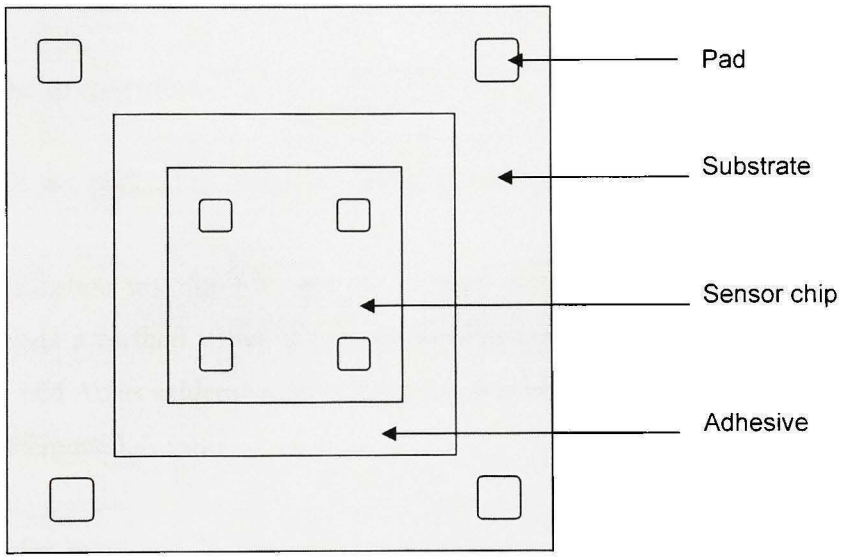

Figure 3.2 Top view of prototype 1 (conventional package prototype).

A schematic diagram of the prototype 1 fabrication processes is shown in Figure 3.3.

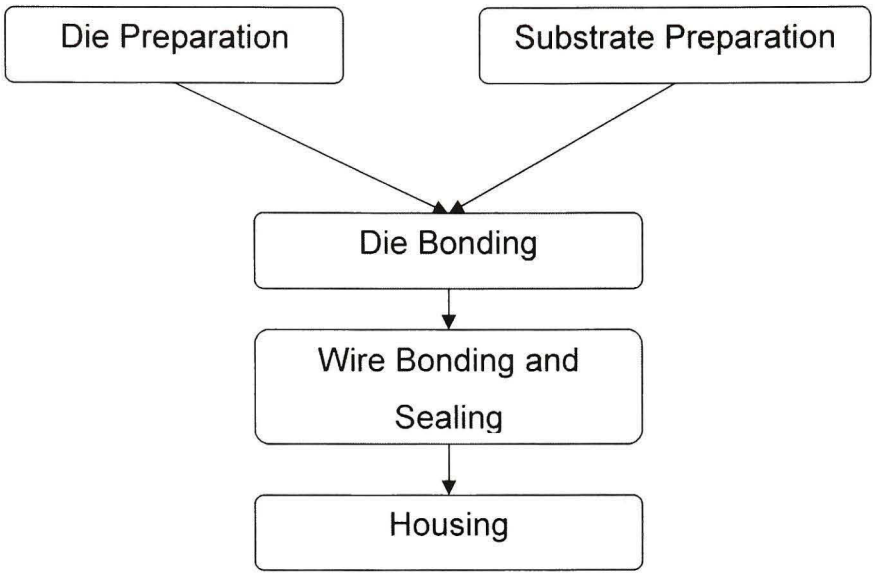

Figure 3.3 Prototype 1 fabrication flow chart.

3.2.1 Die preparation

Before all the packaging processes, metallization of a die should be done with 3 layers structure.

Cu metallization test for SiC and SiCN were done at up to 275°C [40]. This thesis recommends a method which adopts Ti as adhesion layer material, Pt as isolation layer material, and Au as solderable layer material. A schematic diagram of the metallization is shown in Figure 3.4.

After wafer mounting in the set-up, wafer dicing and wafer cleaning, the die of this prototype is 2.4 mm X 2.4 mm X 0.5 mm in size with a hollow coboid area of 1.8 mm X 1.8 mm and 0.48 mm height under the membrane. The membrane is 20 μm in thickness. Because the real die for this project (which is not available for now) probably may be down to 0.2 -0.3 mm, some smaller models have also been simulated in chapter 5.

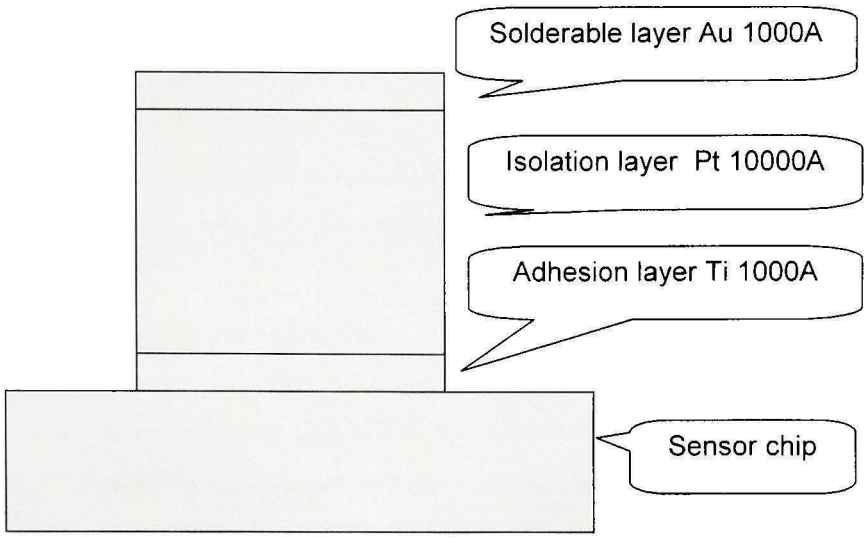

Figure 3.4 Side view of metallization sketch.

3.2.1.1 SiC Metallization

Ti/Pt/Au system metallization is mature in the industry [41]. In 1990, Drost's work presented a Ti/Pt/Au system by using electroplating and photolithographic process.

The stability of metal layers on semiconductors is a key issue for the device electrical performances. A SiC/Ti/Pt/Au system was investigated using storage steady-stress testing, AES (Auger Electron Spectrometry), and SIMS (Secondary Ions Mass Spectrometry) analysis by Sozza [42]. Auger and SIMS analysis showed important modifications in the three-metal structure without reactions with the SiC substrate. The resistance degradation was assigned to interdiffusion phenomena [42].

'Sozza's work underlines the important modifications in the tri-metal structure Ti–Pt–Au deposited on SiC during high-temperature long-term annealing. The resistance changes of the structure were studied using steady state life curves and the calculation gives activation energy of nearly 1.1 eV. A MTF (Mean Time to Failure) value of 0.45 × 105 h at 150 °C was obtained for 10% resistance increase' [42].

Therefore the tri-level metallization is suitable candidate for interconnection directly deposited on SiC for operation at temperatures around 150 °C. The rise of resistivity at higher temperature could become more severe. SiC/Ti/Pt/Au has a stable behaviour in terms of electrical characteristics as reported by Kassamakova [43, 44], but presents low MTF predictions for the resistivity evolution at high-channel temperatures.

3.2.2 Substrate preparation

In chapter 2.2, AlN, Alumina and SiCN are shown as suitable substrate materials. Substrate (i.e. constraint base) processes for ceramic material are casting, potting and mechanical machining. Once it is finished, its connected pins have been already plated in it. Some commercial ceramic materials which could be used in high temperature MEMS application are shown as followings.

3.2.2.1 SiCN

In Liew's work, a cost-effective technology for the fabrication of high-temperature MEMS based on injectable polymer-derived ceramics is described [45, 46]. First, a mold is fabricated using standard photolithographic techniques (Figure 3.5 a and b). The liquid polymer precursor is then cast into the mold, and the mold and polymer precursor are then heated or thermal-set at about 250°C to solidify the polymer (Figure 3.5 c and d). After thermal-setting, the polymer becomes a transparent solid, and may be separated from the mold if suitable techniques are used. After thermal-setting, the polymer part is crosslinked by heating to about 400°C under isostatic pressure (Figure 3.5 e). After crosslinking, the polymer becomes infusible, remaining transparent. In the final stage (pyrolysis), the crosslinked polymer part is heat-treated at about 1000°C to convert it to a monolithic ceramic part.

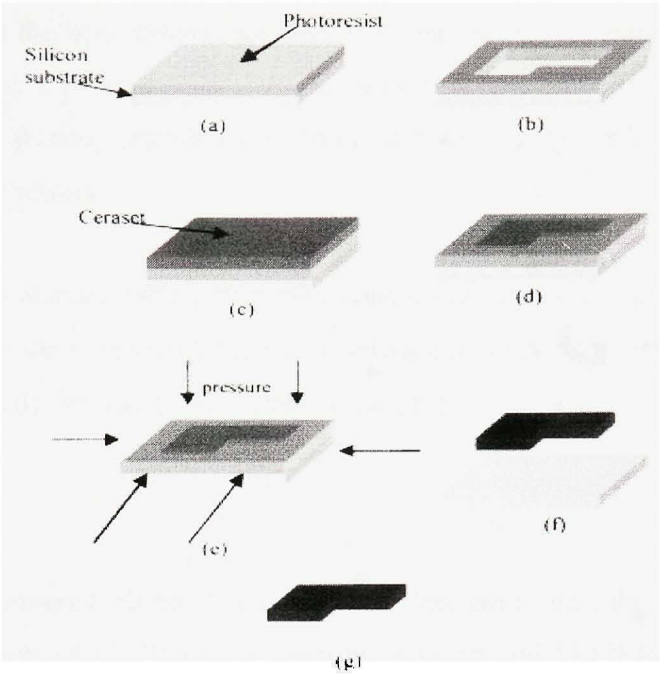

Figure 3.5 SiCN injectable polymer-derived ceramics process.
Cited from Sensors and Actuators (2001, P. 66)

3.2.2.2 Alumina potting compounds and casting compounds

COTRONICS CORP. has some interesting alumina compounds for high temperature purpose. They could be used as packaging substrates.

Durapot™ 801 is a specially formulated, room temperature curing, 99% pure Alumina Ceramic. It offers high electrical resistance, even at high temperatures and is ideal for many electrical and metallurgical applications.

Durapot™ 804 and 805 were formulated to provide a high strength, low cost, Alumina potting and casting material where the purity of type 801 is not required. Their electrical and metallurgical properties are excellent. Durapot™ 804 is ideal for small parts and Durapot™ 805 for larger castings.

Durapot™ 809 is the best, general purpose, ceramic potting compound which based on Magnesium Oxide. It is electrically resistant and offers excellent chemical resistance and it can be used for potting, sealing and bonding. It is also easily used, just mix, apply and cure at room temperature.

Durapot™ 810 is alumina based, thermally conductive potting compound and adhesive, developed to provide excellent electrical resistance at high temperature and improved thermal conductivity for high power applications [47].

3.2.2.3 AlN

A translucent aluminum nitride (AlN) substrate has come into the market which has thermal conductivity of 140 W/mK at room temperature and 130 W/mK at 100°C, eight times that of alumina (Al_2O_3) and one-half to two-thirds that of beryllia (BeO). Its excellent electrical and mechanical properties as well as inherent light transmitting property ensure that the new AlN material can be used as high-performance ceramic substrates for high temperature semiconductor modules. 'Metallization of the ceramic has been done by three methods: tungsten metallization by a co-firing process, which is a fundamental technology for the coming multilayer AlN packages; metallization with silver-palladium (Ag/Pd) conductor and ruthenium-oxide (RuO_2) resistor, which was developed for the translucent AlN substrate; molten metal metallization, which gives very high adhesive strength. Development of an improved AlN ceramic with a thermal conductivity exceeding that of BeO is also described' [48].'

Typical data of its chemical composition are shown in Table 3.1. Sintering is a method for making objects by heating powder without melting. The high-purity submicron AlN powder with a sharp particle size distribution has excellent sinterability. Figure 3.6 shows a typical sintering behavior of the powder. As a sintering aid, $Ca(NO_3)_2$ estimated as 1.0 wt% CaO was added to AlN powder. It shows that fully dense translucent AlN ceramics can be made not only by hot-pressing but by pressureless sintering. For the commercial

production of the translucent AlN substrates trade named SHAPAL, tape casting with a doctor blade and uniaxial dry pressing has been chosen.

Table 3.1

Elemental analysis of AlN powder

Element	Content (ppm)	Element	Content (wt%)
Fe	15	C	0.05
Ca	72	O	1.0
Si	37	N	33.5
		Al	65.3

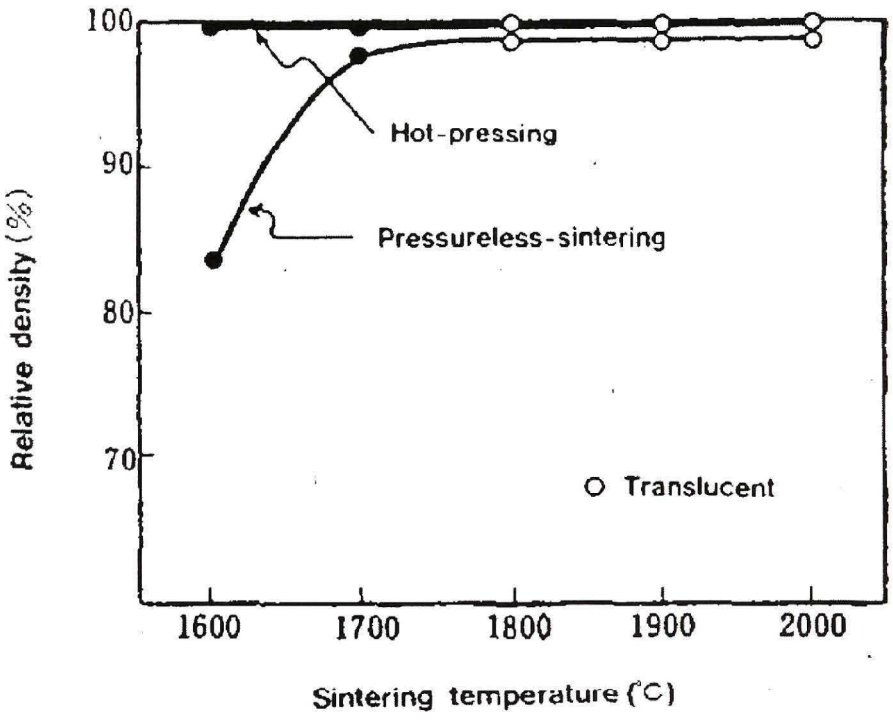

Figure 3.6 Sinterability of AlN powder with sintering aid.

Cited from IEEE Transaction on Components, Packaging, and Manufacturing Technology (1986, VOL. 9, NO. 4 p. 386)

The bonding mechanism between aluminum nitride substrate and silver-copper-titanium solder was studied [49] by Kurihara. 'The AlN surface was bonded to the solder with the TiN intermediate layer containing free Ti and Al, produced at the interface between the AlN substrate and the solder.'

A metallization structure of Ti-Pt-thick Au-Ti-Cr-Au was designed and implemented, and the metallurgical stability of this metallization scheme was reported by Liu [50]. It was found that, without a diffusion barrier, the thick Au layer in the epitaxial-side metallization would be mostly consumed and form intermetallics with the Sn from the AuSn solder during soldering and thermal aging. The Ti-Pt-thick Au-Ti-Cr-Au metallization scheme prevents the diffusion of Sn into the thick Au layer and preserves the integrity of the metallization system [50].

Pads in the substrate of this prototype which use the same structure than the die corresponding to the substrate (see 3.2.1) are made by using metallization process.
The substrate is cuboid and was assumed to be 5.6 mm X 5.6 mm X 1 mm in size.
A schematic model of the substrate (i.e. constraint base) is shown in Figure 3.7.

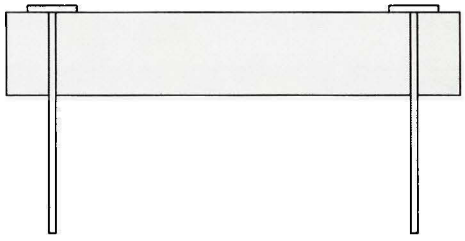

Figure 3.7 Prototype 1 constraint base preparation (side view).

3.2.3 Die attach and sealing

Although there are a number of techniques which can bond die with substrate base, but most of them are for silicon only e.g. silicon fusion and anodic bonding. Adhesives are common to be used for non silicon dies. Polymer adhesives cannot suffer 600 degrees

Celsius high temperature and eutectic die attach need a high temperature process which could damage sensor chip. Cotronics Corporation has some high temperature adhesives which can be cured at room temperature or low temperature [51]. The adhesives for die attach in this prototype are a kind of aluminum compound (alumina) or metal-base adhesives such as Resbond™ 940HT, Resbond™ 919, Resbond™ 920 and Durabond 950. A schematic model of this die bonding process is shown in Figure 3.8.

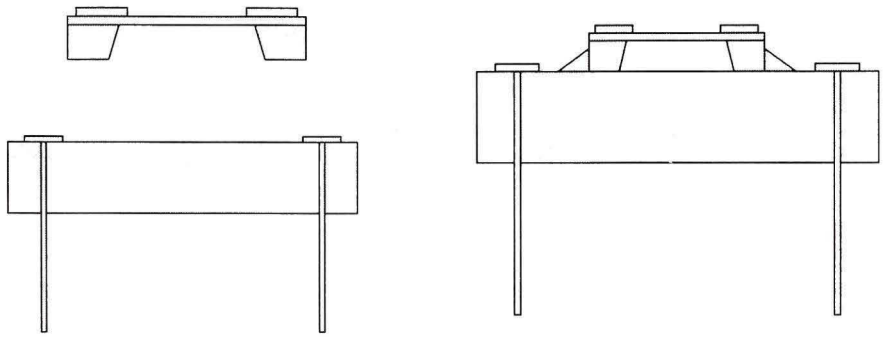

Figure 3.8 Prototype 1 die bonding (side view).

Resbond 940HT Adhesive is a new, fast setting, ultra high temperature alumina adhesive that can be used continuously to 1538°C (2800°F). Resbond 940HT has excellent adhesion to ceramics, metals, glass, composites, etc. It can be resistant to liquid metals, most chemicals and solvents, oxidizing and reducing atmospheres and has good electrical properties. Resbond 940HT sets in 15 minutes and cures in 5 minutes at 80°C (175°F) or in 8-16 hours at room temperature.

Resbond™ 919 has exceptionally high electrical resistance. Dielectric strength is 270 volts/mil and volume resistivity is 1011 ohm-cm (at room temperature). It can maintain its high electrical resistance and dielectric strength at high temperature 1538°C (2800°F). Resbond 919 is ideal for: potting, sealing, coating cable end seals, igniters, heating coils, instrumentation, thermocouples, electronics, and many other electrical applications.

Resbond™ 920 is easy for use (Just mix, apply and let dry). Resbond 920 cures at room temperature to bond, seal, insulate, encapsulate and protect delicate electronics components against heat, electricity, chemicals, corrosion and moisture. It based on high purity alumina ceramic, and it is ideal for use when rapid dissipation of heat is required. Its applications include: bonding, encapsulating, protecting and electrically insulating, high watt resistors, electrodes, extension wires, thermocouples, heat sensors, heating coils, igniters and critical electronic components [51].

Durabond adhesives and putties were specially formulated to bond metals, ceramics, and dissimilar materials for use to 1093°C (2000°F). These metallic composite adhesives overcome the brittle bonds and offer some of the ductility and impact resistance associated with soldering and welding. Durabond adhesives can also be drilled, tapped, machined, etc. They are safe and easy to use. Durabond 940HT bases on Al_2O_3 and is developed for bonding low expansion metals such as 400 series stainless steel, low expansion, high temperature alloys, metals, ceramics etc. Durabond 950 could also be adhesive in this packaging prototype. It bases on aluminum and has similar properties than Resbond 940HT.

3.2.4 Wire bonding

To the wire bonding process, platinum wire is rarely used in the industry, as an example, 5-mil annealed Pt wire to a 5000 A-Pt pad (with an underlying base of Ti, MO, and W) sputter deposited on a sapphire substrate has been reported [36], and most processes use aluminum wire and gold wire techniques even though platinum wire does not oxidize in air at any temperature and gold wire only can suffer 500-600 °C in the air.

In this process, 3 mil gold wires are bonded to Au pads on the gold-plated substrate and die by using conventional thermosonic wire bonding. A schematic model of this wire bonding process is shown in Figure 3.9.

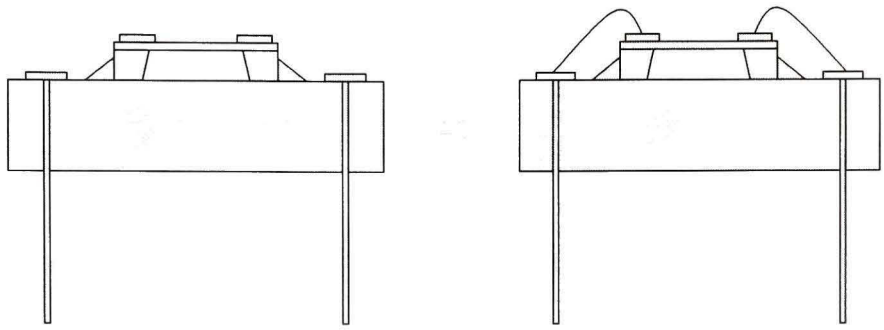

Figure 3.9 Prototype 1 wire bonding (side view).

3.2.5 Housing

The MEMS pressure sensor includes a sensor chip within a substantially sealed cavity formed by a housing (constraint base) and a cover for the housing. The method includes providing an area between a portion of the cover and a portion of the substrate, using adhesive (Durabond 940HT which bases on Al_2O_3 is chosen) to fix them. The cover is a Kovar alloy shell. A schematic model of this process is shown in Figure 3.10. This structure has a potential weakness: bonding wires and metallization pads have no protection. It is difficult to find a protective gel that can suffer -20°C to 600°C temperature cycle and corrosive gas. Protective gel also decreases sensitivity of sensor.

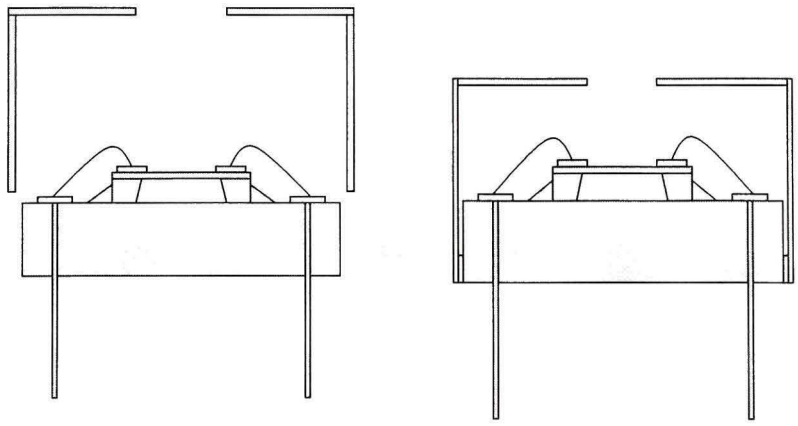

Figure 3.10 Prototype 1 housing (side view).

3.3 Designed prototype 2 (flip-chip package prototype)

This prototype uses flip-chip technique. The idea for this prototype is to avoid bonding wires which is inappropriate to 600 degrees Celsius environment. The prototype consisted of a pressure sensor die mounted on a substrate (i.e. constraint base). The die could be SiC or SiCN and it is attached to a ceramic substrate (it could AlN, Al_2O_3 or SiCN) by using flip-chip technique and adhesives (Al_2O_3). A schematic model of this prototype is shown in Figure 3.11.

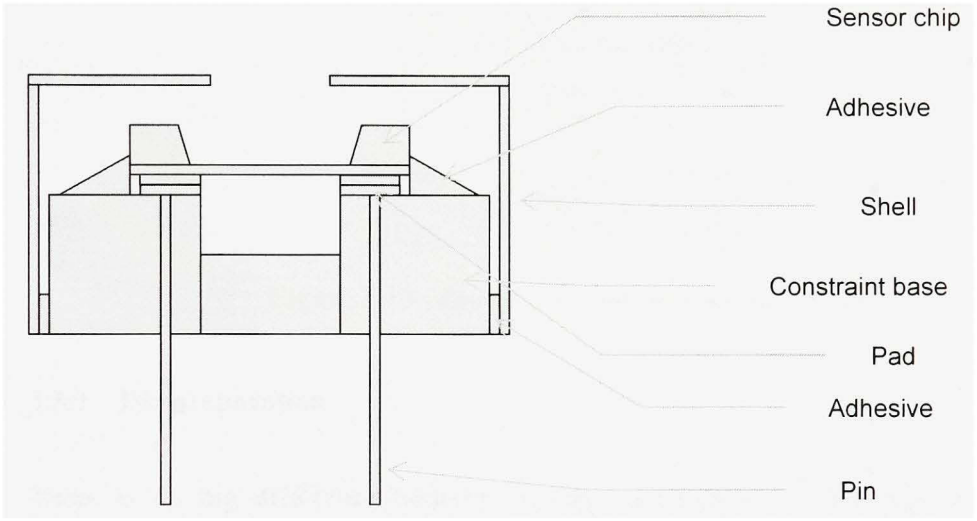

Figure 3.11 Side view of prototype 2 (flip-chip package).

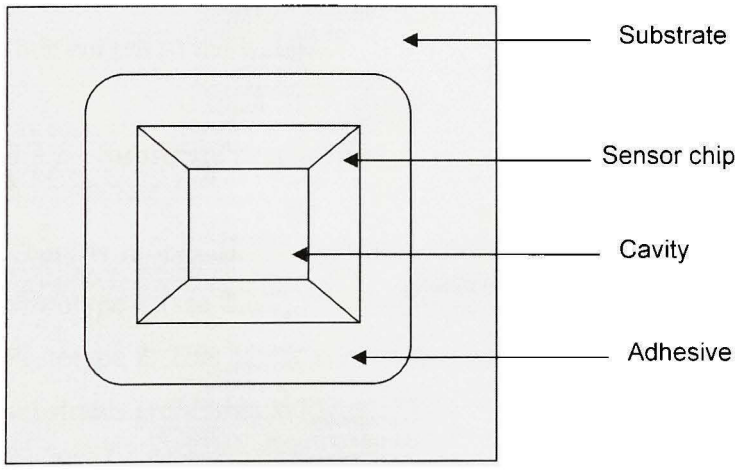

Figure 3.12 Top view of prototype 2 (flip-chip package).

A schematic diagram of the prototype 2 fabrication processes is shown in Figure 3.13.

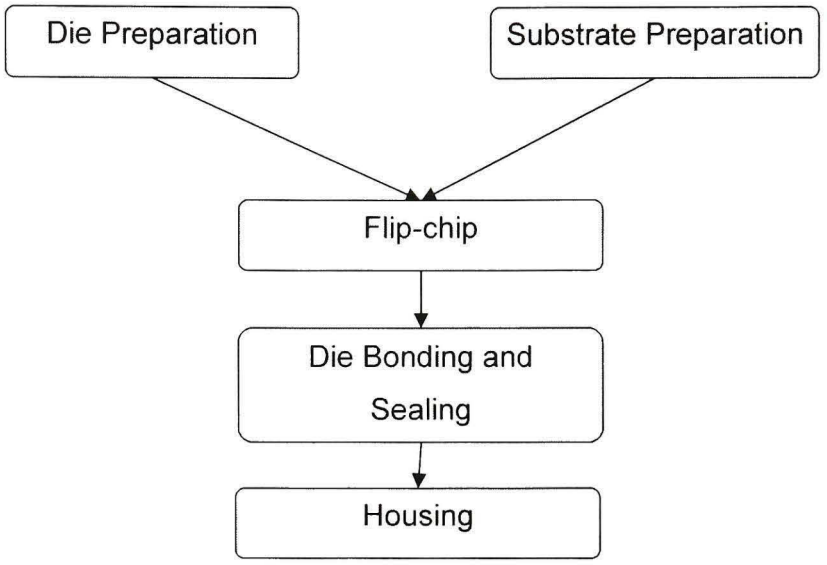

Figure 3.13 Prototype 2 fabrication flow chart.

3.3.1 Die preparation

There is no big difference between the die preparation of Prototype 2 and that of Prototype 1 (see 4.2.1). The major distinction is metallization process to pads. A small dot of solder is then deposited on each of the pads before wafer sawing. The chips are then cut out of the wafer.

3.3.2 Substrate preparation

There is no big difference between the substrate preparation of Prototype 2 and that of Prototype 1 (see 4.2.2). The major distinction is that there is a cavity in the substrate of Prototype 2. This cavity permits the displacement of the sensor chip membrane. The two substrates are shown in Figure 3.14.

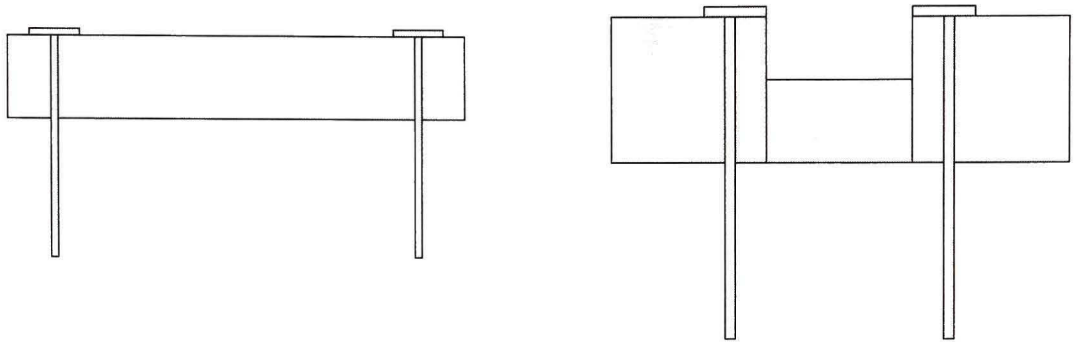

Figure 3.14 Difference between prototype 2 and prototype 1 (side view).

3.3.3 Flip-chip technology description proposed for prototype 2

To attach the flip chip into a circuit, it is inverted to bring the solder dots (gold balls or platinum balls; platinum balls is only for simulation) down onto connectors on the underlying electronics or circuit board. The solder is then remelted to produce an electrical connection, using an ultrasonic process. This also leaves a small space between the chip's circuitry and the underlying mounting. In this case an electrically-insulating adhesive is then "under filled" to provide a stronger mechanical connection, provide a heat bridge, and to ensure the solder joints are not stressed due to differential heating of the chip and the rest of the system. A schematic model of this process is shown in Figure 3.15.

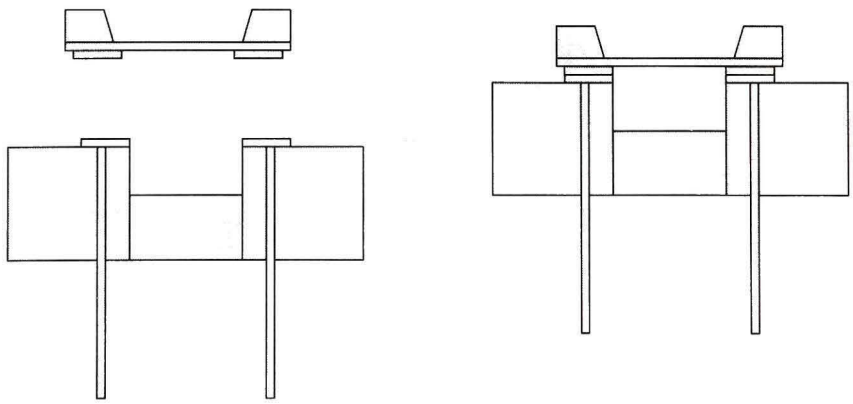

Figure 3.15 Prototype 2 flip-chip (side view).

3.3.4 Die bonding and sealing description proposed for prototype 2

This process is almost identical with that of prototype 1 (see 4.2.3). A schematic model of this process is shown in Figure 3.16.

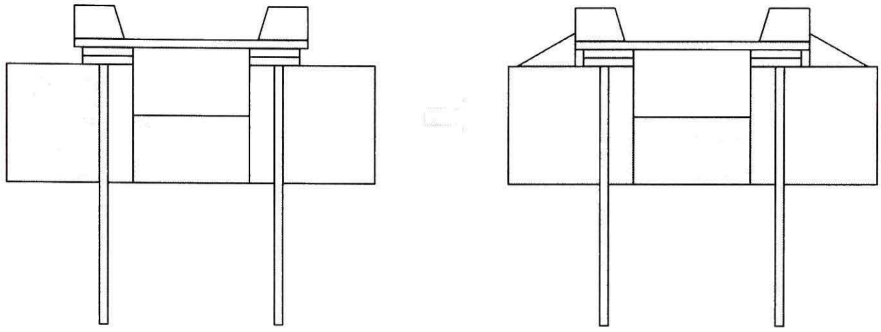

Figure 3.16 Prototype 2 die bonding and sealing (side view).

3.3.5 Housing technology description proposed for prototype 2

This process is similar with that of prototype 1 (see 4.2.5). A schematic model of this process is shown in Figure 3.17.

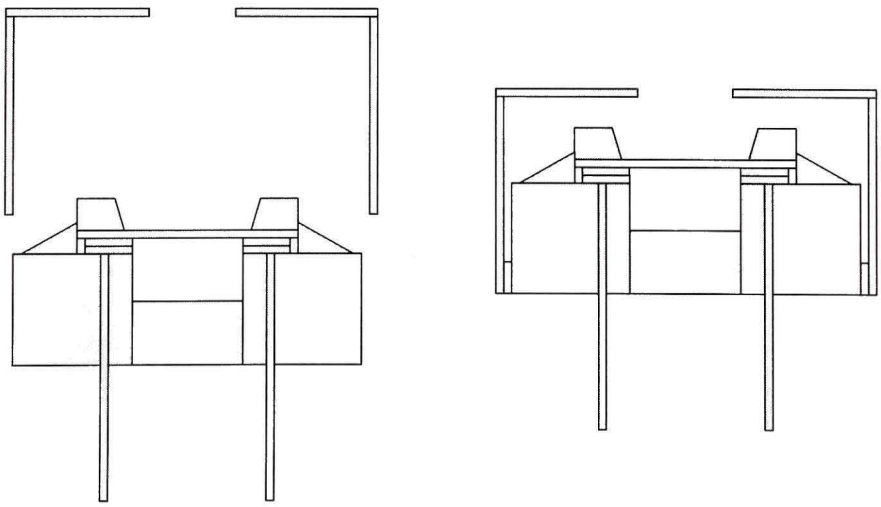

Figure 3.17 Prototype 2 housing (side view).

3.4 Summary

In this chapter, two detailed high temperature MEMS pressure sensor packaging prototypes are presented. Sensor chips (dies) could be SiCN chips (the researchers at Concordia is working on this process) or SiC chips (the most popular material for high temperature application). Ti/Pt/Au system metallization is mature and it could grow on dies and substrates by the chemical vapor deposition method. Three candidate substrate materials which will be simulated in Chapter 5 are AlN, alumina compound and SiCN ceramic. Alumina compound substrates can be prepared by casting or potting. SiCN ceramic substrates can also be cast by pouring into a mold. AlN substrates can be made by hot-pressing or pressureless sintering. All substrates should be embedded Pt pins when they are made. Electrical attachment material is gold wire (wire bonding, prototype 1) or gold solder dots (flip chip, prototype 2). Die bonding and sealing adhesive choose alumina-based Resbond 940HT which is from Cotronics Corporation. This adhesive is also used to bond a substrate to a Kovar alloy shell which is designed to protect sensor and make sensor be installed easily.

CHAPTER 4

SIMULATION TOOLS AND MODELING

A simulation is an imitation of some real thing, state of affairs, or process. The act of simulating something generally entails representing certain key characteristics or behaviors of a selected physical or abstract system.

Simulation is useful for MEMS design. It can provide some future vision about and help to find optimized parameters, find mistakes before fabrication, and reduce time and money. Solving a system like a MEMS sensor is a complex work. It's difficult to apply theoretic analysis to resolve this kind of problem. That's why we apply Finite Element Analysis (FEA) to analyze it. The traditional procedure using FEA is designing FE model, meshing strategy, element solution and assembly etc. For those dynamic problems, the procedure is more complex and it has much more difficulties in designing FE model. Thanks to CAE (Computer-Aided Engineering) technology, FEA becomes easier and more efficient. ANSYS is a kind of CAE software [52] and COMSOL [53] (FEMLAB as former name) is another one.

4.1 Finite element analysis

Finite Element Analysis (FEA) is a computer simulation technique used in engineering analysis. It uses a numerical technique called the Finite Element Method (FEM).

'FEA uses a complex system of points called nodes which make a grid called a mesh. This mesh is programmed to contain the material and structural properties which define how the structure will react to certain loading conditions. Nodes are assigned at a certain density throughout the material depending on the anticipated stress levels of a particular area. Regions which will receive large amounts of stress usually have a higher node

density than those which experience little or no stress. Points of interest may consist of: fracture point of previously tested material, fillets, corners, complex detail, and high stress areas. The mesh acts like a spider web in that from each node, there extends a mesh element to each of the adjacent nodes. This web of vectors is what carries the material properties to the object, creating many elements' [54].

A common use of FEA is for the determination of stresses and displacements in mechanical objects and systems. However, it is also routinely used in the analysis of many other types of problems, including those in heat transfer, solid state diffusion and reactions with moving boundaries, fluid dynamics, and electromagnetism. FEA is able to handle complex systems that defy closed-form analytical solutions.

4.1.1 Analysis contents

FEA can provide a number of outputs but several results have been used to analyze pressure sensor packaging in this thesis.

4.1.1.1 Heat transfer

In thermal physics, heat transfer is the passage of thermal energy from a hot to a cold body. When a physical body, e.g. an object or fluid, is at a different temperature than its surroundings or another body, transfer of thermal energy, also known as heat transfer, occurs in such a way that the body and the surroundings reach thermal equilibrium. Heat transfer always occurs from a hot body to a cold one, a result of the second law of thermodynamics. Heat transfer can never be stopped; it can only be slowed down.

Classical transfer of thermal energy occurs only through conduction, convection, radiation or any combination of these. Heat transfer associated with carriage of the heat of phase change by a substance (such as steam which carries the heat of boiling) is sometimes treated as a variety of convection heat transfer [55].

4.1.1.2 Heat deformation

In engineering mechanics, deformation is a change in shape due to an applied force or an inside stress. In this thesis, the high temperature MEMS pressure sensors must work in a temperature range more than 600 degrees Celsius. During heat transfer, the energy that is stored in the intermolecular bonds between atoms changes. When the stored energy increases, so does the length of the molecular bond. As a result, solids typically expand in response to heating and contract on cooling. Different materials have diverse CTE. These make sensors deform. Deformation may be temporary, as a spring returns to its original length when tension is removed, or permanent as when an object is irreversibly bent or broken.

4.1.1.3 Thermo mechanical stress

Stress is a measure of force per unit area within a body. It is a body's internal distribution of force per area that reacts to external applied loads. Stress is often broken down into its shear and normal components as these have unique physical significance. In short, stress is to force as strain is to elongation.

Von Mises stress is a scalar function of the deviatoric components of the stress tensor that gives an appreciation of the overall magnitude of the shear components of the tensor. This allows the onset and amount of plastic deformation under triaxial loading to be predicted from the results of a simple uniaxial tensile test. It is most applicable to ductile materials [56].

'Residual stress is that which remains in a body which is stationary and at equilibrium with its surroundings. Residual stresses occur for a variety of reasons, including inelastic deformations and heat treatment. Heat from welding may cause localized expansion. When the finished weldment cools, some areas cool and contract more than others,

leaving residual stresses. Castings may also have large residual stresses due to uneven cooling' [57].

4.2 Ansys

The ANSYS computer program is a large-scale multipurpose finite element program which may be used for solving several classes of engineering analyses. The analysis capabilities of ANSYS includes the ability to solve static and dynamic structural analyses, steady-state and transient heat transfer problems, mode-frequency and buckling eigenvalue problems, static or time-varying magnetic analyses, and various types of field and coupled-field applications. The program contains many special features which allow nonlinearities or secondary effects to be included in the solution, such as plasticity, large strain, hyperelasticity, creep, swelling, large deflections, contact, stress stiffening, temperature dependency, material anisotropy, and radiation. As ANSYS has been developed, other special capabilities, such as substructuring, submodeling, random vibration, kinetostatics, kinetodynamics, free convection fluid analysis, acoustics, magnetic, piezoelectric, coupled-field analysis and design optimization have been added to the program. These capabilities contribute further to making ANSYS a multipurpose analysis tool for varied engineering disciplines [58].

The ANSYS program has many finite element analysis capabilities, ranging from a simple, linear, static analysis to a complex, nonlinear, transient dynamic analysis. The analysis guide manuals in the ANSYS documentation set describe specific procedures for performing analyses for different engineering disciplines [52]. Figure 4.1 shows modules of ANSYS. A model consists of some different simple form. After meshing and parameters inputting, ANSYS program calculates it and finds solutions. Post-processor could process solutions and output results visually in different ways.

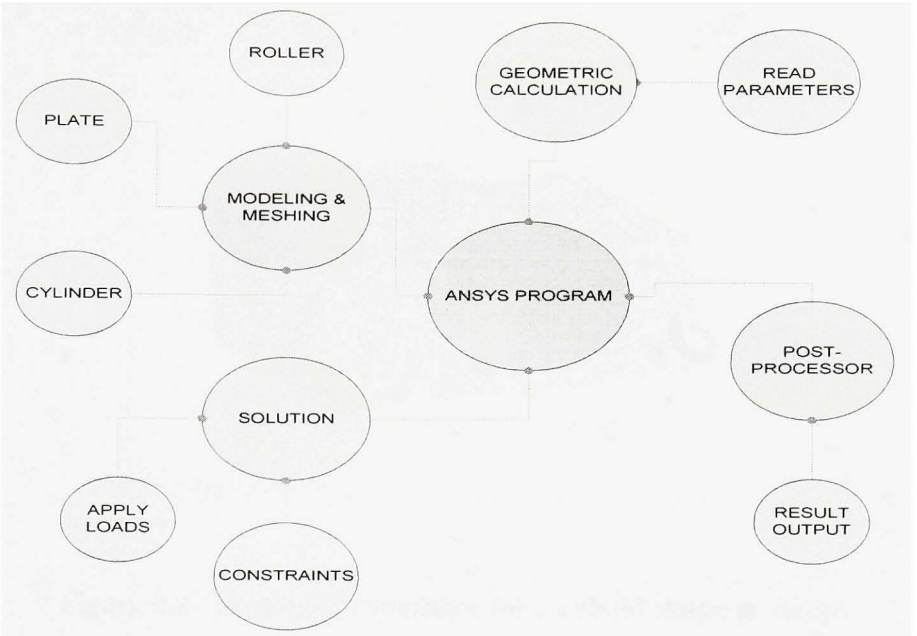

Figure 4.1 Modules of ANSYS program.

4.2.1 Analysis procedure using ANSYS

A typical ANSYS analysis has three distinct steps: [52]

1. Build the model. (PREP7)
2. Apply loads and obtain the solution. (SOLU)
3. Review the results. (POST1 and POST26)

4.2.2 Modular Design

Module design is that using ANSYS script created according to prototypes proposed before. How to mesh is a key process for a simulation and meshing takes more than 50% of time of a simulation workload. An improper meshing can bring on an incorrect simulation result. Employing symmetry considerations, only a quarter portion of the structure has been modeled. Some simulation meshings of this thesis are shown in Figure 4.4, Figure 4.5, Figure 4.2 and Figure 4.3.

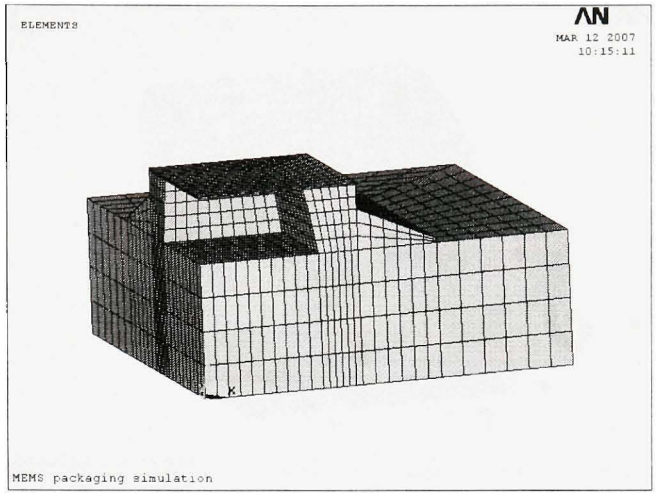

Figure 4.2 Prototype 1 meshing for a cuboid shape package.

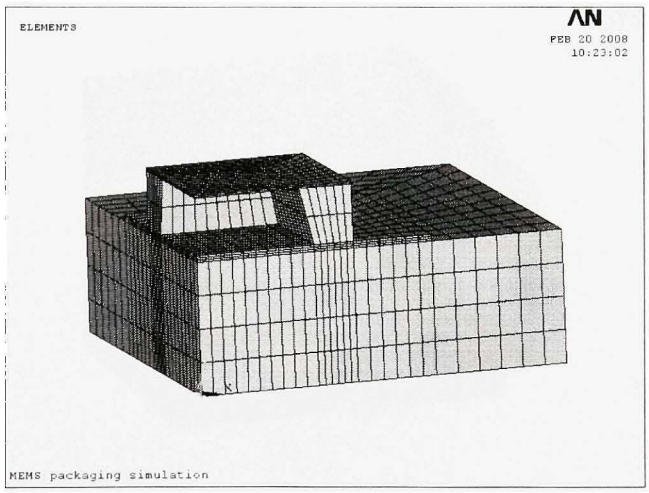

Figure 4.3 Prototype 1 variation meshing for a cuboid shape package.

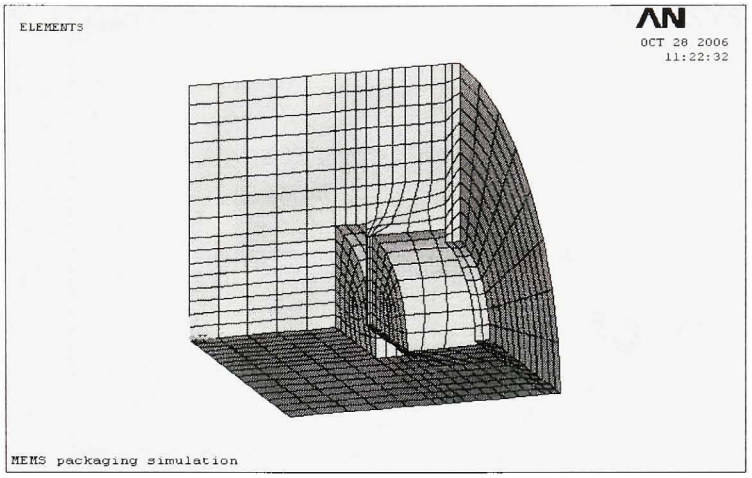

Figure 4.4 Prototype 2 meshing for a cylinder shape package.

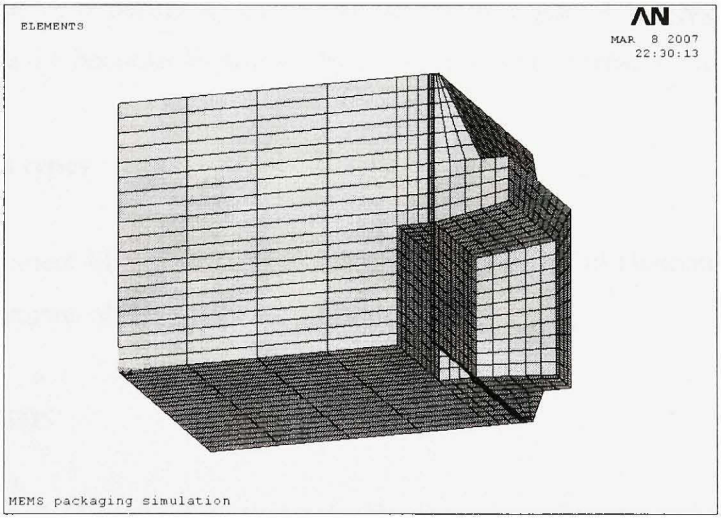

Figure 4.5 Prototype 2 meshing for a cuboid shape package.

Figure 4.6 Prototype 2 meshing for a cuboid shape package (before its rotation).

The difference between Figure 4.2 and Figure 4.3 is die bonding adhesive position. In Figure 4.2, adhesive is beside die and substrate, and in Figure 4.3, it is between die and substrate. Figure 4.6 becomes Figure 4.5 by a 90 degrees clockwise rotation.

4.2.3 Element types

The ANSYS element library consists of more than 100 different element formulations or types. Some elements of this thesis are introduced below.

4.2.3.1 SOLID5

SOLID5 has a 3-D magnetic, thermal, electric, piezoelectric and structural field capability with limited coupling between the fields. The element has eight nodes with up to six degrees of freedom at each node. Scalar potential formulations (reduced RSP, difference DSP, or general GSP) are available for modeling magnetostatic fields in a static analysis. When used in structural and piezoelectric analyses, SOLID5 has large deflection and stress stiffening capabilities. SOLID5 has all the fields that we need in this

thesis except thermal field, and it can easily couple with SOLID90 which is a 3-D thermal element.

4.2.3.2 SOLID90

SOLID90 is a higher order version of the 3-D eight node thermal element (SOLID70). The element has 20 nodes with a single degree of freedom, temperature, at each node. The 20-node elements have compatible temperature shapes and are well suited to model curved boundaries.

4.2.4 Output of solution

The output from the solution consists of the nodal solution (or the primary degree of freedom solution) and the element solution (or the derived solution). The main analyzed outputs are displacement and Von Mises stress.

4.2.4.1 Element Solution

The element output items (and their definitions) are shown along with the element type description. Not all of the items shown in the output table will appear at all times for the element. Normally, items not appearing are either not applicable to the solution or have all zero results and are suppressed to save space.

4.2.4.2 Failure Criteria

Failure criteria are commonly used for orthotropic materials. They can be input using either the FC commands or the TB commands. The FC command input is used in POST1. The TB command input is used directly in the composite elements.

4.3 COMSOL Multiphysics (FEMLAB)

COMSOL Multiphysics (formerly FEMLAB) is a finite element analysis and solver software package for various physics and engineering applications, especially coupled phenomena, or multiphysics. COMSOL Multiphysics also offers an extensive and well-managed interface to MATLAB and its toolboxes for a large variety of programming, preprocessing and postprocessing possibilities. A similar interface is offered to COMSOL Script. The packages are cross-platform (Windows, Mac, Linux, Unix.) In addition to conventional physics-based user-interfaces, COMSOL Multiphysics also allows for entering coupled systems of partial differential equations (PDEs). The PDEs can be entered directly or using the so called weak form. COMSOL has some modules which make it become an easy-using FEA tool.

Heat Transfer Module: Consists of advanced application modes for the analysis of heat transfer by conduction, convection and radiation. It is specific for industrial applications such as electronics cooling and process engineering.
MEMS Module: It represents coupled processes in microelectromechanical and microfluidic devices and it incorporates specific multiphysics couplings for applications such as electroosmotic flow, film damping, piezoelectricity and fluid-structure interaction.

4.4 Summary

In this chapter, firstly FEM and brief steps of FEA were introduced, and analysis contents are discussed. Secondly, 4 designed prototypes have been modeled and meshed. Two elements have been applied in model and material parameters and model dimensions have been inputted, then ANSYS program have calculated and results have been shown by ANSYS post processor. This chapter also introduced COMSOL Multiphysics which are used in this thesis intended to compare and verify ANSYS simulation results.

CHAPTER 5

SIMULATION RESULTS AND DISCUSSION

5.1 Introduction

Simulation results are not always accurate, but they can still show some interesting clues. In this chapter, different prototypes were simulated in ANSYS and FEMLAB in order to compare the prototypes, choose materials, find out better parameters, and verify simulation results. Table 5.1 shows all the simulation contents of this chapter.

Table 5.1

Simulation content

Simulation objectives	Designed Prototype	Materials				Condition	
		Die	Substrate	Adhesive	Electrical Attachment	Temperature (°C)	Pressure (M Pa)
5.2 Thermo mechanical stress distribution	Prototype 1	SiC	AlN	Al_2O_3		20-600	0
	Prototype 2	SiC	AlN	Al_2O_3	Pt	20-600	0
	Prototype 1	SiC	AlN	Al_2O_3		20-600	1
	Prototype 2	SiC	AlN	Al_2O_3	Pt	20-600	1
5.3 Comparison of Conventional package and flip-chip	Prototype1 variation	SiC	AlN	Al_2O_3		20-600	1
	Prototype 2	SiC	AlN	Al_2O_3	Au	20-600	1
5.4 Sensor chip size	Prototype 1 0.24X0.24X0.05mm 1.2X1.2X0.25mm 2.4X2.4X0.5mm	SiC	AlN	Al_2O_3		20-600	1

5.5 Membrane thickness	Prototype 2 cylinder 0.02mm 0.04mm	SiC	AlN				100
5.6 Heat deformation	Prototype 2	SiC	AlN	Al_2O_3	Au	0 100 200 300 400 500 600	1
5.7 Comparison of different materials	Prototype 2	SiCN	AlN	Al_2O_3	Pt	20-600	1
	Prototype 2	SiCN	SiCN	Al_2O_3	Pt	20-600	1
	Prototype 2	SiC	Al_2O_3	Al_2O_3	Au	20-600	1
	Prototype 2	SiC	AlN	Al_2O_3	Au	20-600	1
	Prototype 2	SiCN	Al_2O_3	Al_2O_3	Au	20-600	1
	Prototype 2	SiCN	AlN	Al_2O_3	Au	20-600	1
	Prototype 2	SiCN	SiCN	Al_2O_3	Au	20-600	1
5.8 Heat transfer inside a package	Prototype 1	SiC	AlN	Al_2O_3		20-600	0
	Prototype 1	SiCN	AlN	Al_2O_3		20-600	0
5.9 Heat transfer calculation	Prototype 1	SiC	AlN	Al_2O_3		20-600	0
5.10 Stress-free temperature	Prototype 1 Ref. Temp. 0-600°C	SiCN	AlN	Al_2O_3		0	1
	Prototype 1 Ref. Temp. 0-600°C	SiCN	AlN	Al_2O_3		600	1
5.11 ANSYS and FEMLAB	Prototype 2 cylinder	SiC	AlN			20-600	0
5.12 Porosity	Prototype 2	SiC	AlN	Al_2O_3	Au 100% 80%	20-600	1

5.2 Thermo mechanical stress distribution

High temperature brings on big thermo mechanical stresses and too big stress makes a sensor fail. So, stress distribution in a sensor should be known in order to optimize the design of the pressure sensor.

First simulation in this section uses the model: prototype 1 with a SiC die, AlN substrate, Al_2O_3 adhesives, without pressure load, and reference temperature (stress-free temperature) 20 degrees Celsius. The sensor is subjected to a temperature cycle of 20 degrees Celsius to 600 degrees Celsius. Sensor cavity is at vacuum. A schematic model of this pressure sensor is shown in Figure 5.1.

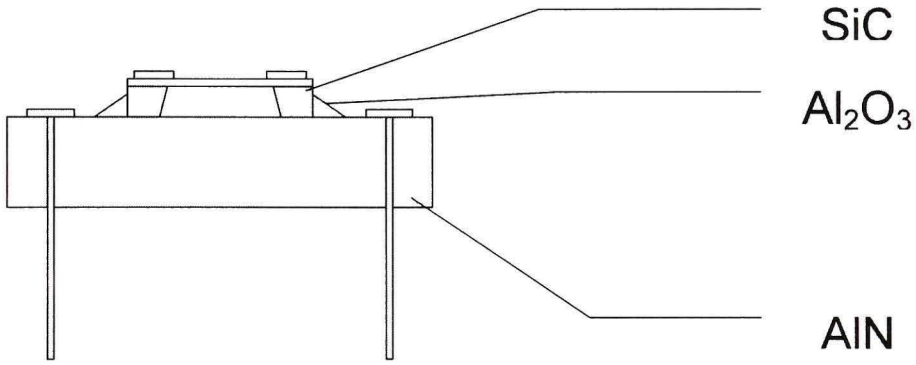

Figure 5.1 SiC die, AlN substrate, Al_2O_3 adhesives (side view).

The simulation has been done in ANSYS by using a meshing like Figure 4.2. As a result Von Mises stress distribution in this model from the simulation is shown in Figure 5.2. The color bar in the bottom of Figure 5.2 represents Von Mises stress (unit Pascal). The stress represented by color. The increase of stress is shown from the blue to the red.

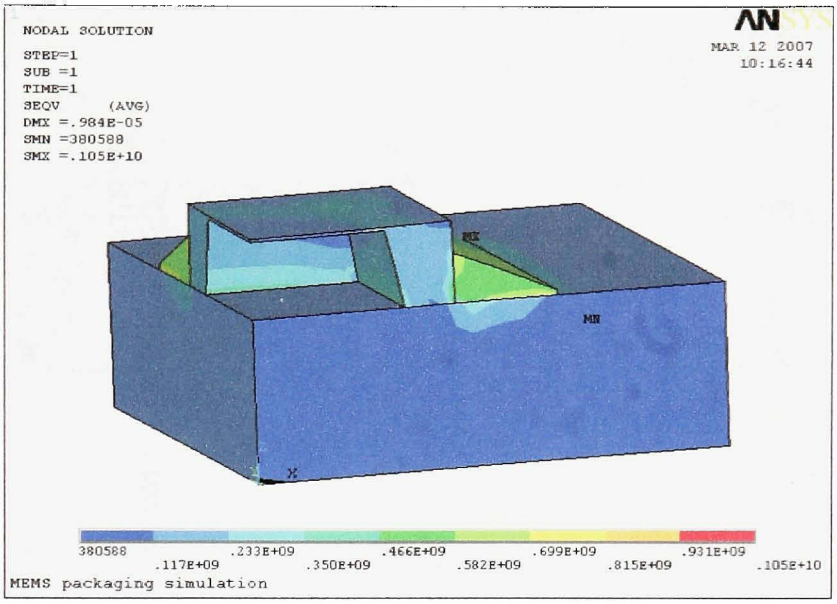

Figure 5.2 Von Mises stress of prototype 1 (temp. from 20 to 600 °C).

Due to mismatch of the coefficient of thermal expansion (CTE) of the sensor chip material (SiC), constraint base material (AlN), and adhesive material (Al_2O_3), thermo mechanical stresses are significant in the adhesive part and the sensor chip, especially on the surface of different materials. Because the CTE of the adhesive (Al_2O_3) is the highest among those three materials, adhesive part also suffer the highest thermo mechanical stress.

Second simulation in this section has used the model: prototype 2 cuboid shape with a SiC die, AlN substrate, Al_2O_3 adhesives, Pt attach, without pressure load, and reference temperature (stress-free temperature) 20 degrees Celsius. The sensor is also subjected to a temperature cycle of 20 degrees Celsius to 600 degrees Celsius. Sensor cavity is at vacuum. A schematic model of this pressure sensor is shown in Figure 5.3.

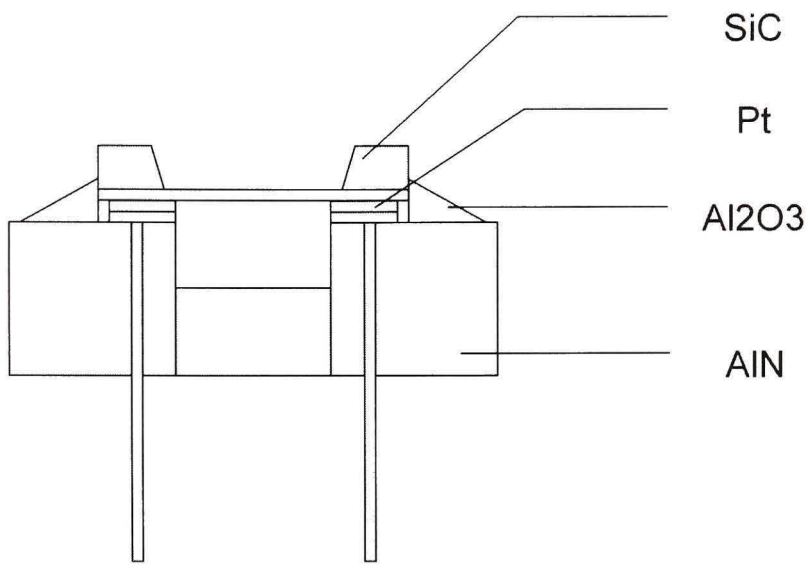

Figure 5.3 SiC die, AlN substrate, Al_2O_3 adhesives, Pt attach (side view).

The simulation has been done in ANSYS by using a meshing like Figure 4.5. As a result Von Mises stress distribution in this model from the simulation is shown in Figure 5.4.

Due to mismatch of the coefficient of thermal expansion (CTE) of the different parts of the whole package which includes sensor chip material (here is SiC), constraint base material (AlN), Pt attach part and adhesive material (Al_2O_3), thermo mechanical stresses are considerable in the adhesive part and the Pt attach part, especially on the surface of different materials. The thermo mechanical stresses distribution in each part of the sensor package depends on the CTE of each part. The higher CTE, the bigger Von Mises stress. Comparing to the first simulation, the maximum Von Mises stress is 5% bigger.

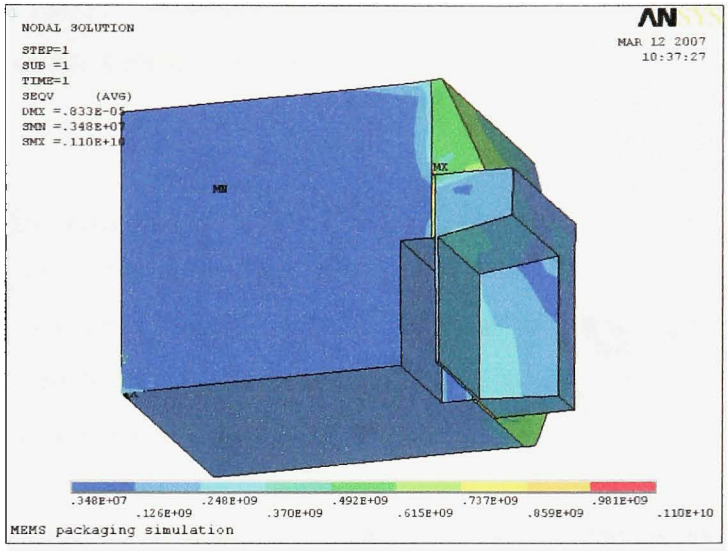

Figure 5.4 Von Mises stress of prototype 2 (SiC die, AlN sub., Al_2O_3, Pt attach).

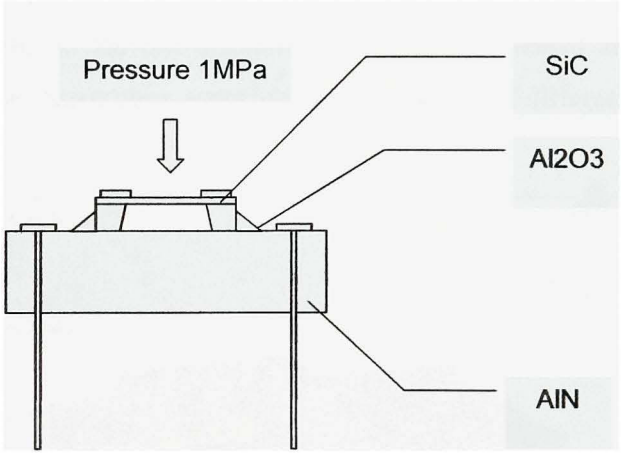

Figure 5.5 Prototype 1 SiC die, AlN, Al_2O_3 adhesives, 1 M Pa (side view).

The first two simulations are without pressure load. In a real application, pressure load should be put in simulations. The third simulation in this section has used the model: prototype 1 with a SiC die, AlN substrate, Al_2O_3 adhesives, with 1 M Pa pressure load, and reference temperature (stress-free temperature) 20 degrees Celsius. According to an engine test result that Pratt & Whitney Canada gave to us, the operation pressure in a jet

engine is about 1MPa. The sensor is subjected to a temperature cycle of 20 degrees Celsius to 600 degree Celsius. A schematic model of this pressure sensor is shown in Figure 5.5.

The simulation has been done in ANSYS by using a meshing like Figure 4.5. As a result, the Von Mises stress distribution and the displacements along Z axis (vertical to the membrane) from the simulation are shown in Figure 5.6 and Figure 5.7. The color bar in the bottom of Figure 5.7 represents displacement (unit meter). The increase of distance is shown from the blue to the red.

The Von Mises stress distribution is different than the one without pressure load. The reason is obvious: 1 M Pa pressure load changes a lot on the sensor chip. The membrane of the sensor chip has big stresses. The maximum stress now is not on the surface of the different parts of the package. It appears near the edge of the membrane. The other parts of stresses are similar to the one without pressure load; stresses are significant in the adhesive part and the sensor chip, especially on the surface of different materials.

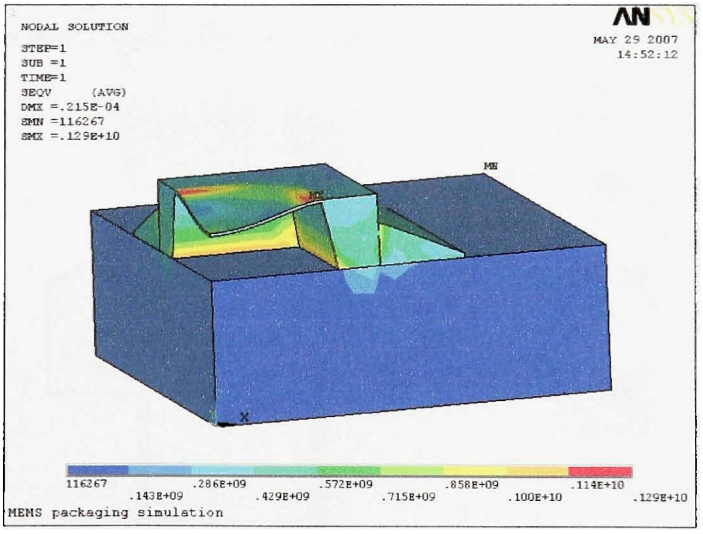

Figure 5.6 Von Mises stress of prototype 1 (SiC die, AlN, Al_2O_3 adhesives, 1MPa).

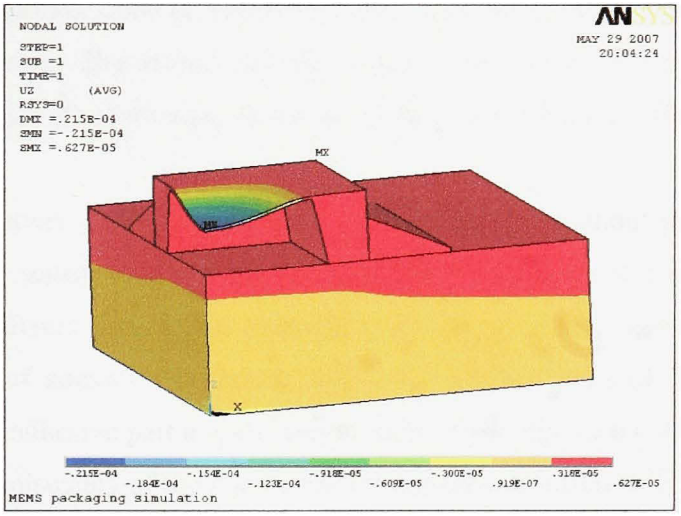

Figure 5.7 Displacement of prototype 1 (SiC die, AlN, Al_2O_3 adhesives, 1MPa).

Fourth simulation in this section is similar to the second simulation. It also has used the model: prototype 2 cuboid shape with a SiC die, AlN substrate, Al_2O_3 adhesives, Pt attach, and reference temperature (stress-free temperature) 20 degree Celsius. The sensor is also subjected to a temperature cycle of 20 degrees Celsius to 600 degrees Celsius. The only difference is that it applies1M Pa pressure load.

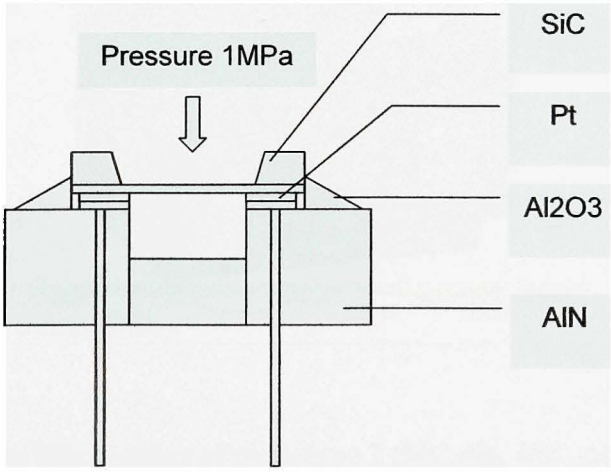

Figure 5.8 Prototype 2 SiC die, AlN substrate, Al_2O_3 adhesives, Pt attach, 1 M Pa (side view).

The simulation has been done in ANSYS by using a meshing like Figure 4.5. As a result, the Von Mises stress distribution and the displacements along Z axis (vertical to the membrane) from the simulation are shown in Figure 5.9 and Figure 5.10 respectively.

The Von Mises stress distribution is different than the one without pressure load. The membrane of the sensor chip has big stresses. The maximum stress now is not on the surface of the different parts of the package. It appears near the edge of the membrane. The other parts of stresses are similar to the one without pressure load; stresses are significant in the adhesive part and the sensor chip, especially on the surface of different materials due to mismatch of the coefficient of thermal expansion (CTE) of the different parts of the whole package. Comparing to the third simulation, the maximum Von Mises stress is much bigger. Sensor cavity is at vacuum. Adding some noble gases in the cavity will counteract sensor membrane displacement (due to damping factor change), and that will decrease sensor sensibility and sensor precision.

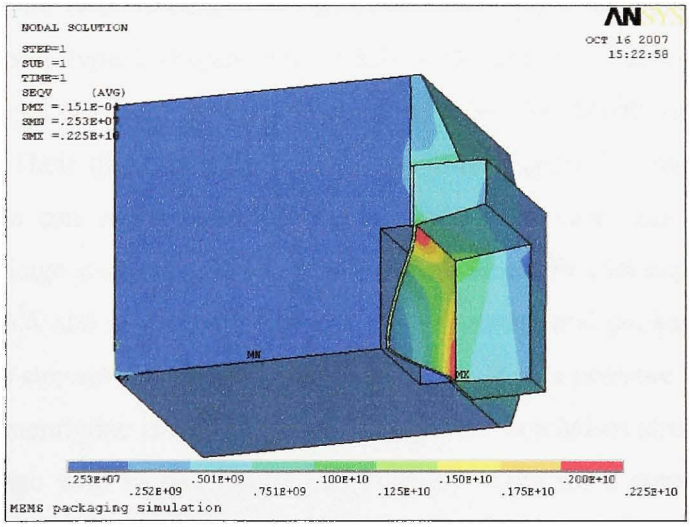

Figure 5.9 Von Mises stress of prototype 2 (SiC die, AlN, Al_2O_3, Pt attach).

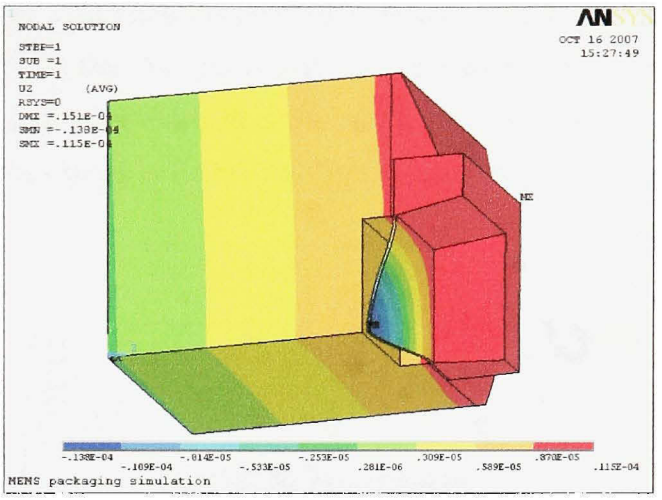

Figure 5.10 Displacement (SiC die, AlN substrate, Al_2O_3 adhesives, Pt attach).

5.3 Comparison of Conventional package and flip-chip

Firstly, we compare two conventional packages: prototype 1 and its variant. The Von Mises stress of prototype 1 (Figure 5.6) is 1.29 GPa, and for a variant of prototype 1 (Figure 5.11) it is 1.62GPa. Prototype 1 has much less Von Mises stress than its most popular variant. Their displacements are almost same (Figure 5.7 and Figure 5.12). A flip-chip package can avoid wire bonding because gold wires are uncovered for a conventional package and they may react with corrosive gas in a jet engine at 600 degree Celsius. Figure 5.6 and Figure 5.9 demonstrate a conventional package that has much lower Von Mises stresses than a flip-chip package in a 1M Pa pressure environment. The displacement of membrane is similar, but the maximum Von Mises stress is 2.25G Pa for a flip-chip package with Pt attachment and it is 1.29 GPa for a conventional package (these sensor chips have the same size in the models). In order to be general, a simulation has been done by using the model: prototype 2 cuboid shape with a SiC die, AlN substrate, Al_2O_3 adhesives, Au attach, with 1M Pa pressure load and reference temperature (stress-free temperature) 20 degrees Celsius. The sensor is also subjected to a

temperature cycle of 20 degrees Celsius to 600 degrees Celsius. The only difference than previous simulation is that Au attachment has replaced Pt attachment. A different die bonding position (adhesive between a die and a substrate) is also simulated and the maximum Von Mises stress is 1.62 G Pa. Compared to Prototype 1, it does not have any advantage.

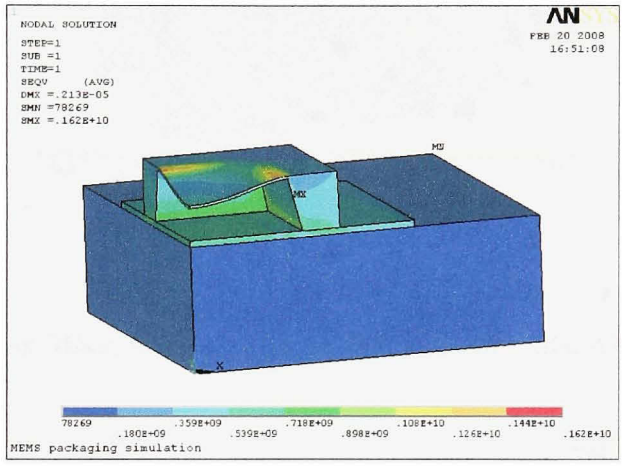

Figure 5.11 Von Mises stress of prototype 1 variation (SiC die, AlN, Al_2O_3, 1MPa).

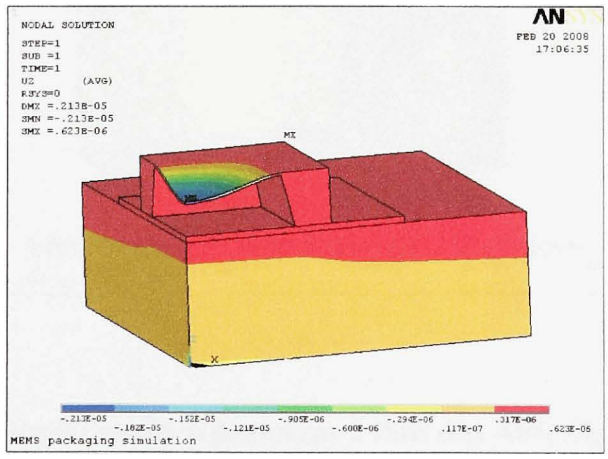

Figure 5.12 Displacement of prototype 1 variation (SiC die, AlN, Al_2O_3, 1MPa).

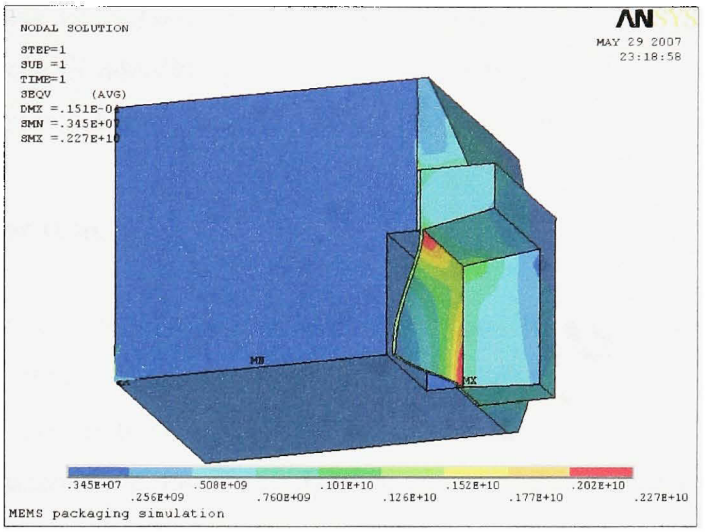

Figure 5.13 Von Mises stress of prototype 2 (SiC die, AlN, Al_2O_3, Au attach).

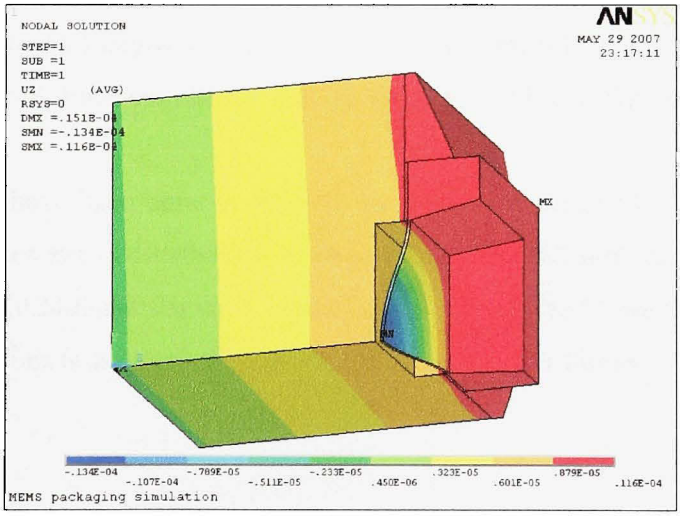

Figure 5.14 Displacement of prototype 2 (SiC die, AlN, Al_2O_3, Au attach).

Figure 5.9, Figure 5.10, Figure 5.13 and Figure 5.14 demonstrate that there is only small difference between Pt attachment (Von Mises stress is 2.25 G Pa) and Au attachment (Von Mises stress is 2.27 G Pa) for the Von Mises stresses and displacements.

5.4 Sensor chip size

Even though a sensor chip is done before its packaging, it is necessary to discuss in the packaging point of view. A sensor chip size determinates the minimal whole package size. The sensor chip size is from 1-2 mm (diameter) and down to 0.2 -0.3 mm (these data have been obtained from the researchers of Concordia University). The following simulation tries to describe the relation of a sensor chip size and thermo mechanical stress.

The simulations in this section have used the model: prototype 1 with a SiC die, AlN substrate, Al_2O_3 adhesives, with 1 M Pa pressure load, and reference temperature (stress-free temperature) 20 degree Celsius. The sensor is subjected to a temperature cycle of 20 degrees Celsius to 600 degrees Celsius. A schematic model of this pressure sensor is shown in Figure 5.8. Each simulation uses the same model but different size.

The simulations have been done in ANSYS by using a meshing like Figure 4.2. As the results, Von Mises stress distribution in this model with different size parameters (SiC dies are 0.24mmX0.24mmX0.05mm, 1.2mmX1.2mmX0.25mm and 2.4mmX2.4mm X0.5mm) from the simulations is shown in Figure 5.15, Figure 5.16 and Figure 5.17 respectively.

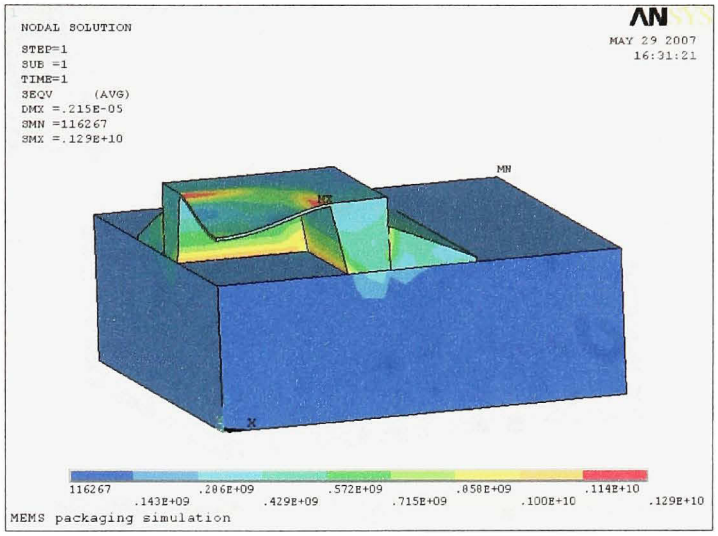

Figure 5.15 Von Mises stress prototype 1 (chip 0.24x0.24x0.05mm SiC+AlN+Al_2O_3).

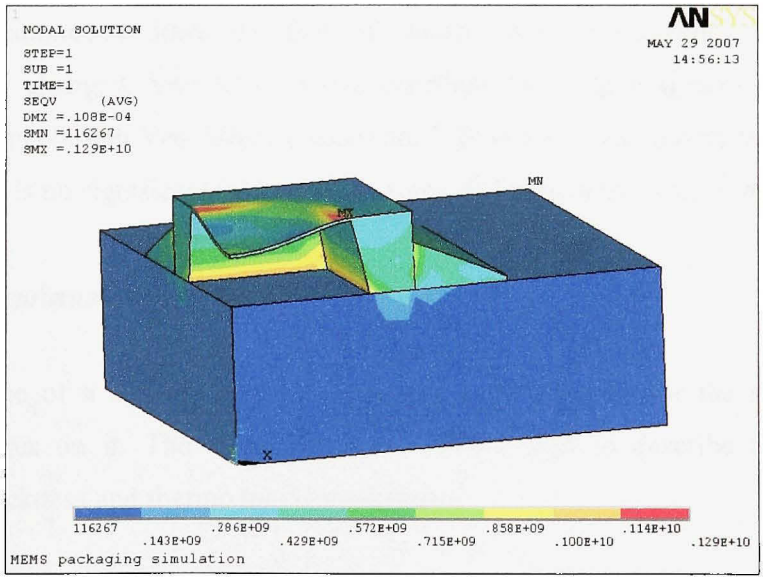

Figure 5.16 Von Mises stress of prototype 1 (chip 1.2x1.2x0.25mm SiC+AlN+Al_2O_3).

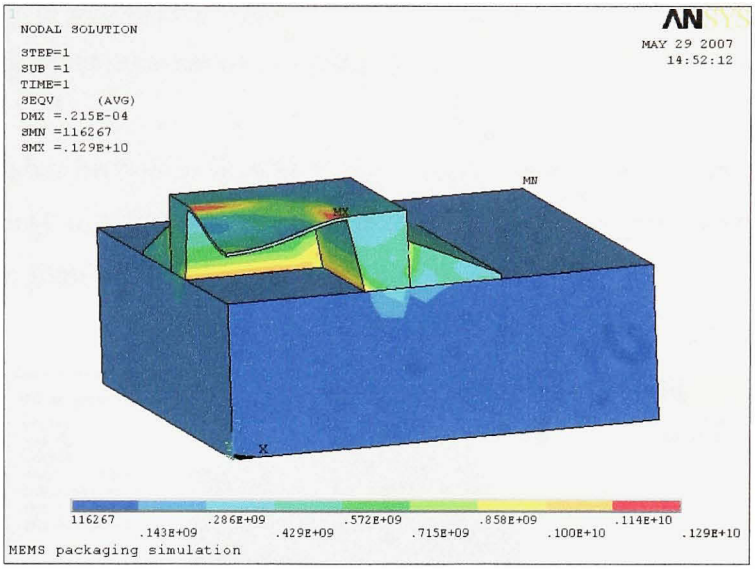

Figure 5.17 Von Mises stress of prototype 1 (chip 2.4x2.4 x0.5mm SiC+AlN+Al_2O_3).

The simulation figures (Figure 5.15, Figure 5.16 and Figure 5.17) which use different dimension parameters illustrate that if sensor chip dimensions are geometric proportionally changed, Von Mises stress distributions in these figures are almost the same and the maximum Von Mises stresses are 1.29 G Pa. From the thermal stress point of view, there is no significant difference between different sensor chip sizes.

5.5 Membrane thickness

The membrane of a MEMS pressure sensor is a pivotal part for the sensor because pressure gauges on it. The simulation that follows tries to describe the relation of membrane thickness and thermo mechanical stress.

The simulation in this section has used the model: prototype 2 cylinder shape with a SiC die, AlN substrate, with 100M Pa pressure load, and reference temperature (stress-free temperature) 20 degrees Celsius. The sensor is subjected to a temperature cycle of 20

degrees Celsius to 600 degrees Celsius. In the simulation, only membrane thickness is changed and the other dimensions of a package are kept the same in the model.

The simulation has been done in ANSYS by using a meshing like Figure 4.4. As results, Von Mises stress distribution figures (0.02mm and 0.04mm thick membrane) in this model from the simulation are shown in Figure 5.18 and Figure 5.19.

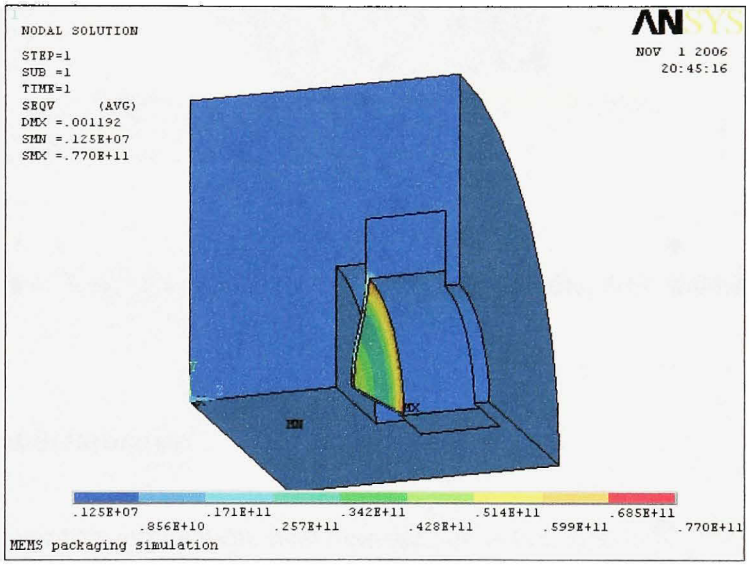

Figure 5.18 Von Mises stress of prototype 2 (SiC die, AlN, 0.02mm thick).

The stress distributions are similar. The stresses concentrate in the membranes of these sensor chips and they appear near the edge of the membranes. The maximum Von Mises stress of 0.04mm thick membrane sensor is much lower than the one of 0.02mm thick membrane sensor (0.02mm thick membrane's stress is 4.45 times than 0.04mm thick membrane). So, increasing a sensor chip membrane thickness can decrease stress. But a thicker membrane is less sensitive to applying pressure load.

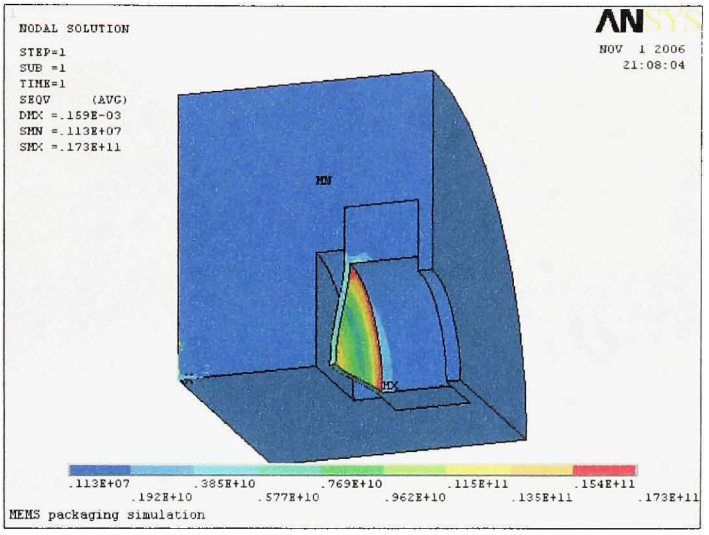

Figure 5.19 Von Mises stress of prototype 2 (SiC die, AlN, 0.04mm thick).

5.6 Heat deformation

For a high temperature application, heat deformation is not ignorable. The simulation that follows tries to describe the relation of displacement and temperature.

The simulations in this section have used the model: prototype 2 cuboid shape with a SiC die, AlN substrate, Al_2O_3 adhesives, Au attachment, with 1 M Pa pressure load, and reference temperature (stress-free temperature) 0 degree Celsius. The sensor is subjected to a temperature cycle of 0 degree Celsius to 600 degree Celsius. A schematic model of this pressure sensor is shown in Figure 5.8.

The simulations have been done in ANSYS by using a meshing like Figure 4.5. As the results, the displacements in different temperature condition from the simulations are shown in Figure 5.20 (a, b, c, d, e, f and g).

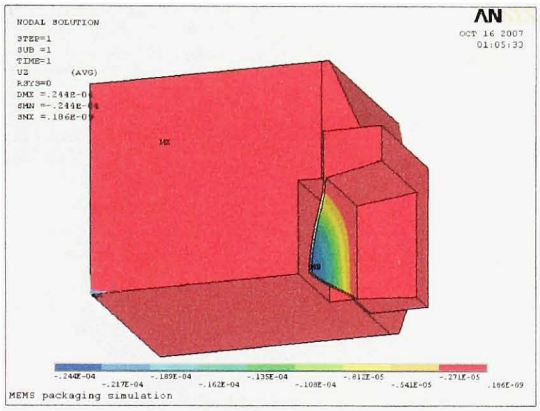

(a) 0 degree Celsius

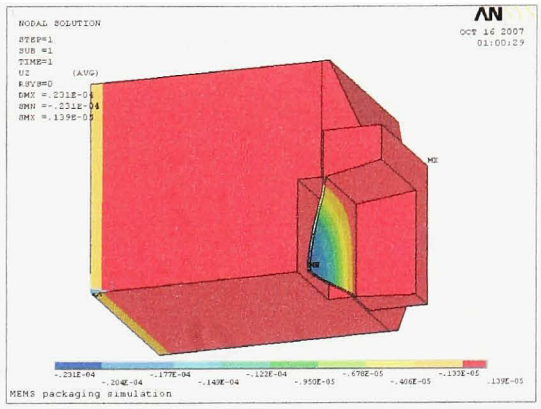

(b) 100 degrees Celsius

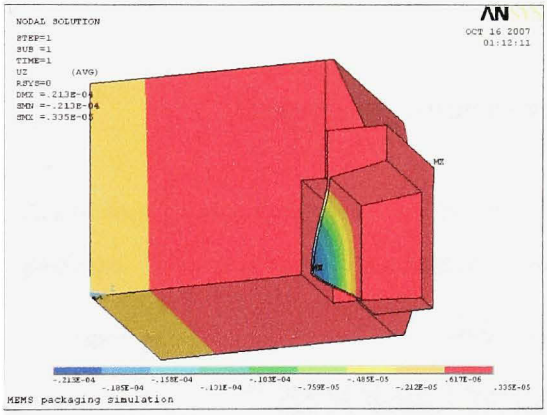

(c) 200 degrees Celsius

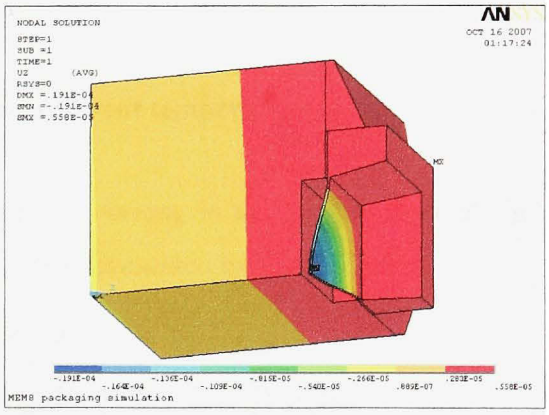

(d) 300 degrees Celsius

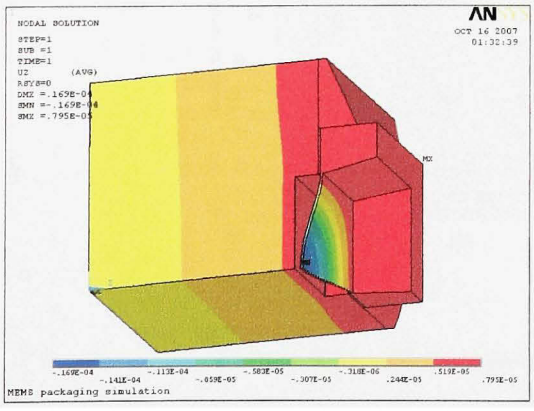

(e) 400 degrees Celsius

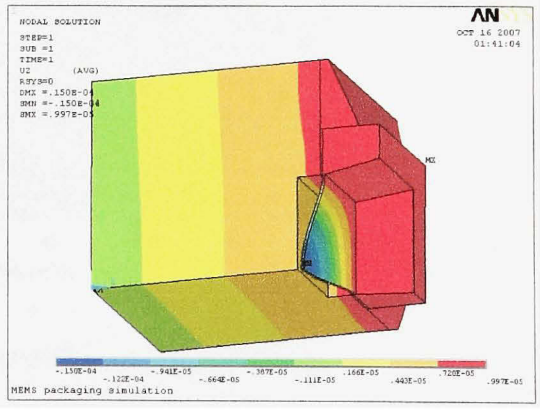

(f) 500 degrees Celsius

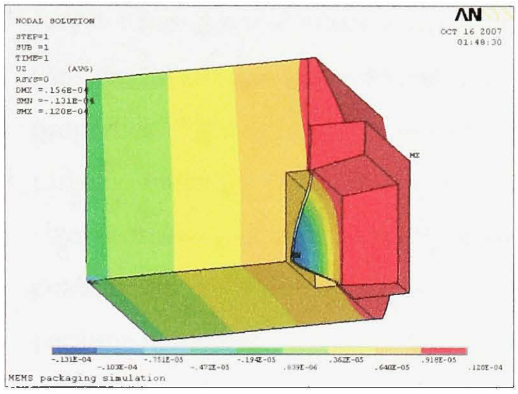

(g) 600 degrees Celsius

Figure 5.20 Displacement at different temperature.

According to simulation results, there has been an increase in the displacement of the package. The membrane displacement data have been presented by Figure 5.21.

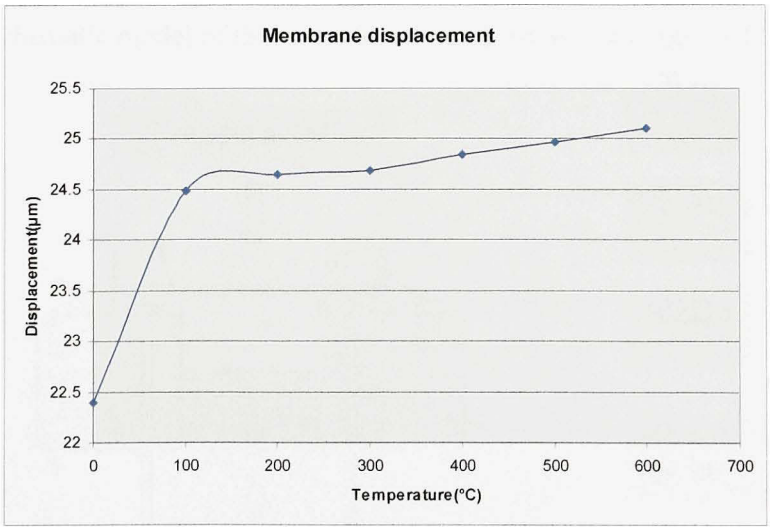

Figure 5.21 Displacements in different temperatures.

For membrane deformation, there has been a 12% increase in the displacement in the center of membrane when temperature changes from 0 degree Celsius to 600 degrees Celsius. Most membrane deformation occurs at first 100 degree Celsius. If we see SiC properties (Figure 2.4), we will see that CTE of SiC increases fast at first 100 degree Celsius. From the numbers given in Figure 5.21, it can be seen that the whole package size increased at time that temperature grows up. In fact, once the materials are determined, the whole package heat deformation is also certain because of the CTE of the package materials.

5.7 Comparison of different materials

Choosing appropriate materials is pivotal to high temperature sensor design. In this section, different materials apply the model of prototype 2 cuboid shape with a die (SiC or SiCN), a substrate (SiCN, Al_2O_3 or AlN), Al_2O_3 adhesives, Au or Pt attach, with 1M Pa pressure load, and reference temperature (stress-free temperature) 20 degrees Celsius. The sensor is also subjected to a temperature cycle of 20 degrees Celsius to 600 degrees Celsius. A schematic model of this pressure sensor is shown in Figure 5.22.

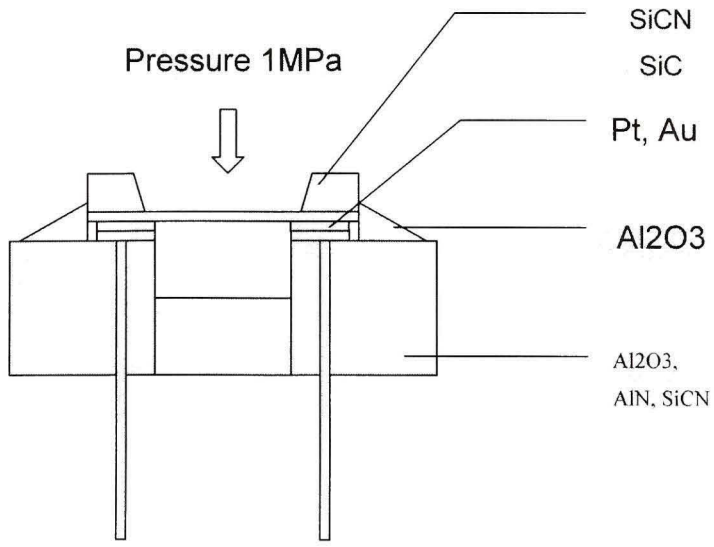

Figure 5.22 Scheme for material comparison (side view).

The simulations have been done in ANSYS by using a meshing like Figure 4.5. As results, the Von Mises stresses corresponding to the different materials are shown in Figure 5.23 to Figure 5.32.

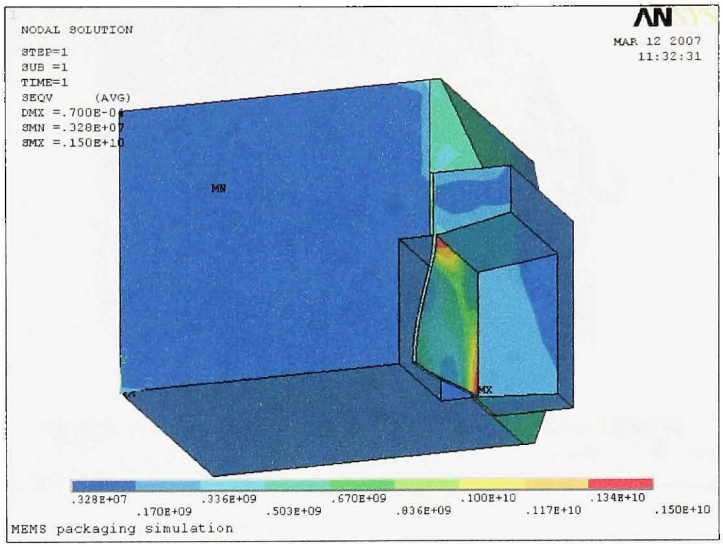

Figure 5.23 Von Mises stress (SiCN die, AlN sub., Al_2O_3, Pt).

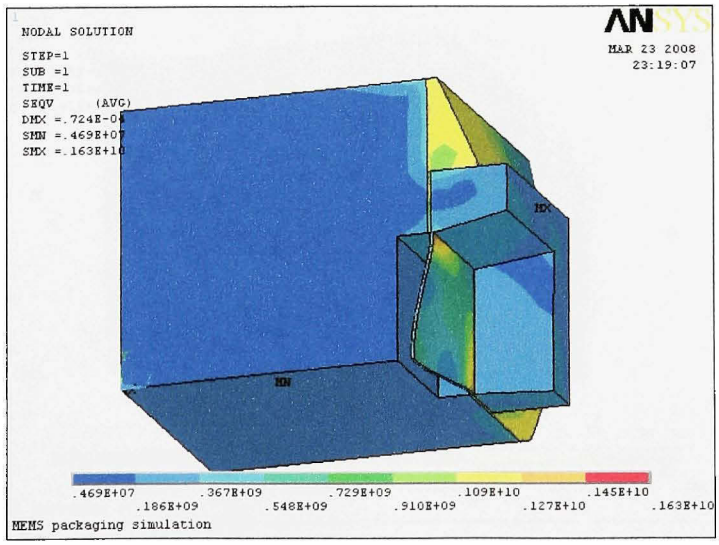

Figure 5.24 Von Mises stress (SiCN die, SiCN sub., Al_2O_3, Pt).

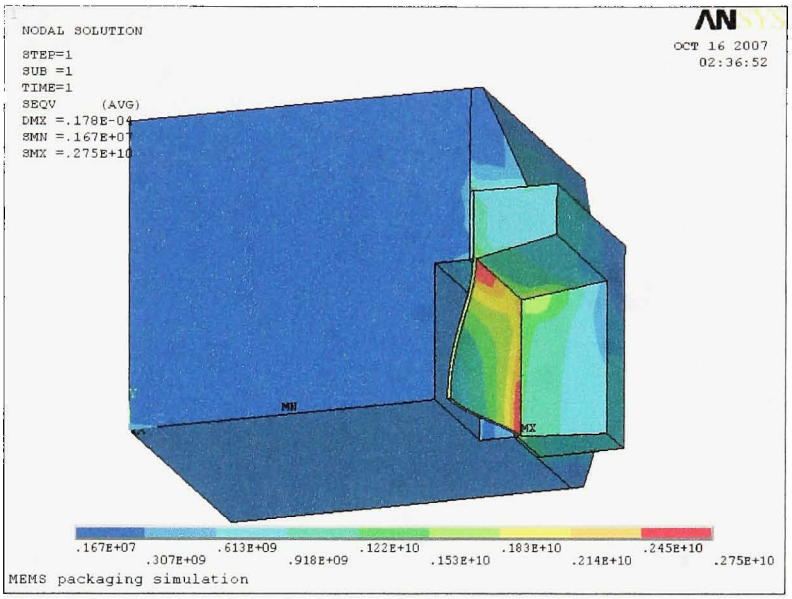

Figure 5.25 Von Mises stress (SiC, Al_2O_3 sub., Al_2O_3, Au).

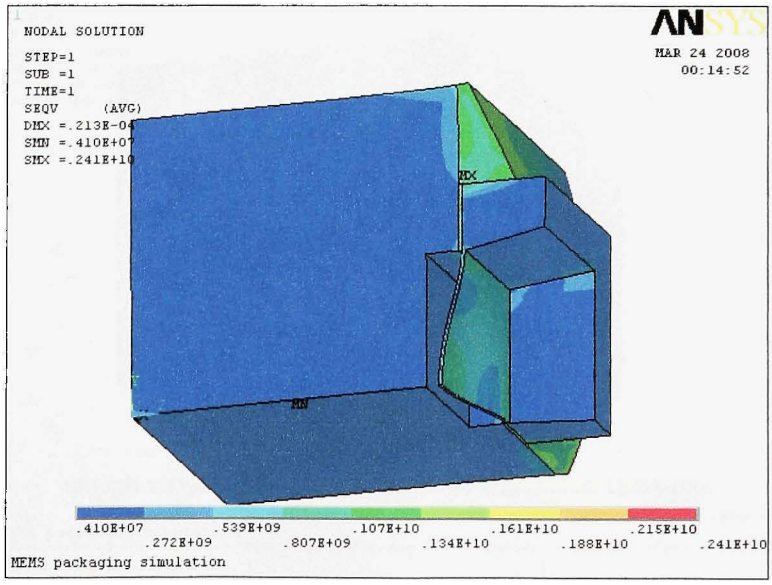

Figure 5.26 Von Mises stress (SiC die, SiCN sub., Al_2O_3, Au).

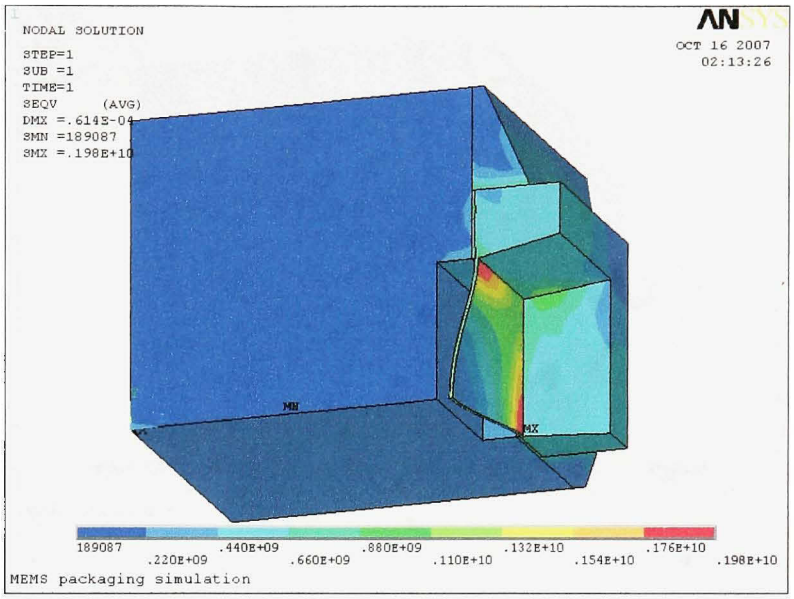

Figure 5.27 Von Mises stress (SiCN die, Al_2O_3 sub., Al_2O_3, Au).

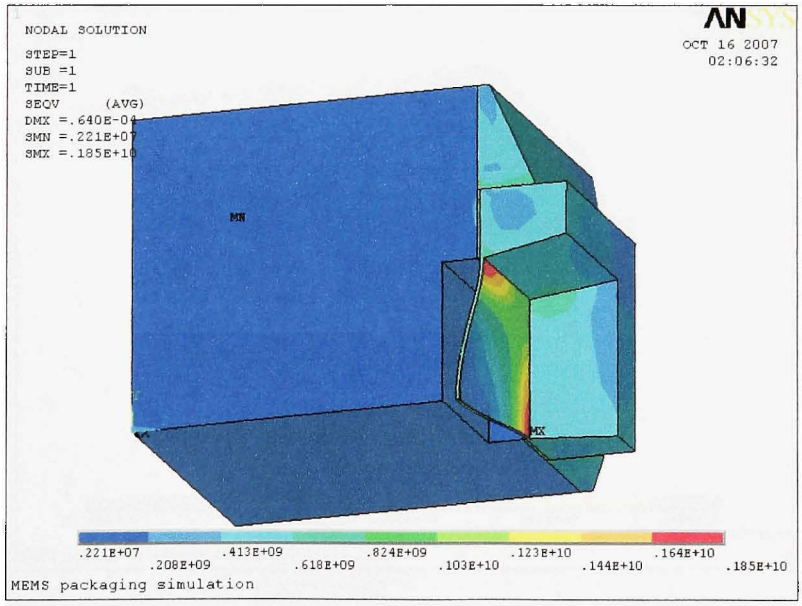

Figure 5.28 Von Mises stress (SiCN die, AlN sub., Al_2O_3, Au).

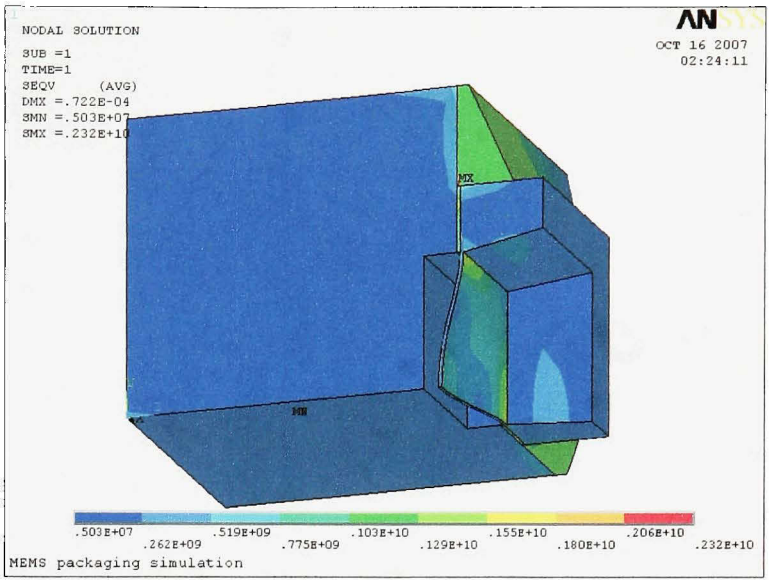

Figure 5.29 Von Mises stress (SiCN die, SICN sub., Al_2O_3, Au).

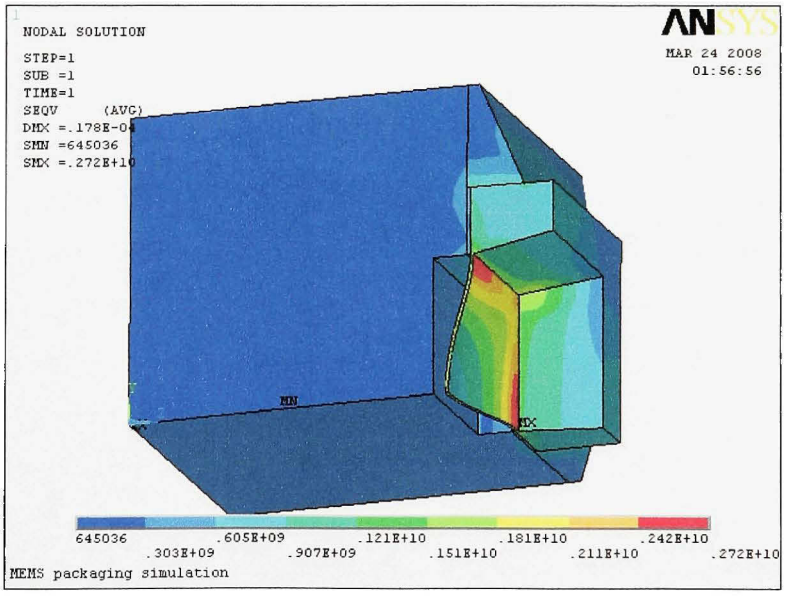

Figure 5.30 Von Mises stress (SiC die, Al_2O_3 sub., Al_2O_3, Pt).

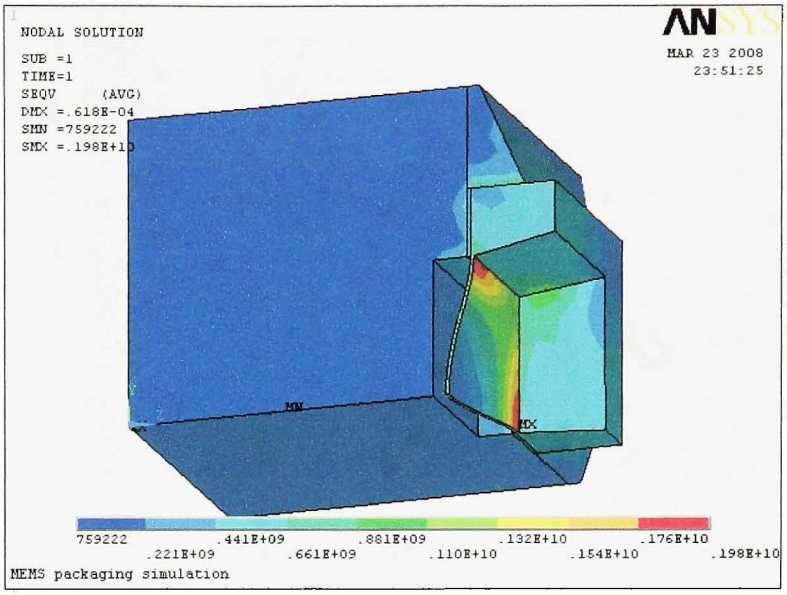

Figure 5.31 Von Mises stress (SiCN die, Al_2O_3 sub., Al_2O_3, Pt).

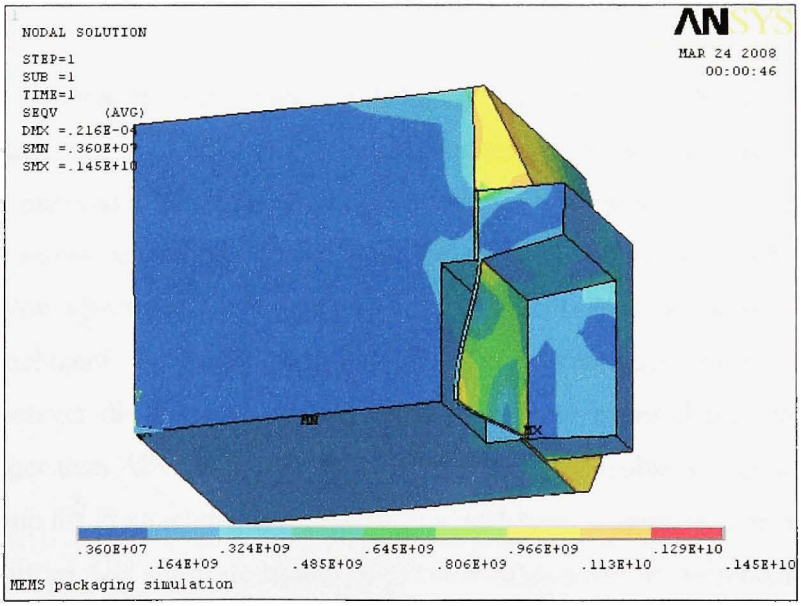

Figure 5.32 Von Mises stress (SiC die, SICN sub., Al_2O_3, Pt).

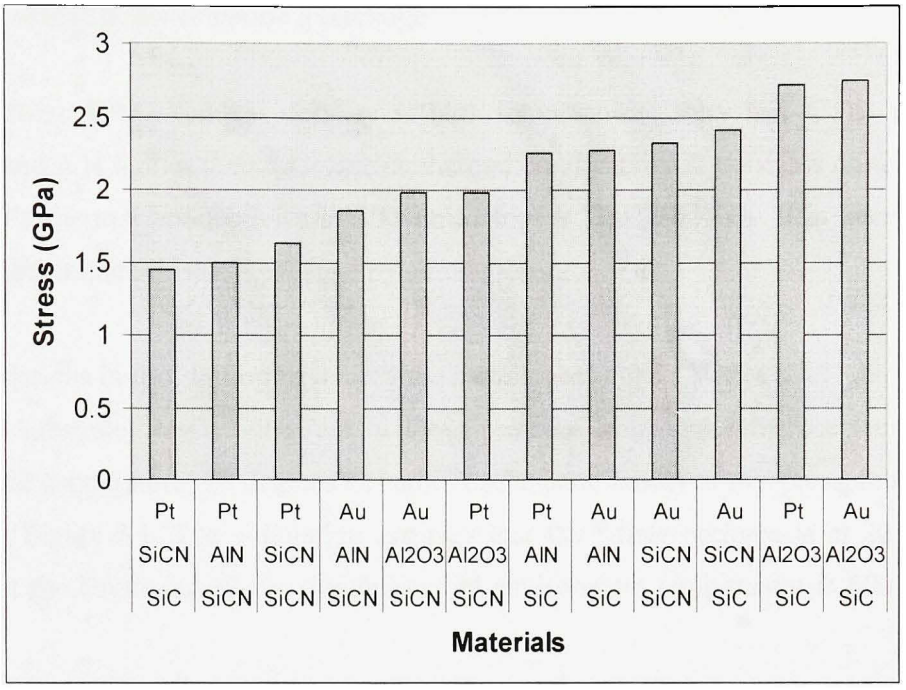

Figure 5.33 Maximum Von Mises stress comparison in different materials packaging.

Figure 5.33 is made by using Figure 5.9, Figure 5.13, and from Figure 5.23 to Figure 5.32, the blue bars represent Von Mises stress and each column under the blue bars represents a material combination: the first row represents electrical attachment material, the second shows substrate material and the third means sensor chip material. The maximum Von Mises stresses are significantly different. Pt attachment is always better than Au attachment if die and substrate material are fixed. Al_2O_3 is not good substrate material whatever die material and electrical attachment material are, because thermal stress is bigger than AlN and SiCN. A SiC die plus a SiCN substrate seem to be the best material group for Pt attachment, because it has the lowest maximum Von Mises stress. A SiCN die plus an AlN substrate is also good for Pt attachment or Au attachment. Most of SiCN combinations are better than SiC. These results were obtained by using static simulation which means that time was not considered and all sensor part were assumed at the same temperature.

5.8 Heat transfer inside a package

SiCN has excellent chemical stability at high temperatures, very low CTE, and high strength and it is lighter than SiC. But its thermal conductivity is very low comparing to SiC (SiC's thermal conductivity is 300 times higher that SiCN's.). It is necessary to observe heat transfer inside a package by simulations.

The simulations in this section have used the model: prototype 1 with a SiCN die or a SiC die, AlN substrate, Al_2O_3 adhesives, without pressure load, and reference temperature (stress-free temperature) 20 degrees Celsius. A schematic model of this pressure sensor is shown in Figure 5.1. The simulation assumes that the whole package is at 20 degrees Celsius at the beginning of the simulation and environment temperature is 600 degrees Celsius.

The simulation has been done in ANSYS by using a meshing like Figure 4.2. As results, temperature contour figures in this model from the simulation are shown in Figure 5.34 and Figure 5.35.

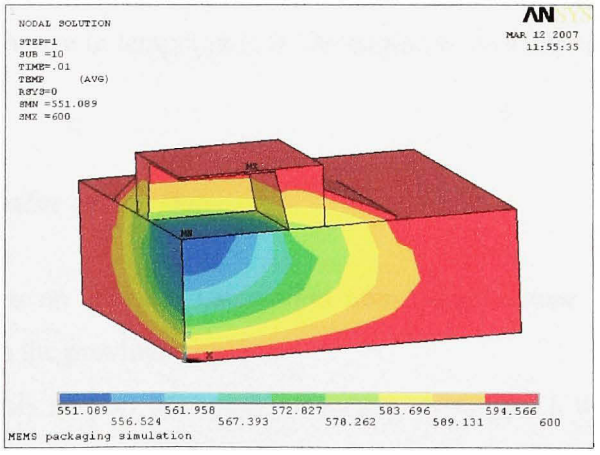

Figure 5.34 Temperature contour SiC+AlN+Al_2O_3 after 10ms.

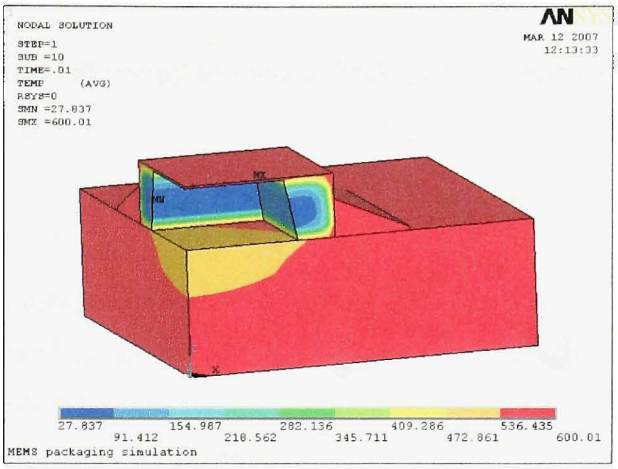

Figure 5.35 Temperature contour SiCN+AlN+Al_2O_3 after 10ms.

The temperature in the center of SiCN die is 27.837 degrees Celsius in the figure. Compared with that of SiC die, the temperature is 551 degree Celsius. There is a big difference inside a SiCN die sensor. If environment temperature changes rapidly, temperature inside the package will be much different and thermo mechanical stress will grow up because material expanses or shrinks disproportionally. It may cause sensor damage or failure. So, a SiCN sensor is not suitable for temperature rapid changing applications. If the change in temperature in the engine is slow, then this point will not be a concern.

5.9 Heat transfer calculation

This section includes an analysis calculation about temperature inside a sensor chip which is simulated in the previous section.

The calculation in this section has used the model: prototype 1 with a SiCN die, AlN substrate, Al_2O_3 adhesives, without pressure load. This calculation assumes the whole package is at 20 degrees Celsius at the beginning of the simulation and environment temperature is 600 degrees Celsius.

The equation relating heat energy to specific heat capacity, where the unit quantity is in terms of mass is:

$$Q = m\ c\ \Delta T \qquad \textbf{(2)}$$

where

Q is the heat energy put into or taken out of the substance,

m is the mass of the substance,

c is the specific heat capacity,

ΔT is the temperature differential.

This is heat capacity equation.

By integrating the differential form over the material's total surface *S*, the integral form of Fourier's law is:

$$\frac{\partial Q}{\partial t} = -k \oint_S \nabla T * dS \qquad \textbf{(3)}$$

where

Q is the amount of heat transferred,

t is the time taken,

k is the materials conductivity.

S is the area through which the heat is flowing,

T is the temperature.

The differential equation (3), when integrated for a simple linear situation, where uniform temperature across equally sized end surfaces and perfectly insulated sides exist, gives the heat flow rate between the end surfaces as:

$$\frac{\Delta Q}{\Delta t} = -k A \frac{\Delta T}{\Delta x} \qquad \textbf{(4)}$$

where

A is the cross-sectional surface area,

ΔT is the temperature difference between the ends,

Δx is the distance between the ends.

A small MATLAB script (.M file) has been written according to Equation (4) and run in MATLAB and the result is shown in Figure 5.36 (Appendix II).

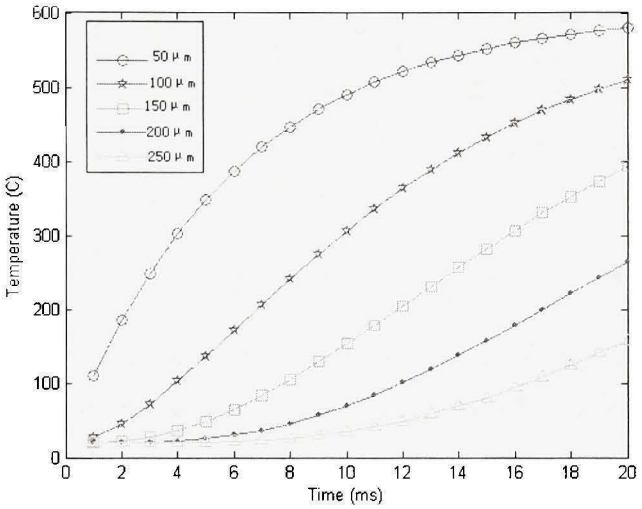

Figure 5.36 Temperature change inside a SiCN die.

Figure 5.36 shows how temperature changes in the first 20ms. The X axis represents time (unit 1ms) and the Y axis represents temperature (unit degree Celsius). The o line represents temperature inside the sensor 50μm far away from the surface. The others are the * line 100μm, the □ line 150μm, the ▪ line 200μm, and the Δ line 250μm far away from the surface. The calculation result is similar to the simulation results (Figure 5.35).

5.10 Stress-free temperature

Stress free temperature is the temperature when all inner stresses are zero. It is also used as reference temperature to simulation.

The stress-free temperature in the earlier simulations is 20 degrees Celsius or 0 degree Celsius. It means that the stress inside a sensor equals to 0 when temperature is 20 degrees Celsius or 0 degree Celsius. In fact, residual stresses always exist because of high temperature process during the fabrication of sensor. The stress-free temperature may change when the fabrication techniques modify. The simulations in this section try to describe how Von Mises stress changes when the stress-free temperature varies.

The first simulations in this section have used the model: prototype 1 cuboid shape with a SiCN die, AlN substrate, Al_2O_3 adhesives, with 1 M Pa pressure load, and environment temperature 0 degree Celsius. Reference temperature (stress-free temperature) has changed from 0 degree Celsius to 600 degrees Celsius. A schematic model of this pressure sensor is shown in Figure 5.5.

The simulations have been done in ANSYS by using a meshing like Figure 4.2. As the results, the displacements in different temperatures condition from the simulations are shown in Figure 5.37 (a, b, c, d, e, f and g).

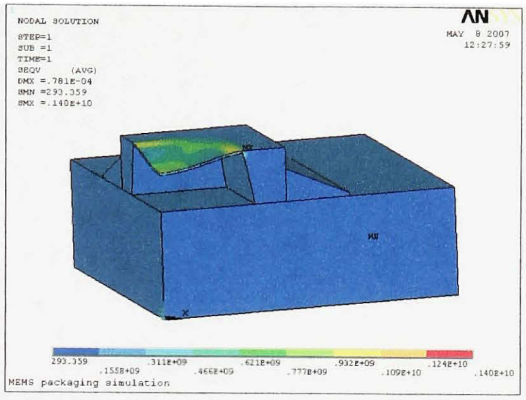

(a) 0 degree Celsius

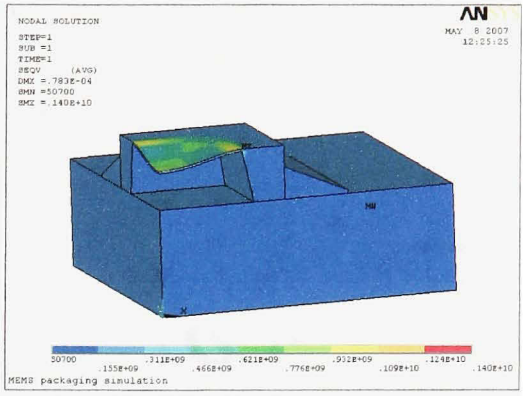

(b) 100 degrees Celsius

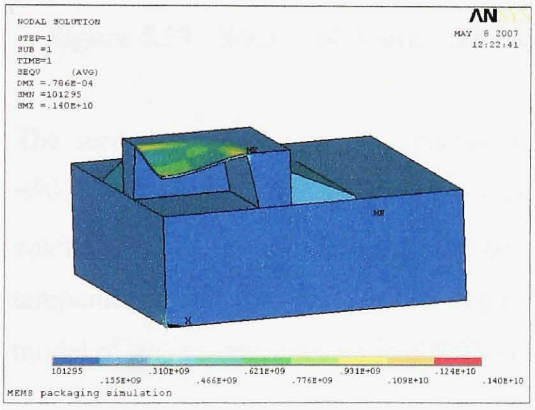

(c) 200 degrees Celsius

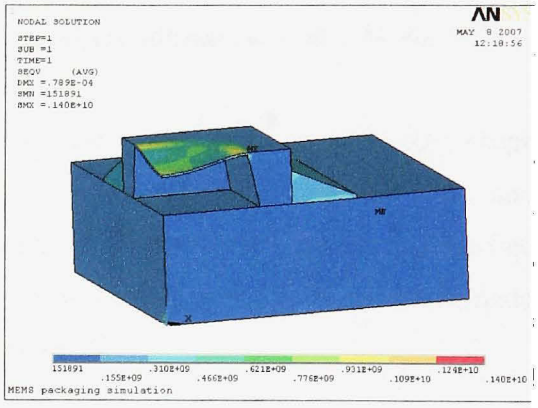

(d) 300 degrees Celsius

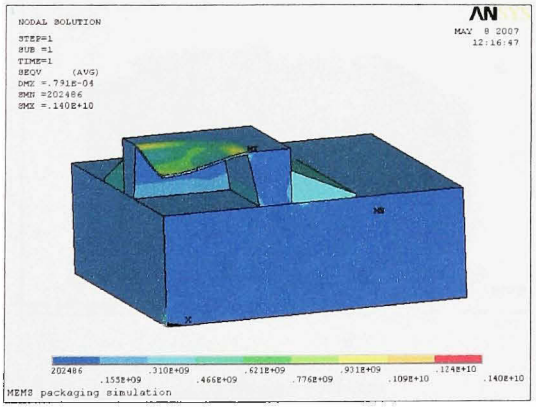

(e) 400 degrees Celsius

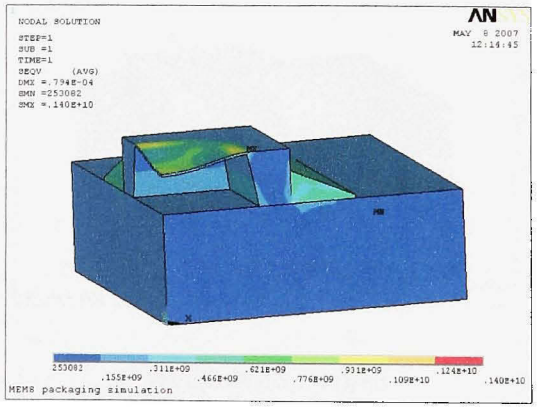

(f) 500 degrees Celsius

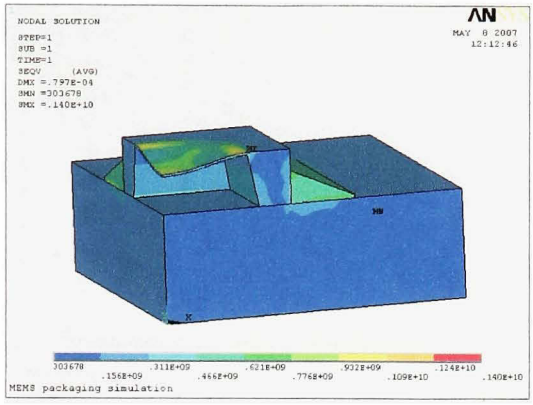

(g) 600 degrees Celsius

Figure 5.37 Stress SiCN die, AlN substrate, Al_2O_3 adhesives, with 1 M Pa, 0°C.

The second simulations in this section have used the model: prototype 1 cuboid shape with a SiCN die, AlN substrate, Al_2O_3 adhesives, with 1 M Pa pressure load, and environment temperature 600 degrees Celsius. Reference temperature (stress-free temperature) has changed from 0 degree Celsius to 600 degrees Celsius. A schematic model of this pressure sensor is also shown in Figure 5.5.

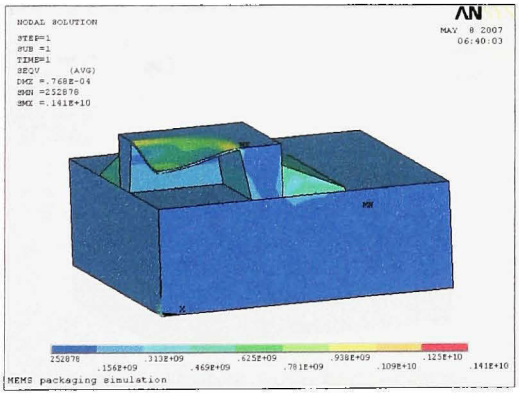

(a) 0 degree Celsius

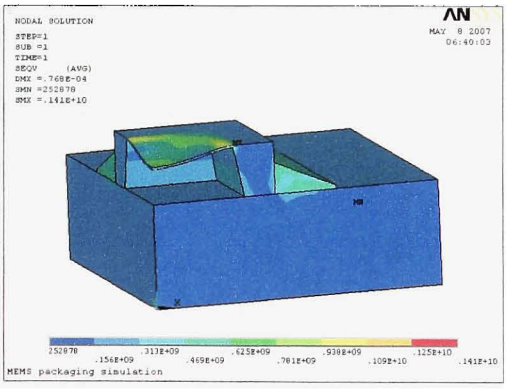

(b) 100 degrees Celsius

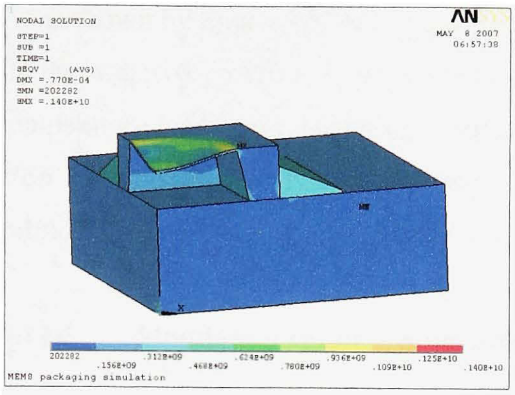

(c) 200 degrees Celsius

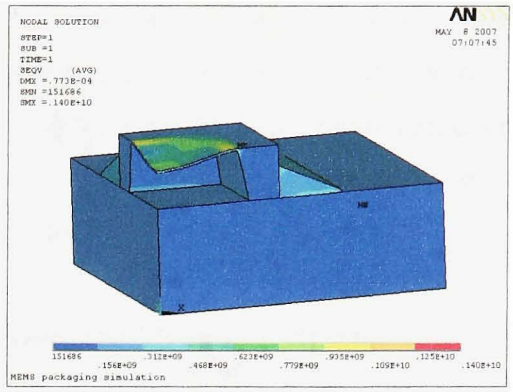

(d) 300 degrees Celsius

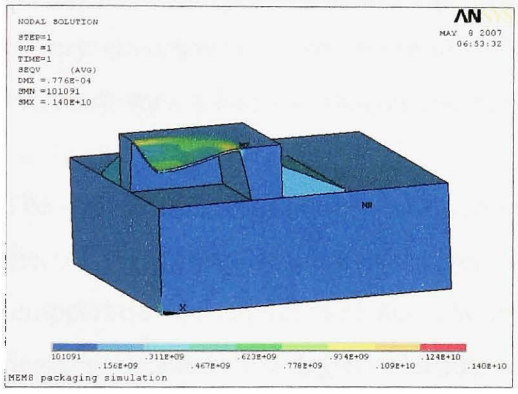

(e) 400 degrees Celsius

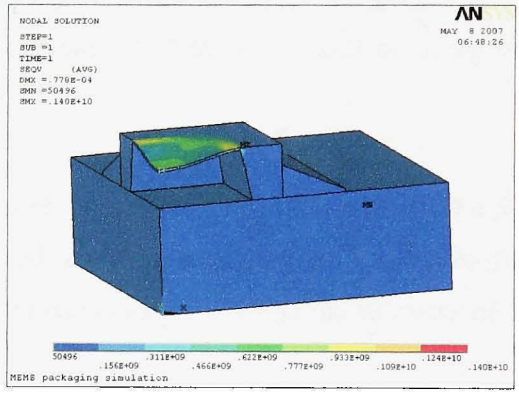

(f) 500 degrees Celsius

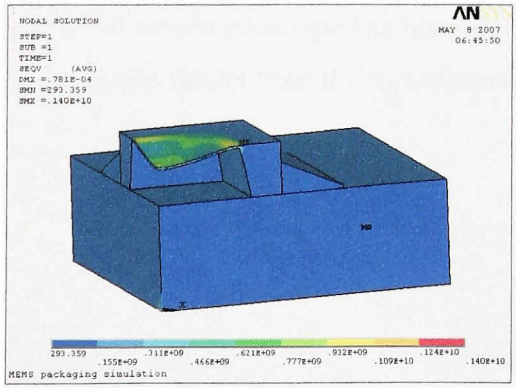

(g) 600 degrees Celsius

Figure 5.38 Stress SiCN die, AlN substrate, Al_2O_3 adhesives, 1 M Pa, 600 °C.

As is shown by Figure 5.37 and Figure 5.38, Von Mises stresses in the sensor are reduced in the adhesive portion if the reference temperature is close to the midpoint of the temperature load range. It is observed that reducing the reference temperature reduces the Von Mises stresses. If it is possible to change stress-free temperature in the sensor fabrication process, it will be helpful to optimize the sensor design.

5.11 Simulation result comparison between ANSYS and FEMLAB

FEA almost always can give us a result but the result should be analyzed carefully. "Finite Element Analysis makes a good engineer great, and a bad engineer dangerous!" It is very important to verify the results. There is a way to check the results by using two FEA software systems to analyze one model.

The simulation in this section has used the model: prototype 2 cylinder shape with a SiC die, AlN substrate, with 100M Pa pressure load, and reference temperature (stress-free temperature) 20 degrees Celsius. The sensor is subjected to a temperature cycle of 20 degrees Celsius to 600 degrees Celsius.

The simulation has been done in ANSYS by using a meshing like Figure 4.4. Only a quarter of sensor prototype has been simulated. As results, Von Mises stress distribution figure in this model from the simulation is shown in Figure 5.39.

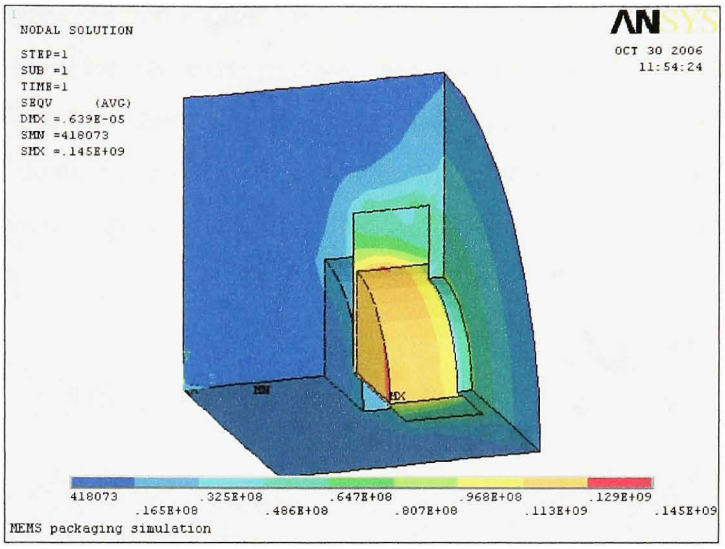

Figure 5.39 Von Mises stress (SiC die, AlN substrate, 0.02mm thick) in ANSYS.

The simulation has been done in FEMLAB by using an automatic meshing. As results, Von Mises stress distribution figure in this model from the simulation is shown in Figure 5.40.

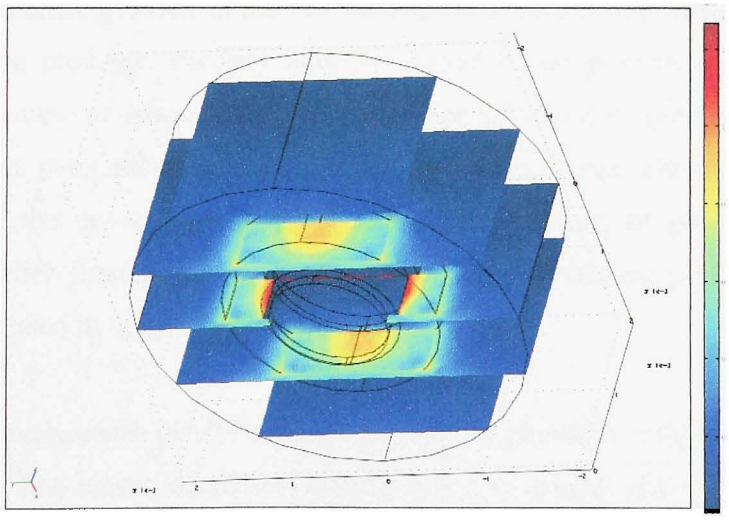

Figure 5.40 Von Mises stress (SiC die, AlN, 0.02mm membrane) in FEMLAB.

Comparing Figure 5.39 and Figure 5.40, we can see that sensor membranes and sensor chip cavity surfaces are the most stressful, and bonding surfaces between sensor chips and packages have less stress than the membranes. Sensor chips have more stress than their packages. Both results have similar stress distributions. The maximum Von Mises stresses are shown in Table 5.2. There is no big difference between ANSYS result and FEMLAB result.

Table 5.2

ANSYS and FEMLAB simulation result comparison

Simulation software	Maximum Von Mises stress
ANSY	1.45 G Pa
FEMLAB	1.267 G Pa

5.12 Porosity

Porosity is a measure of the void spaces in a material, and is measured as a fraction, between 0–1, or as a percentage between 0–100%. In manufacturing of metal or plastic parts and assemblies, porosity in the raw material is a serious issue affecting the quality of the resulting products. Porosity may be caused by temperature control problems, material impurities, or other causes in the casting of metal or plastic parts. Porosity internal to cast parts may become external or surface pores when material is then removed from the raw part material by machining, grinding or other manufacturing operations. Earlier simulations are based on that all materials are perfect. So, porosity should be simulated in order to reflect reality.

In addition, some research results indicate the effect of porosity on the elastic modulus of silver powder. The elastic decreases with decrease in density (for a 20% decrease in density, the modulus of elasticity reduces by about 37%. Beyond a 20% decrease in density, the modulus of elasticity stabilizes [59]). From the study of the Ag powder, it is

evident that the porosity level affects the modulus. Such a study has not been conducted for gold attach. However, the gold attach is also assumed to be affected by varying porosity levels. Hence, the stress patterns in the die and attach layers have been studied for another modulus of elasticity corresponding to the silver porosity data.

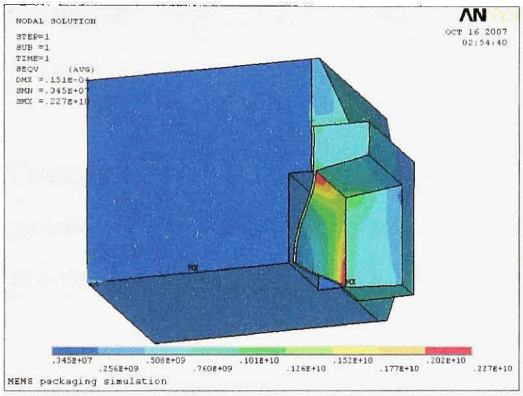

(a) stress (perfect Au attach)

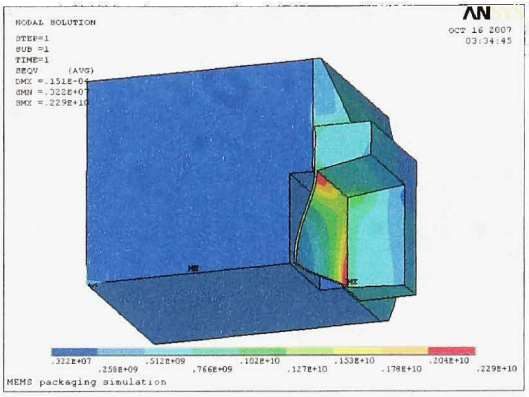

(b) stress (Au 80% density)

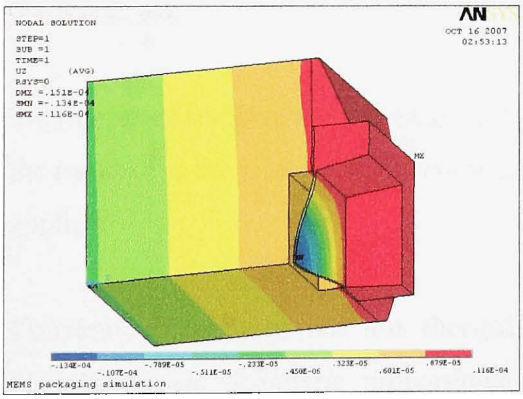

(c) displacement (perfect Au attach)

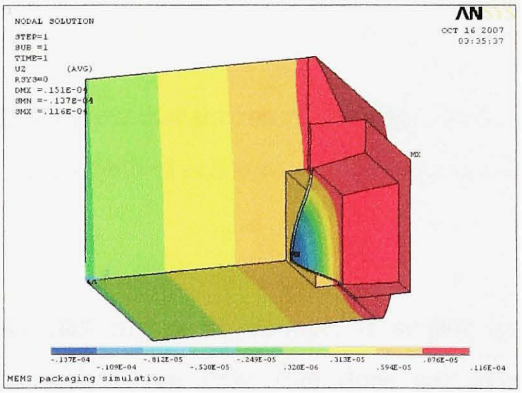

(d) displacement (Au 80% density)

Figure 5.41 Porosity simulation results.

The simulation in this section has been done by using the model: prototype 2 cuboid shape with a SiC die, AlN substrate, Al_2O_3 adhesives, Au attach (80% density, 63%

modulus), with 1M Pa pressure load and reference temperature (stress-free temperature) 20 degree Celsius. The sensor is also subjected to a temperature cycle of 20 degrees Celsius to 600 degree Celsius.

The simulations have been done in ANSYS by using a meshing like Figure 4.5. As results, the displacement and Von Mises stress from the simulations are shown in Figure 5.41.

Compared with the perfect gold attach, there is a minute difference in the Von Mises stress distribution. The maximum stress in (b) is 2.29 G Pa and that in (a) is 2.27 G Pa. For the displacements, (c) and (d) are almost identical.

5.13 Summary

In this chapter, different kinds of simulation have been done, and the simulation results are presented.

Thermo mechanical stress distribution simulations show that the most stressful portion in the package is the joint of sensor membrane with an applied pressure, or without pressure applied.

Conventional package has less thermal stress than flip chip package. If sensor chip dimensions are geometric proportionally changed, sensor chip size does not affect thermal stress. Moreover If only sensor membrane thickness changes (other portion keep the same dimension), increasing a sensor chip membrane thickness can decrease thermal stress.

With the increase in temperature, heat deformation will also increase. For membrane deformation, there has been a 12% increase in the displacement in the center of membrane when temperature changes from 0 degree Celsius to 600 degrees Celsius.

Different materials will get different thermal stress. Pt attachment is better than Au attachment. Al_2O_3 is not good substrate material comparing to AlN and SiCN. A SiC die plus a SiCN substrate and Pt attachment seem to be the best material combination. A SiCN die plus an AlN substrate is also good for Pt attachment or Au attachment. Most of SiCN combinations are better than SiC's.

Transient heat transfer simulation shows that SiCN is not suitable for temperature rapid changing applications because of its low thermal conductivity. A heat transfer calculation in MATLAB was completed as a verification of transient heat transfer simulation.
If the stress-free temperature is close to the midpoint of the temperature load range, it is helpful to reduce thermal stress.

A FEMLAB simulation was done by using the same model than ANSYS, their similar results can verify each other.

A comparison between Au attach (80% density, 63% modulus) and Au attach (100% density, 100% modulus) was processed with 1M Pa pressure load and room temperature environment. The thermal stresses are almost same, but 80% density Au only has 63% modulus.

CONCLUSION

In this study, a literature review about MEMS packaging was done. Some existing MEMS sensor packagings were analyzed. Two packaging designs that met the specifications identified by the involved industrial company were given and simulated by using finite element analysis. Real sensor packages are not obtained because sensor chips are not available for now.

In this thesis, two high temperature MEMS pressure sensor packaging prototypes (conventional package and flip-chip package) have been developed, simulated and discussed. Prototype 2 (flip-chip package) is better than Prototype 1 (conventional package) because Prototype 2 can avoid wire bonding in which gold wire is exposed in the air and it is unstable due to jet engine corrosive environment at 600°C and platinum wire bonding might not be available in the industry even though platinum is more stable than gold in a hot air environment.

Material selecting is a key part of the thesis. To package high temperature MEMS, materials should have high thermal conductivity, thermo mechanical compatibility, high thermal shock resistance, high strength and high chemical compatibility. A candidate material list for high temperature packaging has been listed. In the list, SiC and SiCN are used to be die material; SiCN, Alumina and AlN as constraint base material; platinum and gold as electrical attach material; Aluminum compound as adhesive material.

SiC and SiCN are selected to be sensor chip material because SiC has excellent chemical stability at high temperatures, high thermal conductivity and there are some existing SiC sensor chips which can work at 600 degrees Celsius. SiCN also has excellent chemical stability at high temperatures, very low CTE, and high strength. Moreover, as a part of CRIAQ 6.2, the researchers of Concordia University have found that SiCN has a potential ability to work at 1300 degree Celsius. SiCN material has very low thermal

conductivity. This might limit its application because temperature rapidly changing environment on SiCN will present big temperature difference increasing stress in the die. A SiCN die plus an AlN substrate is the best material group for Au attachment package.

Metallization is mature in the industry. Most metal films are fabricated by CVD. A Ti/Pt/Au system could be recommended.

FEA models have been generated and some simulations have been done. In order to verify the output result, both ANSYS and FEMLAB have applied to an identical model. Von Mises stresses, deformations and temperature distribution in the package models have been obtained. Discussions about sensor chip size, membrane thickness, heat deformation, heat transfer, porosity, stress-free temperature and different material comparison were presented. In all the FEA models, the attachment is assumed to be perfectly bonded to the substrate and the die. In addition, the boundary conditions permit no slip.

In conclusion, if Pt wire bonding technique is available, conventional packaging should be adopted because its package has the less thermal stress and Pt wire has better high temperature stability than gold. Otherwise, flip-chip packaging could protect inside electrical attachment from high temperature and it is more reasonable. The original objectives of the research were achieved except for the fabrication and testing due to the unavailability of the high temperature sensor chip at this time.

RECOMMENDATIONS

The final object for a packaging design is to make one in a factory. In order to achieve this object, a real sensor chip should be done and some key data about packaging should be obtained. New simulations should be performed because model size probably is going to modify and exact material properties (different provider's commercial materials have minor differences) should be input in the ANSYS or other FEA software. Simulation should also be verified by fabrication and testing. Wafer-to-wafer bonding should be considered and simulated in the future work. In Dr. Schmidt's review/invited paper, wafer to wafer bonding was discussed and a pressure sensor example was given [60]. Solder bump material is pivotal for flip-chip. It deserves an investigation.

APPENDIX I

ANSYS SCRIPT

```
!Ansys scripts prototype 2
!SiC die, AlN substrate, alumina adhesive, gold attachment.
!
FINISH
/CLEAR   !clears database, closes all the files and start a new

/FILNAME,simu_pressure
/TITLE,MEMS packaging simulation        ! define simulation name and title

/PREP7   ! enters preprocessor
/PNUM,AREA,1

ET,1,SOLID5   !defines SOLID5 as element 1
!*
KEYOPT,1,1,2
KEYOPT,1,3,0
KEYOPT,1,5,0

!SiC material characteristics
MP,DENS,1,3.21e3   !SiC density kg/m3
MP,KXX,1,300                !Thermal conductivity
MPTEMP,1, -15,20,105,205,305,405,505,605,705
MPDATA,ALPX,1,1,2.93e-6,3.35e-6,3.97E-6,4.23e-6,4.46e-6,4.68e-6,4.68e-6,4.89e-
6,5.1e-6,5.29e-6            !Coefficient of thermal expansion
MP,EX,1,4.7E11              !Young's Modulus
MP,PRXY,1,0.3               !Poisson's ratio   or NUXY
MP,C,1,800                  !specific heat capacity
MP,HF,1,5                   ! CONVECTION COEFFICIENT

!AlN material characteristics
MP,DENS,2,3.31e3   !AlN
MP,KXX,2,200
MP,EX,2,3.2E11
MP,PRXY,2,0.31
MPTEMP,1, -15,20,105,205,305,405,505,605,705
MPDATA,ALPX,2,1,3.14e-6,3.9e-6,5.36e-6,6.51e-6,7.25e-6,7.76e-6,8.25e-6,8.72e-
6,9.09e-6
MP,C,2,710
```

```
MP,HF,2,5              ! CONVECTION COEFFICIENT

!Alumina material characteristics
MP,DENS,3,3.75e3   !Alumina
MP,KXX,3,36
MP,EX,3,3.97E11
MP,PRXY,3,0.31
!MP,ALPX,3,6.57E-6
MPTEMP,1, -15,20,105,205,305,405,505,605,705
MPDATA,ALPX,3,1,5.34e-6,6.20e-6,7.83e-6,8.48e-6,8.89e-6,9.28e-6,9.65e-6,10e-
6,10.33e-6
MP,C,3,800
MP,HF,3,5              ! CONVECTION COEFFICIENT

!Au material characteristics
MP,DENS,4,19.28e3
MP,KXX,4,315
MP,EX,4,7.8e10
MP,PRXY,4,0.44
MPTEMP,1, -15,20,105,205,305,405,505,605,705
MPDATA,ALPX,4,1,14.04e-6,14.24e-6,14.71e-6,15.23e-6,15.75e-6,16.29e-6,16.89e-
6,17.58e-6,18.38e-6
MP,C,4,128.74
MP,HF,4,5              ! CONVECTION COEFFICIENT

!define model dimension variables (m)
SUBL=1800e-6                !substrate length
SUBW=1800e-6                !substrate width
SUBH=2000E-6                !substrate height
CSL=800E-6
CSW=800E-6
CSH=200E-6
DIEL=1200E-6                !die length
DIEW=1200E-6                !die width
DIEH=500E-6                 !die height
CDBL=800E-6
CDBW=800E-6
CDML=860E-6
CDMW=860E-6
CDTL=900E-6
CDTW=900E-6
CDH=480E-6
FILMH=20E-6                 !membrane thickness
SEALH=300E-6
```

```
SEALH1=30E-6
SEALW=600E-6

!define model key point,
K,100,0,0,0
K,101,0,SUBL,0
K,102,SUBW,SUBL,0
K,103,SUBW,0,0
K,111,0,DIEL,0
K,112,DIEW,DIEL,0
K,113,DIEW,0,0
K,121,0,CSL,0
K,122,CSW,CSL,0
K,123,CSW,0,0

K,200,0,0,SUBH-CSH
K,201,0,SUBL,SUBH-CSH
K,202,SUBW,SUBL,SUBH-CSH
K,203,SUBW,0,SUBH-CSH
K,211,0,DIEL,SUBH-CSH
K,212,DIEW,DIEL,SUBH-CSH
K,213,DIEW,0,SUBH-CSH
K,221,0,CSL,SUBH-CSH
K,222,CSW,CSL,SUBH-CSH
K,223,CSW,0,SUBH-CSH

K,300,0,0,SUBH
K,301,0,SUBL,SUBH
K,302,SUBW,SUBL,SUBH
K,303,SUBW,0,SUBH
K,311,0,DIEL,SUBH
K,312,DIEW,DIEL,SUBH
K,313,DIEW,0,SUBH
K,321,0,CSL,SUBH
K,322,CSW,CSL,SUBH
K,323,CSW,0,SUBH

K,400,0,0,SUBH+FILMH
K,401,0,SUBL,SUBH+FILMH
K,402,SUBW,SUBL,SUBH+FILMH
K,403,SUBW,0,SUBH+FILMH
K,411,0,DIEL,SUBH+FILMH
K,412,DIEW,DIEL,SUBH+FILMH
K,413,DIEW,0,SUBH+FILMH
```

```
K,421,0,CDBL,SUBH+FILMH
K,422,CDBW,CDBL,SUBH+FILMH
K,423,CDBW,0,SUBH+FILMH

K,500,0,0,SUBH+FILMH+DIEH-CDH
K,501,0,SUBL,SUBH+FILMH+DIEH-CDH
K,502,SUBW,SUBL,SUBH+FILMH+DIEH-CDH
K,503,SUBW,0,SUBH+FILMH+DIEH-CDH
K,511,0,DIEL,SUBH+FILMH+DIEH-CDH
K,512,DIEW,DIEL,SUBH+FILMH+DIEH-CDH
K,513,DIEW,0,SUBH+FILMH+DIEH-CDH
K,521,0,CDBL,SUBH+FILMH+DIEH-CDH
K,522,CDBW,CDBL,SUBH+FILMH+DIEH-CDH
K,523,CDBW,0,SUBH+FILMH+DIEH-CDH

K,600,0,0,SUBH+FILMH+DIEH-CDH+SEALH
K,601,0,SUBL,SUBH+FILMH+DIEH-CDH+SEALH1
K,602,SUBW,SUBL,SUBH+FILMH+DIEH-CDH+SEALH1
K,603,SUBW,0,SUBH+FILMH+DIEH-CDH+SEALH1
K,611,0,DIEL,SUBH+FILMH+DIEH-CDH+SEALH
K,612,DIEW,DIEL,SUBH+FILMH+DIEH-CDH+SEALH
K,613,DIEW,0,SUBH+FILMH+DIEH-CDH+SEALH
K,621,0,CDML,SUBH+FILMH+DIEH-CDH+SEALH
K,622,CDMW,CDML,SUBH+FILMH+DIEH-CDH+SEALH
K,623,CDMW,0,SUBH+FILMH+DIEH-CDH+SEALH

K,700,0,0,SUBH+FILMH+DIEH
K,701,0,SUBL,SUBH+FILMH+DIEH
K,702,SUBW,SUBL,SUBH+FILMH+DIEH
K,703,SUBW,0,SUBH+FILMH+DIEH
K,711,0,DIEL,SUBH+FILMH+DIEH
K,712,DIEW,DIEL,SUBH+FILMH+DIEH
K,713,DIEW,0,SUBH+FILMH+DIEH
K,721,0,CDTL,SUBH+FILMH+DIEH
K,722,CDTW,CDTL,SUBH+FILMH+DIEH
K,723,CDTW,0,SUBH+FILMH+DIEH

!connect keypoints to lines
L,111,211
L,211,311
L,311,411
L,411,511
L,511,611
L,611,711
```

```
L,311,312
L,313,312
L,302,312
L,312,322

!Defines a area through keypoints.
A,100,121,122,123
A,111,112,122,121
A,101,102,112,111
A,113,112,122,123
A,103,102,112,113

A,101,102,202,201
A,103,102,202,203
A,301,302,202,201
A,303,302,202,203
A,301,302,402,401
A,303,302,402,403
A,501,502,402,401
A,503,502,402,403
A,501,502,602,601
A,503,502,602,603

A,601,602,612,611
A,603,602,612,613
A,711,712,612,611
A,713,712,612,613

A,500,521,522,523
A,521,522,622,621
A,523,522,622,623
A,721,722,622,621
A,723,722,622,623
A,721,722,712,711
A,723,722,712,713

!Defines a volume through keypoints.
V,100,121,122,123,200,221,222,223!ALN
V,111,112,122,121,211,212,222,221
V,101,102,112,111,201,202,212,211
V,113,112,122,123,213,212,222,223
V,103,102,112,113,203,202,212,213

V,311,312,322,321,211,212,222,221
```

```
V,301,302,312,311,201,202,212,211
V,313,312,322,323,213,212,222,223
V,303,302,312,313,203,202,212,213

V,311,312,322,321,411,412,422,421!METALLIZATION
V,301,302,312,311,401,402,412,411!SEALING GLASS
V,313,312,322,323,413,412,422,423
V,303,302,312,313,403,402,412,413

V,400,421,422,423,500,521,522,523!MEMBRANE
V,511,512,522,521,411,412,422,421!SIC
V,501,502,512,511,401,402,412,411!SEALING GLASS
V,513,512,522,523,413,412,422,423
V,503,502,512,513,403,402,412,413

V,511,512,522,521,611,612,622,621!SIC
V,501,502,512,511,601,602,612,611!SEALING GLASS
V,513,512,522,523,613,612,622,623
V,503,502,512,513,603,602,612,613

V,711,712,722,721,611,612,622,621!SIC
V,713,712,722,723,613,612,622,623

! glue volumes, change view angle and plot.
VGLUE,ALL
/PNUM,VOLU,1
/VIEW,,-3,-1,1
!/TYPE,,4
VPLOT

! divide lines in order to mesh.
LESIZE,1,,,4
LESIZE,2,,,3
LESIZE,3,,,2
LESIZE,4,,,2
LESIZE,5,,,3
LESIZE,6,,,2
LESIZE,7,,,10!GOLD
LESIZE,8,,,10
LESIZE,9,,,6  !SEAL
LESIZE,10,,,4!GOLD

!meshing
VSEL,,,,10     !chooses volume No. 10
```

```
MSHKEY,1    !mapped meshing
VATT,4      !associates element attributes to this volume.
VMESH,10    !meshes volume No. 10

VSEL,,,,12
MSHKEY,1
VATT,4
VMESH,12

VSEL,,,,11    !SEAL
MSHKEY,1
VATT,3
VMESH,11

VSEL,,,,13
MSHKEY,1
VATT,3
VMESH,13

VSEL,,,,6
MSHKEY,1
VATT,2
VMESH,6
VSEL,,,,7
MSHKEY,1
VATT,2
VMESH,7
VSEL,,,,8
MSHKEY,1
VATT,2
VMESH,8
VSEL,,,,9
MSHKEY,1
VATT,2
VMESH,9

VSEL,,,,2
MSHKEY,1
VATT,2
VMESH,2
VSEL,,,,3
MSHKEY,1
VATT,2
VMESH,3
```

```
VSEL,,,,4
MSHKEY,1
VATT,2
VMESH,4
VSEL,,,,5
MSHKEY,1
VATT,2
VMESH,5
VSEL,,,,1
MSHKEY,1
VATT,2
VMESH,1

VSEL,,,,15
MSHKEY,1
VATT,1
VMESH,15
VSEL,,,,16
MSHKEY,1
VATT,3
VMESH,16
VSEL,,,,17
MSHKEY,1
VATT,1
VMESH,17
VSEL,,,,18
MSHKEY,1
VATT,3
VMESH,18
VSEL,,,,14
MSHKEY,1
VATT,1
VMESH,14

VSEL,,,,19
MSHKEY,1
VATT,1
VMESH,19
VSEL,,,,20
MSHKEY,1
VATT,3
VMESH,20
VSEL,,,,21
MSHKEY,1
```

```
VATT,1
VMESH,21
VSEL,,,,22
MSHKEY,1
VATT,3
VMESH,22

VSEL,,,,23
MSHKEY,1
VATT,1
VMESH,23
VSEL,,,,24
MSHKEY,1
VATT,1
VMESH,24

!chooses all surfaces and applies 1 M Pa pressure
ASEL,S,,,1,26
SFA,ALL,1,PRES,1E6        !147psi

FINISH

!solves
/SOLU

!symmetry
NSEL,S,LOC,X,0            !selects a subset of nodes
dsym,,X                   !specifies symmetry DOF constraints on nodes above
NSEL,S,LOC,Y,0
dsym,,Y

ALLSEL,ALL
DK,100,UX,0               !defines DOF constraints at keypoints
DK,100,UY,0
DK,100,UZ,0
TREF,20                   !defines reference temperature
BFUNIF,TEMP,600           !defines model temperature
SOLVE
FINISH
```

APPENDIX II

MATLAB SCRIPT

```
%MATLAB script to calculate temperature inside a SiCN sensor chip
clc;
clear all;
clear;
dt=0.0001;
dx=50e-6;
thickness=500e-6/2;          % sensor chip material thickness
totaltime=0.02;              % total simulation time
highTi=600;                  % high end temperature
lowTi=20;                    %low end temperature
ratio=2.2e3;
c=1100;
k=1;
colc=round(thickness/dx)+1;
rowc=0.02/dt+1;
II=lowTi*ones(rowc,colc);
II(:,1)=highTi;
rown=1;
coln=1;
for J=2:1:colc

for I=1:1:rowc
dT=II(I,J-1)-II(I,J);
dTup=k*dt*dT/dx/dx/c/ratio;
II(I+1,J)=dTup+II(I,J);
if I-floor(I/10)*10==0
III(I/10,J)=II(I+1,J);
end
end
end
plot(III(:,:));
xlabel('Time (ms)');
ylabel('Temperature (C)');
```

BIBLIOGRAPHY

1. Bouchaud, J., *MEMS industry and market overview.* 2008.

2. Christian A. Zorman, M.M., *Materials for Microelectromechanical Systems*, in *The MEMS Handbook*, M. Gad-el-Hak, Editor. 2002, CRC Press.

3. Wilson, J., *Sensor Technology Handbook.* 2005: Elsevier.

4. Harman, G., *Pressure Sensors*, in *Sensor Technology Handbook*, J. Wilson, Editor. 2005, Elsevier.

5. Fontes, J., *Temperature Sensors*, in *Sensor Technology Handbook*, J. Wilson, Editor. 2005, Elsevier.

6. Lin, L., *Packaging Schemes for MEMS.* 2004.

7. Chen, L.-Y. and J.-F. Lei, *Packaging of Harsh-Environment MEMS Devices, The MEMS Handbook*, M. Gad-el-Hak, Editor. 2002, CRC Press.

8. Reichl, H. and V. Grosser. *Overview and development trends in the field of MEMS packaging.* in *Micro Electro Mechanical Systems, 2001. MEMS 2001. The 14th IEEE International Conference on.* 2001.

9. CRIAQ, *MEMS Based Gas Turbines Control.* 2007.

10. Boyce, M.P., *Gas Turbine Engineering Handbook (THIRD EDITION).* 2001: Gulf Professional Publishing.

11. Chang, J.C.D.a.C.T., *Active Control of High Frequency Combustion Instability in Aircraft Gas-Turbine Engines.* 2003.

12. Brown, A.S. *MEMS across the valley of death.* 2006

13. Yuan, I.E.S.a.S.W.K., *Prediction of Thermal Acoustic Oscillations (TAOs) in the claes solid CO2/neon system.* 1992.

14. Okojie, R.S.D., J.C. Saus, J.R. . *SiC pressure sensor for detection of combustor thermoacoustic instabilities.* 2005.

15. CRIAQ, *Gas Turbines Control.* 2007.

16. Akin, T., *Piezoresistive Pressure and Temperature Sensor Cluster* 2007.

17. RTCA. *Welcome to RTCA, Inc.* 2007

18. Savrun, E. *Packaging considerations for very high temperature microsystems.* 2002.

19. Li-Anne Liew, W.Z., Linan An,Sandeep Shah, Ruiling Luo,Yiping Liu,Tsali Cross, Martin L. Dunn,Victor Bright,John W. Daily and Rishi Raj, *Ceramic MEMS: New Materials, Innovative Processing and Future Applications.* 2001.

20. Lee, J.P., *Fabrication of SiCN thin film on a substrate and measurement of sheet resistivity.* 2007.

21. Peng, J., *Thermochemistry and Constitution of Precursor-Derived Si-(B-)C-N Ceramics* 2002.

22. Accuratus, *Silicon Nitride (SiN) Properties.* 2008.

23. Accuratus, *Silicon Carbide (SiC) Properties.* 2008.

24. Driver, M.C.H., R.H. Brandt, C.D. Barrett, D.L. Burk, A.A. Clarke, R.C. Eldridge, G.W. Hobgood, H.M. McHugh, J.P. McMullin, P.G. Siergiej, R.R. Sriram, S. , *Advances in silicon carbide (SiC) device processing and substrate fabrication for high power microwave and high temperature electronics*. 1993.

25. Chien-Hung Wu Zorman, C.A.M., M. , *Fabrication and testing of bulk micromachined silicon carbide piezoresistive pressure sensors for high temperature applications*. 2006: Sensors Journal, IEEE

26. Young, D.J.J.D.Z., C.A. Ko, W.H. , *High-temperature single-crystal 3C-SiC capacitive pressure sensor*. 2004.

27. Liang-Yu Chen, R.S.O., Philip G. Neudeck, Gary W. Hunter, and Shun-Tien T. Lin *Material System for Packaging 500 °C SiC Microsystems.* 2001.

28. Accuratus, *Aluminum Nitride (AlN) Properties.* 2008.

29. E. Savnin, C.T., *An Aluminum Nitride Package for 600°C and Beyond.* 1998.

30. Accuratus, *Aluminum Oxide (Al2O3) Properties.* 2008.

31. Lucas F. M. da Silva, R.D.A., *Stress-free temperature in a mixed-adhesive joint.* Journal of Adhesion Science and Technology, 2006.

32. Cotronics, *UNIQUE 1200°F ADHESIVE.* 2007.

33. Lide, D.R., *CRC Handbook of Chemistry and Physics*. 2005: CRC Press.

34. Lab, J., *The Element Platinum.* 2008.

35. Habib A Mustain, A.B.L., William D. Brown, *Evaluation of Gold and Aluminum Wire Bond Performance for High Temperature (500 °C) Silicon Carbide (SiC) Power Modules.* IEEE, 2005.

36. Fendrock, J.J. and L.M. Hong, *Parallel-gap welding to very-thin metallization for high temperature microelectronic interconnects.* Components, Hybrids, and Manufacturing Technology, IEEE Transactions on [see also IEEE Trans. on Components, Packaging, and Manufacturing Technology, Part A, B, C], 1990. 13(2): p. 376-382.

37. www.edfagan.com, *glossary.* 2006.

38. Dacon Systems, *High Temperature Wire & Cables.* 2008

39. Linan, A., et al. *Development of injectable polymer-derived ceramics for high temperature MEMS.* in *Micro Electro Mechanical Systems, 2000. MEMS 2000. The Thirteenth Annual International Conference on.* 2000.

40. Hao Cui, P.A.B., *Time-Dependent Dielectric Breakdown Studies of PECVD H:SiCN and H:SiC Thin Films for Copper Metallization.* J. Electrochem. Soc., 2004.

41. Drost, A., D. Bonfert, and M. Feil. *Reliability investigations of thin film metallizations of AlN-Ceramics.* in *Electronic Manufacturing Technology Symposium, 1990, IEMT Conference., 8th IEEE/CHMT International.* 1990.

42. A. Sozza, C.D., A. Kerlainb, C. Brylinskib and E. Zanonia *Long-term reliability of Ti-Pt-Au metallization system for Schottky contact and first-level metallization on SiC MESFET.* Microelectronics and Reliability, 2004. Volume 44, Issue 7, July 2004.

43. L Kassamakovay, A.K.-G., R Kakanakovy, Ts Marinovaz, I Kassamakovy, Tz Djambovay, O Noblancx, C Arnodox, S Cassettex and C Brylinskix, *Thermostable Ti/Au/Pt/Ti Schottky contacts to n-type 4H-SiC.* Semicond. Sci. Technol., 1998.

44. Kakanakov, R., et al. *Thermally stable low resistivity ohmic contacts for high power and high temperature SiC device applications.* in *Microelectronics, 2002. MIEL 2002. 23rd International Conference on.* 2002.

45. Li-Anne Liew, W.Z., Victor M. Bright, Linan An, Martin L. Dunn and Rishi Raj *Fabrication of SiCN ceramic MEMS using injectable polymer-precursor technique.* Sensors and Actuators A: Physical 2001.

46. Li-Anne, L., et al. *Fabrication of multi-layered SiCN ceramic MEMS using photo-polymerization of precursor.* in *Micro Electro Mechanical Systems, 2001. MEMS 2001. The 14th IEEE International Conference on.* 2001.

47. Cotronics, *Potting Compounds.* Cotronics Corp., 2007.

48. Kuramoto, N., H. Taniguchi, and I. Aso, *Translucent A1N Ceramic Substrate.* Components, Hybrids, and Manufacturing Technology, IEEE Transactions on [see also IEEE Trans. on Components, Packaging, and Manufacturing Technology, Part A, B, C], 1986. 9(4): p. 386-390.

49. Kurihara, Y., et al., *Bonding mechanism between aluminum nitride substrate and Ag-Cu-Ti solder.* Components, Hybrids, and Manufacturing Technology, IEEE Transactions on [see also IEEE Trans. on Components, Packaging, and Manufacturing Technology, Part A, B, C], 1992. 15(3): p. 361-368.

50. Xingsheng, L., et al., *A metallization scheme for junction-down bonding of high-power semiconductor lasers.* Advanced Packaging, IEEE Transactions on [see also Components, Packaging and Manufacturing Technology, Part B: Advanced Packaging, IEEE Transactions on], 2006. 29(3): p. 533-541.

51. Cotronics, *Electrically Resistant Adhesives.* Cotronics Corp., 2007.

52. ANSYS, *ANSYS Basic Analysis Guide*, ANSYS Inc.

53. COMSOL, *COMSOL Installation and Operations GUide*. 2007.

54. Widas, P., *Introduction to Finite Element Analysis.* 1997.

55. engineering.wikia.com. *Heat transfer.* 2007

56. Answer.com, *Von Mises failure criteria.* 2007.

57. Bhadeshia, P.J.W.a.H.K.D.H., *Residual Stress Part 1 - Measurement Techniques.* Materials Science and Technology, 2001. Vol. 17.

58. ANSYS, *ANSYS Verification Manual*, ANSYS Inc.

59. Meyyappan, K., P. McCluskey, and L. Chen, *Thermomechanical analysis of gold-based SiC die-attach assembly.* IEEE Transactions on Device and Materials Reliability, 2003. 3(4): p. 152-158.

60. Schmidt, M.A., *Wafer-to-wafer bonding for microstructure formation.* Proceedings of the IEEE, 1998. 86(8): p. 1575-1585.